LOSS OF INTERACTION IN REINFORCED CONCRETE BEAMS

LOSS OF INTERACTION IN REINFORCED CONCRETE BEAMS

by

ANIS AHMAD BAIG, B.E. (Civil)

A Thesis

Submitted to the Faculty of Graduate Studies

in Partial Fulfilment of the Requirements

for the Degree

Master of Engineering

McMaster University

December, 1969

MASTER OF ENGINEERING (1969) McMASTER UNIVERSITY
(Civil Engineering) Hamilton, Ontario.

TITLE: Loss of Interaction in Reinforced Concrete Beams

AUTHOR: Anis Ahmad Baig, B.E. (Civil) (University of Karachi)

SUPERVISOR: Dr. H. Robinson

NUMBER OF PAGES: xiii, 138

SCOPE AND CONTENTS:

This thesis involves the consideration of the reinforced concrete beam as a composite beam with incomplete interaction. The flexual carrying capacity of the remaining uncracked portion, and the distribution of shear stress throughout the depth of a cracked beam are studied analytically.

ACKNOWLEDGEMENT

I wish to express my deepest gratitude and sincere appreciation to Dr. H. Robinson for his invaluable guidance and encouragement throughout the research program.

I wish to acknowledge the financial support of the project by the National Research Council and to McMaster University for awarding the scholarship and teaching assistantship.

Thanks are also due to my wife and parents for their patience, general assistance and advice.

TABLE OF CONTENTS

LIST OF FIGURES

LIST OF SYMBOLS

A_c	Effective cross-sectional area of concrete (sq. inches)
A_s	Cross-sectional area of the steel reinforcement (sq. inches)
$A_{11}, A_{12}, A_{21}, A_{22}$	Cross-sectional area of each member of a composite beam (sq. inches)
a	Distance from the support to the nearest load point i.e. shear span (inches)
B_1, B_2	Breadth of each member in a composite beam (inches)
B,b	Width of the beam (inches)
$\frac{1}{C}, (\frac{1}{C})_o (\frac{1}{C})_I$	Interaction coefficient, a dimensionless number
Cd, Cd_c	Uncracked concrete depth (inches)
Cd_1, Cd_2	
C_H	Total flexural crack height (inches)
C_{H_c}	Total crack height including inclined crack height (inches)
C_c, C_s	Distances from the centroids of the concrete and steel, respectively, to the pseudo-interface (inches)
D	Effective depth of a reinforced concrete beam (inches)
D_1, D_2	Depth of each member in a composite beam (inches)
D_c	The distance between the root of the flexural crack and the starting point of the inclined crack (inches)
d	Effective depth of the section of a reinforced concrete beam (inches)

d_s	Distance of the concrete cover to centre of reinforcement (inches)
E_c, E_s	Moduli of elasticity of concrete and steel, respectively (lb/sq. in.)
E_1, E_2	Moduli of elasticity of each member of a composite beam (lb/sq. in.)
$\frac{1}{\overline{EA}}$	$\frac{1}{E_c A_c} + \frac{1}{E_s A_s}$
$\frac{1}{\overline{EA}_o}$	$\frac{1}{E_1 A_{11}} + \frac{1}{E_2 A_{21}}$
$\frac{1}{\overline{EA}_I}$	$\frac{1}{E_1 A_{12}} + \frac{1}{E_2 A_{22}}$
ΣEI	$E_c I_c + E_s I_s$
ΣEI_o	$E_1 I_{11} + E_2 I_{21}$
ΣEI_I	$E_1 I_{12} + E_2 I_{22}$
$\overline{EI}$	$\Sigma EI + \overline{EA} \cdot z^2$
$\overline{EI}_o$	$\Sigma EI_o + \overline{EA}_o \cdot z_o^2$
$\overline{EI}_I$	$\Sigma EI_I + \overline{EA}_I \cdot z_I^2$
F, F_1, F_2, F_3, F'	Horizontal direct forces acting at the centroids of the concrete and the steel (lbs.)
G_c	Shear modulus of concrete (lb//sq.in.)
H,H'	Half the uncracked depth of the concrete section (inches)
I_c, I_s	Second moment of area of the concrete and steel, respectively (inches^4)
$I_{11}, I_{12}, I_{21}, I_{22}$	Second moment of area of each member of a composite beam (inches)
jd	Depth of lever arm in the conventional reinforced concrete theory (inches)

K	Bond-slip modulus in case of a reinforced concrete beam or modulus of shear connector (lb/in.)
K_{AG}	Aggregate interlocking modulus (lb/sq.in.)
K_D	Modulus of dowel action (lb/in.)
L	Span length of the beam (inches)
M	Maximum external bending moment (lb-in.)
$M_{11}, M_{22}, M_1, M_2, M_{21}, M_{22}$	Internal moments carried by the each member of a composite beam (lb-in.)
$M_t, M(x)$	External moment on the beam at any distance x from left hand support (lb-in.)
M_u	Maximum computed moment capacity of a beam (lb-in.)
M_{test}	Maximum experimental moment capacity of a beam (lb-in.)
M_{ult}	Computed ultimate flexural capacity of a beam, as obtained by ACI code formula (lb-in.)
n_1, n_2	Depths of neutral axes at sections 1 and 2, respectively (inches)
p	Percentage of reinforcement in a reinforced concrete section (inches)
Q	Load on a connector (lbs.)
Q_o	$\frac{K}{s} \frac{EI_o}{EA_o \Sigma EI_o}$
Q_I	$\frac{K}{s} \frac{EI_I}{EA_I \Sigma EI_I}$
q, q'	Horizontal shear per unit length (lb/in.)
R_o	$\frac{K}{s} \frac{Z_o}{\Sigma EI_o}$
R_I	$\frac{K}{s} \frac{Z_I}{\Sigma EI_I}$

S	Total shear carried by a concrete section (lbs.)
s	Spacing of the connectors (inches)
u	Distance from the support to the nearest load point i.e. shear span (inches)
V	Vertical shear due to external loading (lbs.)
v	Vertical shear stress (lb/sq.in.)
W	Magnitude of the external point load (lbs.)
X,x	Distance from the left hand support to any section within the span (inches)
y	Depth from the top fibre of the concrete to any level within the depth of the section (inches)
Z	Distance between the centroidal axes of the uncracked concrete section and the steel reinforcement (inches).
Z_1, Z_2, Z_o, Z_I	Distances between the centroidal axes of the each member in a composite beam (inches)
α	Distance of the change in cross-section of the first flexural crack from left hand support or the distance between the reduced cross-section and the support (inches).
β	Ratio of the full cross-section to reduced cross-section
γ	Slip between the concrete and the steel or slip between the two members of a composite beam (inches)
γ_{xy}	Shear strain (micro in./in.)
Δx	Distance between the two closely spaced cross-sections
Δ_{ch}	Increment in the flexural crack height (inches)
Δ_{ch_c}	Increment in the inclined crack height (inches)

ΔF_B	Incremental increase in the tensile force in the steel reinforcement (lbs.)
σ, σ_o	Stresses in the concrete (lb/sq.in.)
$\varepsilon, \varepsilon_o$	Strain in the concrete (lb/sq.in.)
ε_{cr}	Critical (cracking) tensile strain of the concrete (micro in/in.)
ε_r	Strain due to the distortion of the concrete 'teeth' in a cracked reinforced concrete beam (micro in./in.)
$\varepsilon_{sb}, \varepsilon_{sm}, \varepsilon_{st}$	Strains at the bottom, mid height and top fibres, respectively of the steel (micro in./in.)
$\varepsilon_{ct_{max}}, \varepsilon_{sm_{max}}$	Maximum permissible compressive strain at the top fibre of concrete and maximum permissible average tensile strain in the steel reinforcement, respectively (micro in./in.)
ε_{max}	Maximum principal strain (micro in./in.)
ε_{xy}	Flexural strain (micro in./in.)
$\varepsilon_{ct_1}, \varepsilon_{ct_2}$	Strains at top fibre of concrete at sections 1-1 and 2-2, respectively (micro in./in.)
$\varepsilon_{y_1}, \varepsilon_{y_2}$	Flexural strains at levels y_1 and y_2 respectively (micro in./in.)
θ	Angle of inclination of the direction of maximum principal strain (degrees)
τ_{12}	Horizontal shear stress (lb./sq.in.)
τ_{xy}	Vertical shear stress (lb./sq.in.)
ν	Poisson's Ratio for concrete, a dimensionless member.

CHAPTER I

INTRODUCTION

1.1 Introduction

In this analysis a reinforced concrete beam is treated as a composite beam with incomplete interaction, a deviation from the conventional concept.

Conventionally it is assumed that in a reinforced concrete beam, concrete and steel acts together such that there is no relative movement between the two materials. However from the experimental evidence[1,2] it has been well recognized that slip does take place and concrete does not act perfectly with the steel.

The phenomenon of so-called 'diagonal failure' still remains unsolved and a rational theory is required. The ACI-ASCE committee 426(326)[3] made an excellent contribution in the field of shear and diagonal tension. The committee stated that the problem of shear failure and diagonal tension has not been fundamentally and conclusively solved and the same committee urged the formulation of a rational theory.

Therefore, new approaches[1,2,4] are being undertaken, especially those which take into account the slip

between the two materials. Robinson[4] suggested that a reinforced concrete beam may well be treated as a composite beam with incomplete interaction.

Treating the reinforced concrete beam in this manner the qualitative explanation of some of the experimental results such as cracking pattern, the ultimate moment carrying capacity of the beam with varying shear-span to depth ratio and the influence of various parameters on it can be provided.

It is hoped that by treating the reinforced concrete beam as composite beam with loss of interaction a rational explanation of so-called diagonal cracking in the shear span might be achieved.

1.2 Historical Survey

Few subjects in the field of concrete have received more attention from research workers than the shear failure of reinforced concrete beams. The phenomenon of shear failure has been the interest of many research workers for quite a long time.

As early as in 1900 one group of thought believed the basic cause of shear failure to be due to diagonal tension and many research workers supported this concept in the light of their experiments.

Mörsch[5] provided the famous and most widely used equation for shear design which is included in many design

codes of practices. The equation is:

$$v = \frac{V}{bjd} \qquad 1.1$$

A few years later in 1909 Talbot[6] observed that the Mörsch equation does not take into account the variables such as shear-span to depth ratio and percentage of reinforcement etc. and it is not in general agreement with the test results.

Two decades ago Clark[7] introduced the equation for shear design which includes the shear-span to depth ratio, percentage of reinforcement and the strength of concrete.

Studies of shear and diagonal tension became a major interest of research workers when a few structural failures occurred, especially the failure at Wilking Air Force Depot in Shelby, Ohio in 1955, and after that considerable research in this field was undertaken experimentally as well as analytically.

Kani[8] in his paper, "The Mechanism of So-Called Shear Failure", used the concept of 'Concrete Teeth' to explain the mechanism of shear and diagonal failure and concluded that the shear failure is a problem of diagonal compression failure, a deviation from earlier concepts. Kani in another paper[9] further pointed out the process of transformation of a "Comb-Like" structure with bond into a 'Tied Arch" without bond due to redistribution of stresses.

A number of authors[10,11,12] attempted to relate the critical cracking load to the maximum principal stress. Ferguson[12] also described the failure pattern in terms of the theory of combined stresses and suggested that if the theory of combined stresses applied more constructively a rational solution could be achieved.

It has been well recognized[2] that the diagonal tension is a combined stress problem, however, in a reinforced concrete beam owing to initial flexural cracks, the stress redistribution near the crack, and changes in the magnitude in the shear and normal stresses, as well as stress concentrations at the tip of the crack, make the calculation of principal stresses extremely complex. Therefore, without taking into account these redistributions of internal stresses, any theoretical treatment of the problem of diagonal tension is a rough approximation.

Broms[13] carried out an analytical study to determine the distribution of shear, flexural and normal stresses in constant moment and in combined bending and shear regions of a simply supported reinforced concrete beam. He reported that the shear stresses near the neutral axis is the cause of diagonal tension failure. However, Brom's approach gave an unrealistically high value of shear stresses[14] and the percentage of shear force carried by uncracked concrete is

more than 300 percent as obtained by Uppal[14], using Brom's method.

Recently the distribution of shear stresses in a cracked beam and the percentage of shear force carried by different components such as uncracked concrete, aggregate interlocking and dowel action have received the attention of many research workers[1,11,15]. Acharya and Kemp[15] argued that the dowel force cannot be ignored in any reliable quantitative analysis of shear failure. They suggested that at least 60 percent of the total shear force is carried by dowel action.

Fenwick and Pauley[1] in their paper "Mechanism of Shear Resistance of Concrete Beams", claim that 70 percent of the shear force is carried by aggregate interlock and dowel actions, in which dowel action contributes $\frac{1}{3}$ to $\frac{1}{4}$ of the 70 percent, and the remaining 30 percent is carried by uncracked concrete.

MacGregor and Walters[11] in their analytical analysis of inclined cracking load suggested that 11 percent of the total shear force is carried by dowel action, 23 percent by aggregate interlock action and the remainder by the uncracked concrete.

In spite of the fact that extensive experimental as well as analytical research has been carried out in order

to give a rational explanation of the so-called shear failure, still the problem remains untractable and the mechanism of shear failure improperly understood.

Robinson[4] in conducting tests on composite beams having a cellular zone between concrete and steel I-beam discovered that in spite of the fact that there was no interfacial plane between the two materials, the distribution of strain has been observed to be essentially linear. He also suggested that the reinforced concrete beam can be treated as a composite beam with incomplete interaction.

In his analytical study Wong[16] following the Robinson notion stated that although a reinforced concrete beam does not have a distinct interfacial plane between steel and concrete, a slight modification of the Newmark[17] theory for composite beams with incomplete interaction makes it applicable to a reinforced concrete beam if a pseudo interface is assumed. He then computed the flexual crack profiles of a simply supported reinforced concrete beam with two symmetrical point loads and observed that the highest crack is under the load points.

Ho[18] in an extension of Wong's work computed the strain trajectories and stated that they do not lead to further understanding of diagonal cracking.

Uppal[14] made an extensive analytical study based

on Robinson's notion and Wong's modified Newmark composite beam theory. He computed the flexural crack profiles and studied the influence of a number of parameters such as degree of interaction between steel and concrete, percentage of longitudinal reinforcement and the intensity of loading. He stated that the crack profiles were greatly affected by these parameters. He also stated that the cracking pattern is affected by the shear-arm to depth ratio. He also determined the effect on moment carrying capacity of a reinforced concrete beam of the variation of shear-arm to depth ratio, percentage of tensile reinforcement and the interaction coefficient. He computed the distribution of shear stresses in the remaining uncracked concrete, but the amount of shear force carried by uncracked concrete did not give a realistic percentage of shear force and hence, he argued for more rigorous analysis of shear distribution in a cracked beam.

1.3 Object and Extent of Investigation

In this analysis an attempt has been made to study the cracking behavior, moment carrying capacity and the distribution of shear stresses in a reinforced concrete beam, by treating it as a composite beam with incomplete interaction.

The Newmark[17] composite beam theory can be applied, with slight modifications to an uncracked reinforced

concrete beam. Its applicability to a cracked reinforced concrete beam has been verified. However, it does not take into account the compatibility conditions at the first flexural crack from the support.

The stability of a tensile crack is discussed and the influence of bond-slip modulus and modulus of elasticity of concrete on the crack height are studied.

Moment carrying capacity curves for a particular 'typical' reinforced concrete beam were computed. It was found that the computed results are in very close agreement with Kani's experimental results[19]. This study was extended further to find the influence of various other parameters on the moment carrying capacity.

An attempt has been made to give the magnitude of bond-slip modulus for different percentages of steel.

Finally the distribution of shear stresses along the depth of a cracked beam are computed and the amount of vertical shear force carried by different components such as uncracked concrete, dowel action and aggregate interlock action are determined. The shear stresses were combined with the flexural stresses in order to compute the magnitude and direction of principal stresses. The results obtained are encouraging and an inclined crack is obtained above the root of the flexural crack. This offers prospects

that further analysis may lead to determination of the development of diagonal cracks if small incremental loading is utilized.

CHAPTER II

COMPOSITE BEAM WITH STEPPED CHANGE IN CROSS-SECTION

2.1 The conventional Newmark[17] theory for composite beams is applicable only to beams with prismatic sections and this does not take into account the compatibility conditions if the profile of the cross-section changes suddently. From here onwards in this chapter this theory is called Newmark 1.

As the reinforced concrete beam cracks the application of Newmark 1 theory (with slight modifications) to the cracked beam is questionable, since the beam is no longer prismatic and the degree of interaction, $\frac{F}{F'}$, at a particular location along the length of the beam will be influenced by this. Therefore, an approach which takes into account the compatibility conditions at the location of change in cross-section, for example at the end of the cracked zone of the beam, would provide more correct mathematical results. Uppal[14] also argued for the development of such an approach.

A cracked reinforced concrete beam can be idealized into two parts, namely, the one which is uncracked (full section) and the other which has cracked (reduced section) and having a sudden change at the limits of the cracked zone.

A particular solution for a simply supported compo-

site beam, with symmetrical situated two point loads at a distance 'u' from each end, having flexible connection and stepped change in cross-section at a distance 'α' from each end, where α is less than u, is obtained.

This approach takes into account the compatibility conditions at the stepped change and will be called Newmark 2B theory in this thesis.

2.2 Assumptions

The basic assumptions and the formulation of the approach is the same as that of Newmark 1. The assumptions are:

1. The two components of the composite beam have equal curvatures at any cross-section.
2. The horizontal force, F, transmitted to each component by the connections are considered to act at the centroids of each section.
3. The shear connection between the beam and slab is assumed to be continuous along the length of the beam,i.e. connectors are of equal capacities and are equally spaced; then

$$\frac{K}{s} = \text{constant.}$$

4. The amount of slip permitted by the shear connection is directly proportional to the load transmitted.

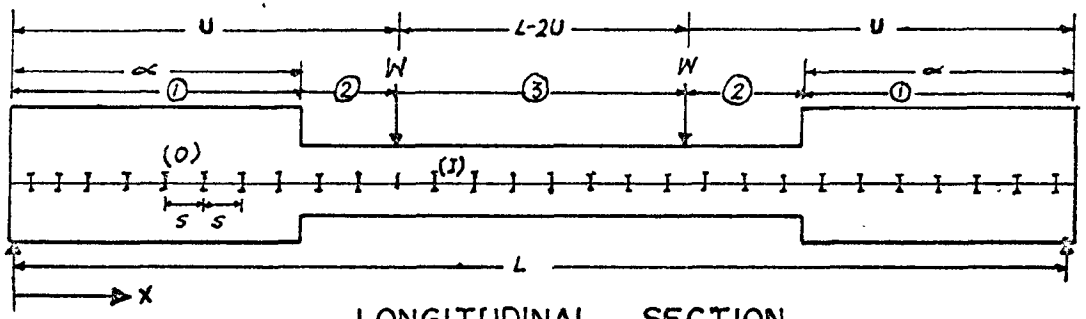

LONGITUDINAL SECTION

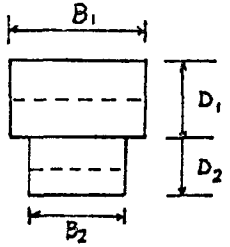

CROSS SECTION

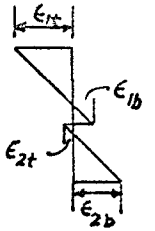

STRAIN DISTRIBUTI

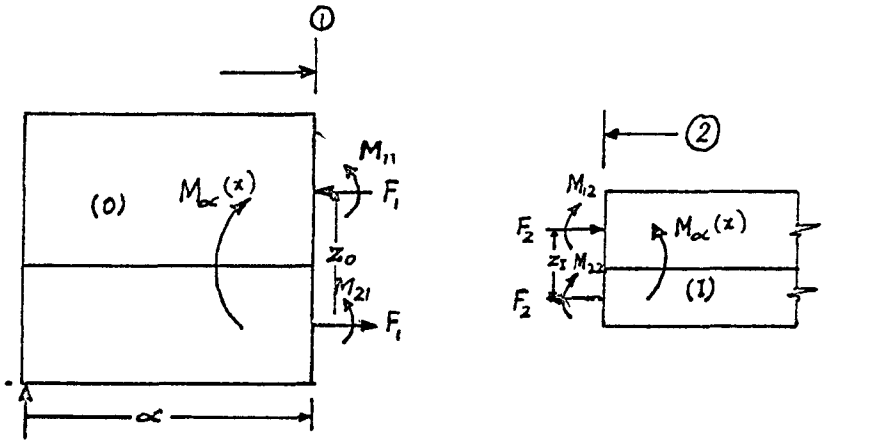

$M_{\alpha}(x) = M_{11} + M_{21} + F_1 \cdot Z_0$ $\qquad$ $M_{\alpha}(x) = M_{12} + M_{22} + F_2 \cdot Z_1$

FREE BODY DIAGRAM AT $X = \alpha$

COMPOSITE BEAM WITH STEPPED PROFILE

FIG. 2.1

$$\text{i.e.} \quad \gamma = \frac{Q}{K} .$$

5. The distribution of strain throughout the depth of the beam, in the two components, is linear.

6. The total internal moment, M, at any location along the beam is equal to the sum of the individual member moments, M_1, M_2 and the additional couple due to horizontal force, F, hence:

$$M = M_1 + M_2 + F \cdot Z \qquad 2.1$$

where Z = distance between the centroids of the individual components as shown in Fig. 2.1.

2.3 Solution of Differential Equation

The basic differential equation[17] for the solution of horizontal force, F, for various loading, compatability and boundary conditions, is: (See Appendix A)

$$\frac{d^2F}{dx^2} - \frac{K}{s} \frac{\overline{EI}}{\overline{EA}\Sigma EI} F = - \frac{K}{s} \frac{Z}{\Sigma EI} M(x) \qquad 2.2$$

The differential equation for the two segments to the left and right of $x = \alpha$, is: (see Fig. 2.1)

$$\frac{d^2F}{dx^2} - Q_o F = - R_o M(x) \qquad 2.3$$

$$\frac{d^2F}{dx^2} - Q_I F = - R_I M(x) \qquad 2.4$$

The subscript zero is used for the full cross-section and suffix I is used for the reduced cross-section.

Here Q_o, Q_I, R_o and R_I incorporate the properties of the sections, as follows:

$$Q_o = \frac{K}{s} \frac{\overline{\overline{EI}}_o}{\overline{\overline{EA}}_o \; \Sigma EI_o} = \left(\frac{1}{C}\right)_o \frac{\pi^2}{L^2}$$

$$Q_I = \frac{K}{s} \frac{\overline{\overline{EI}}_I}{\overline{\overline{EA}}_I \; \Sigma EI_I} = \left(\frac{1}{C}\right)_I \frac{\pi^2}{L^2}$$

$$R_o = \frac{K}{s} \frac{Z_o}{\Sigma EI_o} = \left(\frac{1}{C}\right)_o \frac{\overline{\overline{EA}}_o}{\overline{\overline{EI}}_o} Z_o \frac{\pi^2}{L^2}$$

$$R_I = \frac{K}{s} \frac{Z_I}{\Sigma EI_I} = \left(\frac{1}{C}\right)_I \frac{\overline{\overline{EA}}_I}{\overline{\overline{EI}}_I} Z_I \frac{\pi^2}{L^2}$$

and

$$\frac{R_o}{Q_o} = \frac{\overline{\overline{EA}}_o}{\overline{\overline{EI}}_o} Z_o$$

$$\frac{R_I}{Q_I} = \frac{\overline{\overline{EA}}_I}{\overline{\overline{EI}}_I} Z_I$$

where $\left(\frac{1}{C}\right)_o$ = Interaction coefficient in the full cross-section zone

$\left(\frac{1}{C}\right)_I$ = Interaction coefficient in the reduced cross-section zone.

The particular solutions for equations 2.3 and 2.4 are:

For $o < x \leq \alpha$

$$F_1 = C_1 \cosh x\sqrt{Q_o} + C_2 \sinh x\sqrt{Q_o} + \frac{R_o}{Q_o} W \cdot x. \qquad 2.5$$

For $\alpha < x \leq u$

$$F_2 = C_3 \cosh x\sqrt{Q_I} + C_4 \sinh x\sqrt{Q_I} + \frac{R_I}{Q_I} W \cdot x \qquad 2.6$$

For $u < x \leq \frac{L}{2}$

$$F_3 = C_5 \cosh x\sqrt{Q_I} + C_6 \sinh x\sqrt{Q_I} + \frac{R_I}{Q_I} W \cdot u \qquad 2.7$$

Compatability Conditions

At $x = o$ $\qquad F_1 = 0$

At $x = \alpha$; $\quad \frac{dF_1}{dx} = \frac{dF_2}{dx}$ i.e. $\quad q_1 = q_2$

and $\quad \frac{dq_1}{dx} = \frac{dq_2}{dx}$ i.e. $\quad \frac{d\gamma_1}{dx} = \frac{d\gamma_2}{dx}$

or $\quad \frac{d^2F_1}{dx} = \frac{d^2F_2}{dx}$ or $F_1 = \frac{Q_I}{Q_o} F_2 + \frac{R_o - R_I}{Q_o} M_\alpha$

where M_α = moment at a distance α from support.

At $x = u$; $F_2 = F_3$ and $\frac{dF_2}{dx} = \frac{dF_3}{dx}$

and At $x = \frac{L}{2}$ $\quad \frac{dF_3}{dx} = 0$

here suffix 1, 2, 3 represents the composite beam between o and α, α and u, and u and $\frac{L}{2}$, respectively. Solving for the constants C_1, C_2 ..... C_6.

$$C_4 = -\left[\left(\frac{R_I}{Q_I} + \frac{R_o}{Q_o}\right)\frac{\sqrt{Q_o}}{Q_I} W \sinh a\sqrt{Q_o} + \left(\sqrt{Q_I}\cosh a\sqrt{Q_I}\right.\right.$$

$$\cosh a\sqrt{Q_o} - \sqrt{Q_o}\sinh a\sqrt{Q_I}\sinh a\sqrt{Q_o})\frac{R_I \cdot W}{Q_I\sqrt{Q_I}}$$

$$\left.\frac{\cosh\sqrt{Q_I}\left(\frac{L}{2}-u\right)}{\sinh\frac{L}{2}\sqrt{Q_I}}\right] \div \left[\frac{\cosh\frac{L}{2}\sqrt{Q_I}}{\sinh\frac{L}{2}\sqrt{Q_I}}\left(\sqrt{Q_I}\cosh a\sqrt{Q_I}\right.\right.$$

$$\cosh a\sqrt{Q_o} - \sqrt{Q_o}\sinh a\sqrt{Q_I}\sinh a\sqrt{Q_o}) +$$

$$\left.\left.(\sqrt{Q_o}\cosh a\sqrt{Q_I}\sinh a\sqrt{Q_o} - \sqrt{Q_I}\sinh a\sqrt{Q_I}\cosh a\sqrt{Q_o})\right]\right|$$

$$C_3 = -\frac{1}{\sinh\frac{L}{2}\sqrt{Q_I}}\left[C_4\cosh\frac{L}{2}\sqrt{Q_I} + \frac{R_I W}{Q_I\sqrt{Q_I}}\cosh\sqrt{Q_I}\left(\frac{L}{2}-u\right)\right]$$

$$C_5 = C_3 - \frac{R_I}{Q_I\sqrt{Q_I}} W \sinh u\sqrt{Q_I}$$

$$C_6 = C_4 + \frac{R_I}{Q_I\sqrt{Q_I}} W \cosh u\sqrt{Q_I}$$

$$C_2 = \frac{Q_I}{Q_o}\frac{1}{\sinh a\sqrt{Q_o}}\left[C_3\cosh a\sqrt{Q_I} + C_4\sinh a\sqrt{Q_I}\right]$$

$$C_1 = 0.$$

2.4 Comparison of Newmark 1 and Newmark 2B

2.4.1 The results obtained by both the approaches have been plotted in Figs. 2.3, 2.4, 2.5 and 2.6 for various ratios of reduced depth to full depth, β. The beam considered for this purpose is shown in Fig. 2.2. It is a simply supported beam having two symmetrical point loads of W = 5000 lbs. at a distance, u = 21 in. from each support, having the change in cross-section at a distance, a = 15 in. Specific dimensions have been considered to overcome complexities involved in attempting to non-dimensionalize the equations obtained.

The values of β considered are 0.4, 0.6, 0.8 and 1.0 and the degree of interaction, $\frac{F}{F'}$, along the length of the beam, horizontal force, F, horizontal shear, q, and the top fibre strain of the above member have been plotted.

2.4.2 The effect of β on the magnitude of $\frac{F}{F'}$, as obtained by the two approaches is shown in Fig. 2.3. It can be observed that the difference between $\frac{F}{F'}$ is not much in the region of the reduced section. However, there is a difference in the region of the full cross-section and this increases as the value of β decreases. For example, when β = 0.4 the value of $\frac{F}{F'}$ has a sudden reduction in magnitude at the change of cross-section, moving towards

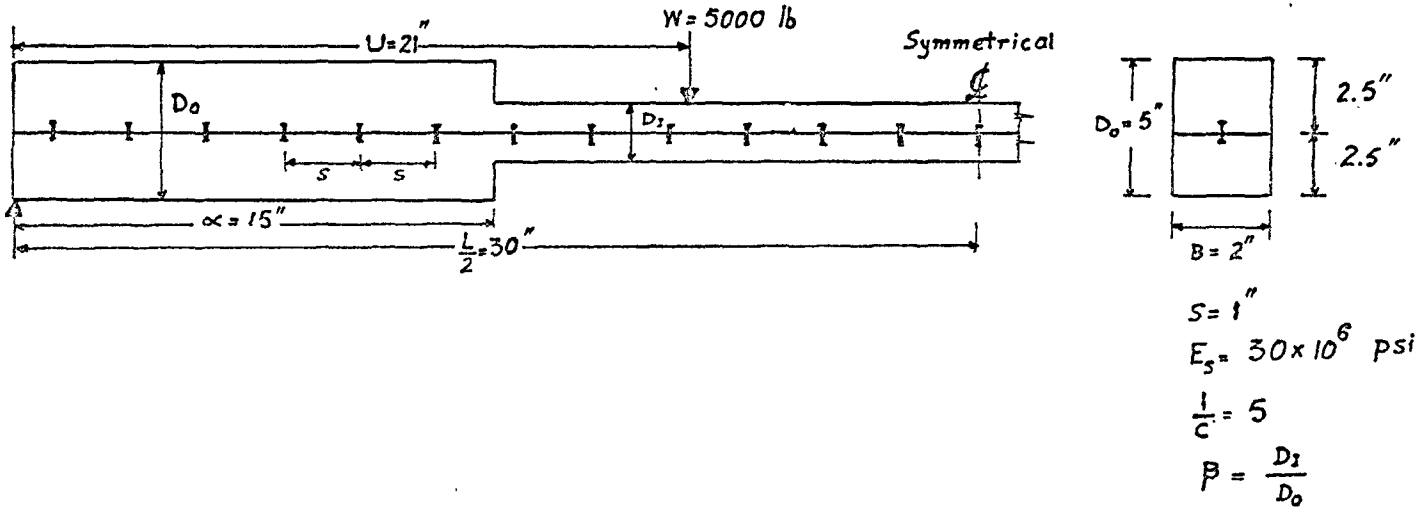

DIMENSIONS OF COMPOSITE BEAM WITH STEPPED PROFILE

FIG. 2.2

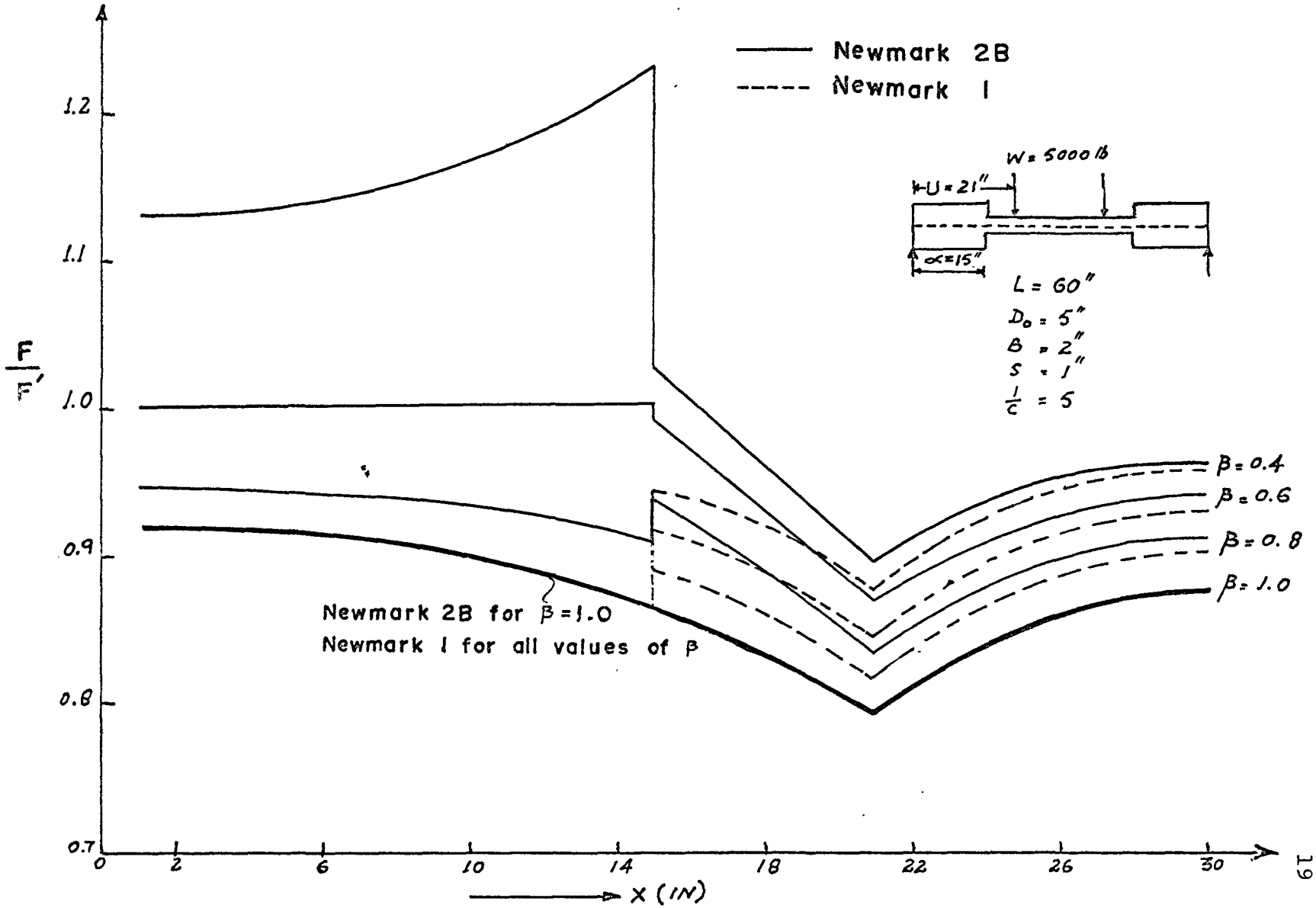

COMPARISON OF DEGREE OF INTERACTERACTION

FIG. 2.3

mid-span, for Newmark 2B, while on the other hand the value of $\frac{F}{F'}$, has a sudden increase in magnitude for Newmark 1; and for $\beta = 0.8$ the magnitude of $\frac{F}{F'}$, has a sudden increase by both the methods. It is also to be noted that $\frac{F'}{F}$, up to the change of cross-section is the same by Newmark 1, whatever may be the value of β, though it is different in the reduced section for various values of β. However, in Newmark 2b the $\frac{F}{F'}$, is different throughout the length of the beam for every different value of β and in some instances, for example $\beta = 0.4$, $\frac{F}{F'}$, is more than 1 up to the change in cross-section. This is because, as the section reduces for the same applied bending moment , a redistribution of forces occurs, see Fig. 2.4 for F and F'.

2.4.3 Figure 2.4 shows the variation in the magnitude of interaction force, F, along the length of the beam for various values of β. The horizontal forces, F, computed by the two methods are generally in agreement in the reduced section, but the difference is in the full section zone and it increases for the lower values of β, however, it is not more than 24 percent.

2.4.4 The distribution of horizontal shear, q, is shown in Fig. 2.5 and in this case the difference is significant. In the Newmark 2B approach q follows a smooth curve

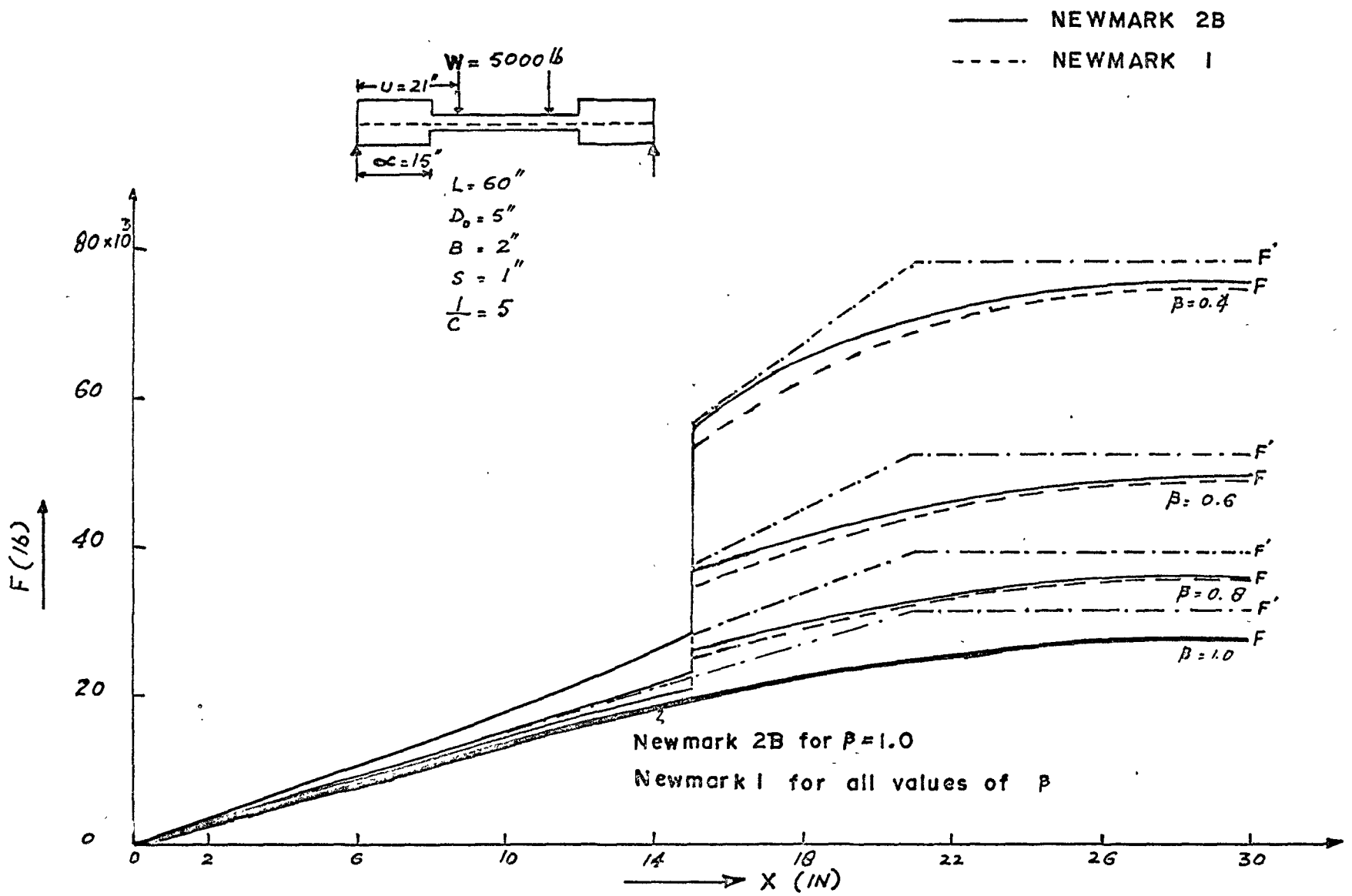

COMARISON OF INTERACTION FORCE

FIG. 2.4

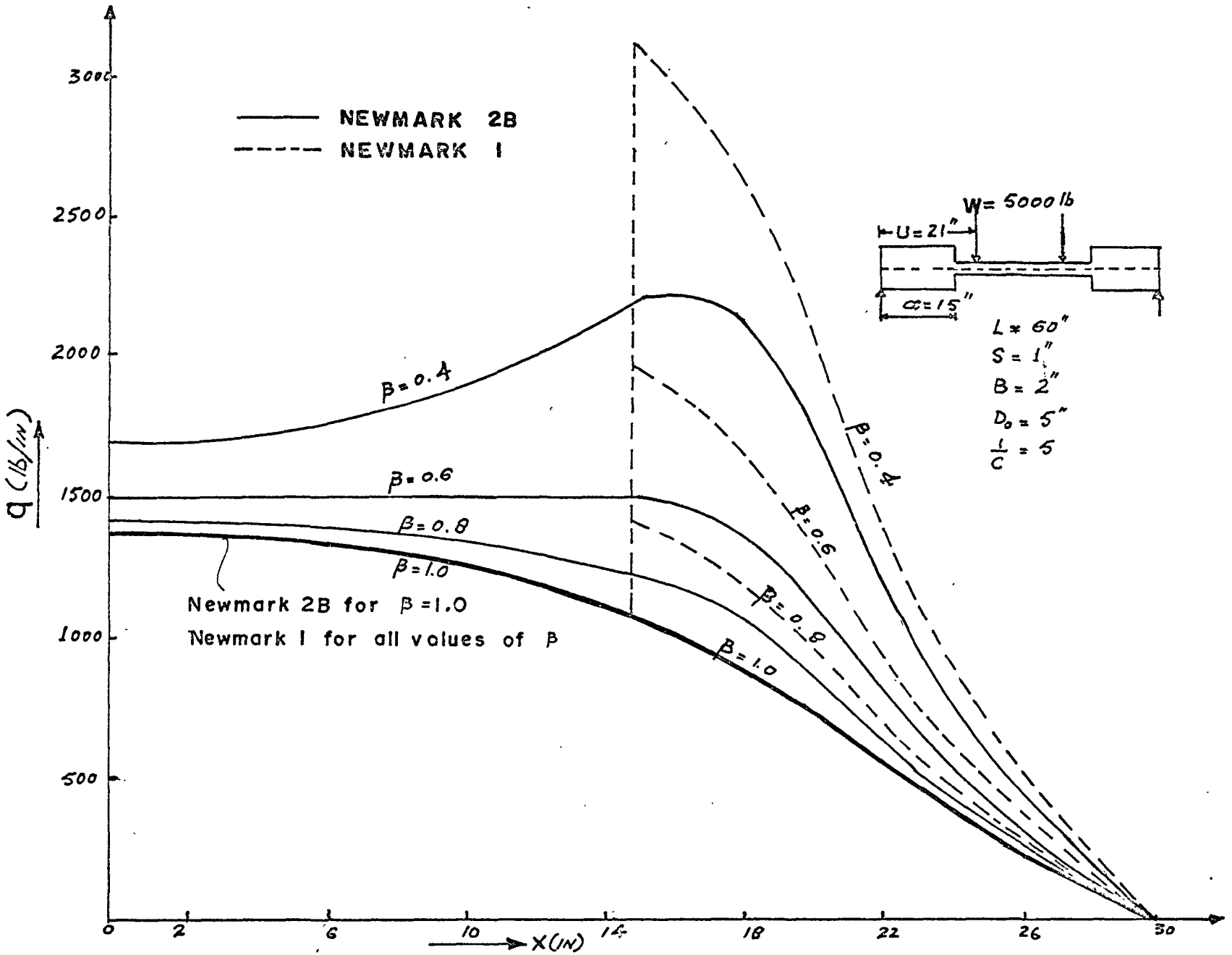

COMPARISON OF HORIZONTAL SHEAR

FIG. 2.5

throughout the length of beam, in accordance with the chosen compatibility conditions, while on the other hand for Newmark 1,q has a sudden increase at the change of cross-section, moving towards mid-span . Also for any different value of β, the magnitude of horizontal shear, q, is the same from the support to the change of cross-section, as computed by Newmark 1.

2.4.5 Fig. 2.6 shows the variation in the magnitude of top fibre strain of the upper member, ε_{1t} (or the bottom fibre strain of the lower member) along the length of the beam for various values of β. It can be observed that the difference in the strain computed by both the approaches is not much in the reduced section zone and the maximum is about 8 percent for β=0.4. However, there is a considerable difference in the magnitude of strains in the full section portion for smaller values of β, but the difference is insignificant for higher values of β. It is also to be noted that the magnitude of strains computed by Newmark 2B are lower than those obtained by Newmark 1 method.

2.5 Comparison of Crack Profiles

The flexural crack profiles have been computed by the two methods. The method is presented in Appendix A and chapter III.

The approximation made for computation by Newmark 2B is that the beam has two different cross-sections, namely, a

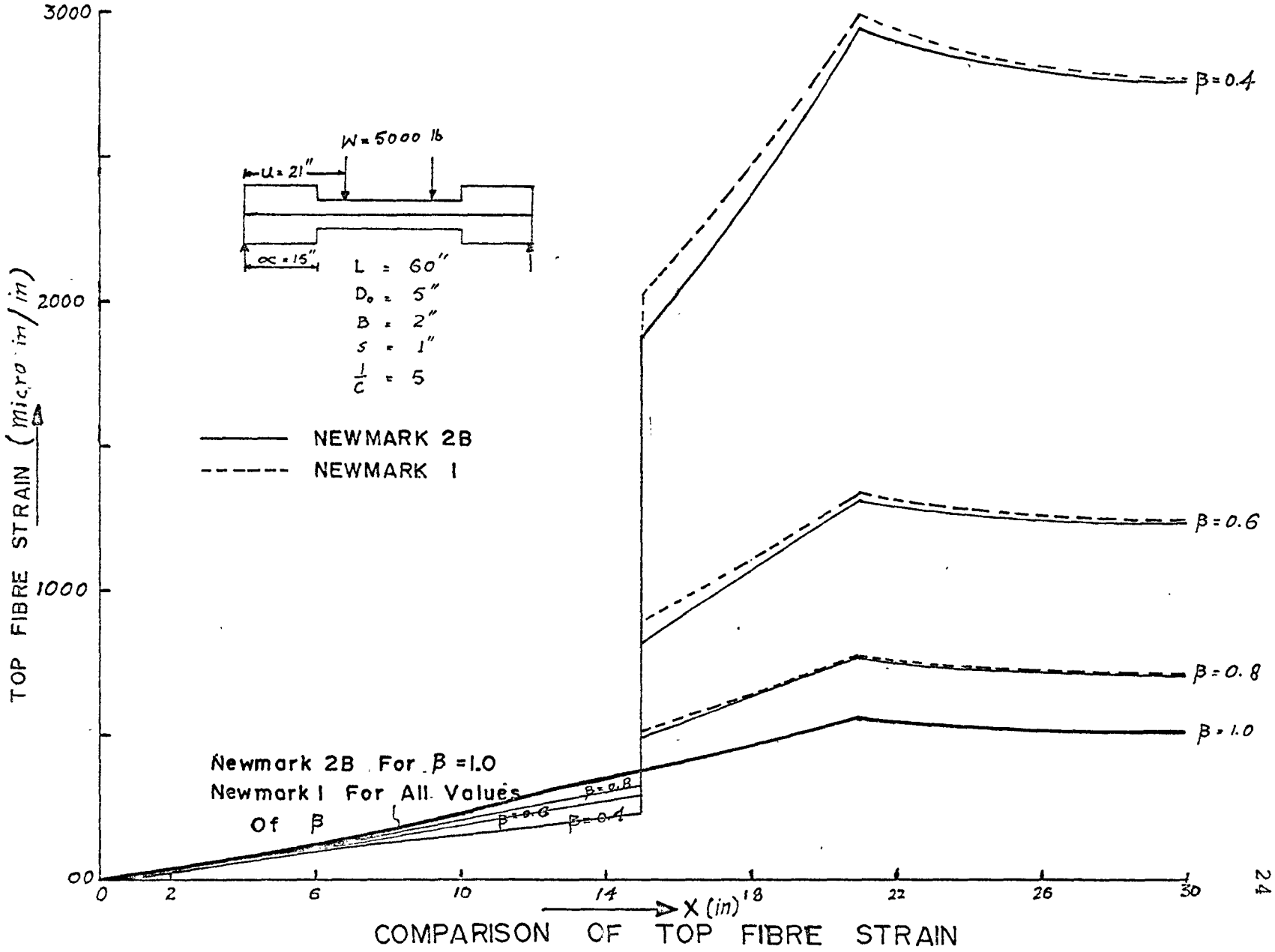

COMPARISON OF TOP FIBRE STRAIN

FIG. 2.6

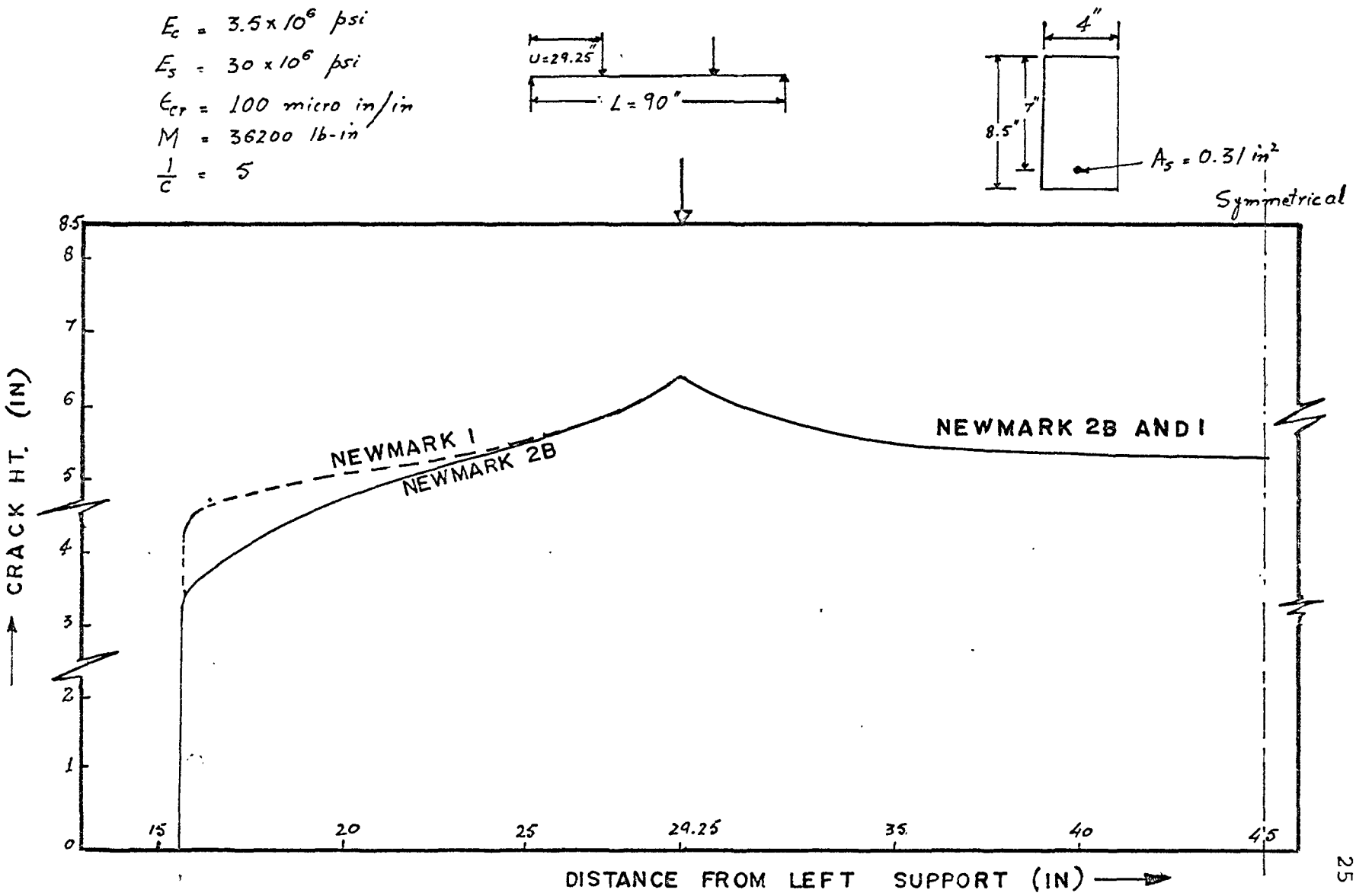

COMPARISON OF CRACK PROFILES

FIG. 2.7

full section from the support to the first flexural crack and a reduced section, which depends upon the crack height at any particular section under consideration in the potential cracking zone. In the Newmark 1 method, the approximation is that the beam has the same reduced or full section throughout the length of the beam depending upon the section under consideration.

The crack profiles of the reinforced concrete beam, obtained by the two approaches, are shown in Fig. 2.7. It can be seen that the first flexural crack starts at the same point by the two methods. The reason is that, first the crack profile is computed using Newmark 1 and then the distance of the first flexural crack from the support is used as the length of full section, α, in Newmark 2B. The height of the crack at the extremity of the cracked zone is significantly different and is lower in the case for Newmark 2B; the difference is about 1 in., but this difference goes on reducing until near the load point,and after it,the profiles are almost the same and there is practically no difference. Also the maximum crack height obtained under the load point is almost the same by both the methods.

The difference in the crack height is obvious; in the beginning the magnitude of horizontal force, F, varies considerably when computed by the two methods (as can be

seen in Fig. 2.4), but this difference decreases as the section moves towards mid-span. According to theory if F is greater the crack height will be lower and vice versa.

2.6 Discussion

The variation in the magnitude of horizontal force, F, degree of interaction, $\frac{F}{F'}$, , and the top fibre strain of the upper member (or the bottom fibre strain of the lower member) agrees closely in the reduced section zone, when computed by the two methods. However, in the full section portion, the difference is considerable for smaller values of β, but for higher values of β the difference is not significant. The horizontal shear, q, has remarkably different magnitudes, as computed by the two methods. This is due to the compatibility conditions applied at the change of cross-section in Newmark 2B, while Newmark 1 solution does not consider any compatibility conditions at the change of cross-section.

A different set of compatibility conditions were tried at the change of cross-section, in order to see the results of $\frac{F}{F'}$, F and q. The solution of the differential equations obtained from these conditions is called Newmark 2A, but the results obtained are far from Newmark 2B and Newmark 1. The compatibility conditions at the change of cross-section are:

at $x = \alpha$

$$F_1 = F_2$$

and $q_1 = q_2$.

The solution of the differential equation can be obtained in the same way as the solution of Newmark 2B.

Although the solution obtained with Newmark 2A is in very close agreement with the Stussi method[20] using finite difference equations, it is concluded that the Newmark 2A is not correct and the agreement with Stussi solution is due to the fact that the Stussi method does not take into account the compatibility conditions if the section is non-prismatic or has a stepped profile, and violates the condition that $\frac{d\gamma}{dx}$ must be equal at the change of cross-section. If similar conditions were imposed in the Stussi method then it is expected that this will give the same results as obtained by Newmark 2B.

The flexural crack profiles obtained by the two methods give maximum crack height under the load point and the magnitude is almost the same. It is thought that the crack profile obtained by Newmark 2B gives better results as compared to experimental observations, because crack heights are not as high towards the extremities of the cracked zone as those obtained by Newmark 1.

As mentioned earlier the discrepancy in the crack height is in the initial cracking zone and the profiles are virtually the same near the load point and after it up to mid-span. Hence, it is concluded that the Newmark 1 solution; although it does not take into account the compatibility conditions at the change of cross-section can well be applied to study the reinforced concrete beam especially to find the flexural capacity and maximum crack height.

CHAPTER III

STABILITY OF TENSILE CRACK

3.1 The Newmark composite beam theory has been used with slight modifications to furnish an estimated flexural crack profile based on the attainment of flexural crack stability. The theory is summarized in Appendix A.

Apart from assumptions made for composite theory and also made in Appendix A for a reinforced concrete beam it is assumed that the concrete is capable of withstanding a certain tensile strain, ε_{cr}, that is a strain level at which cracking will occur. If the lower fibre strain of the concrete, ε_{cb}, is greater than the limiting tensile strain, ε_{cr}, then a flexural crack starts and propogates upwards into the beam until ε_{cb} is equal to ε_{cr}, as well as there being equilibrium between internal and external forces.

From the geometry of the distribution of strains at any section, as shown in Fig. 3.1, the following equation can be derived:

$$\Delta_{ch} = 2H \frac{\varepsilon_{cb}-\varepsilon_{cr}}{\varepsilon_{cb}+\varepsilon_{cr}} \qquad 3.1$$

where Δ_{ch} = first increment in the crack height.

The remaining uncracked depth will be:

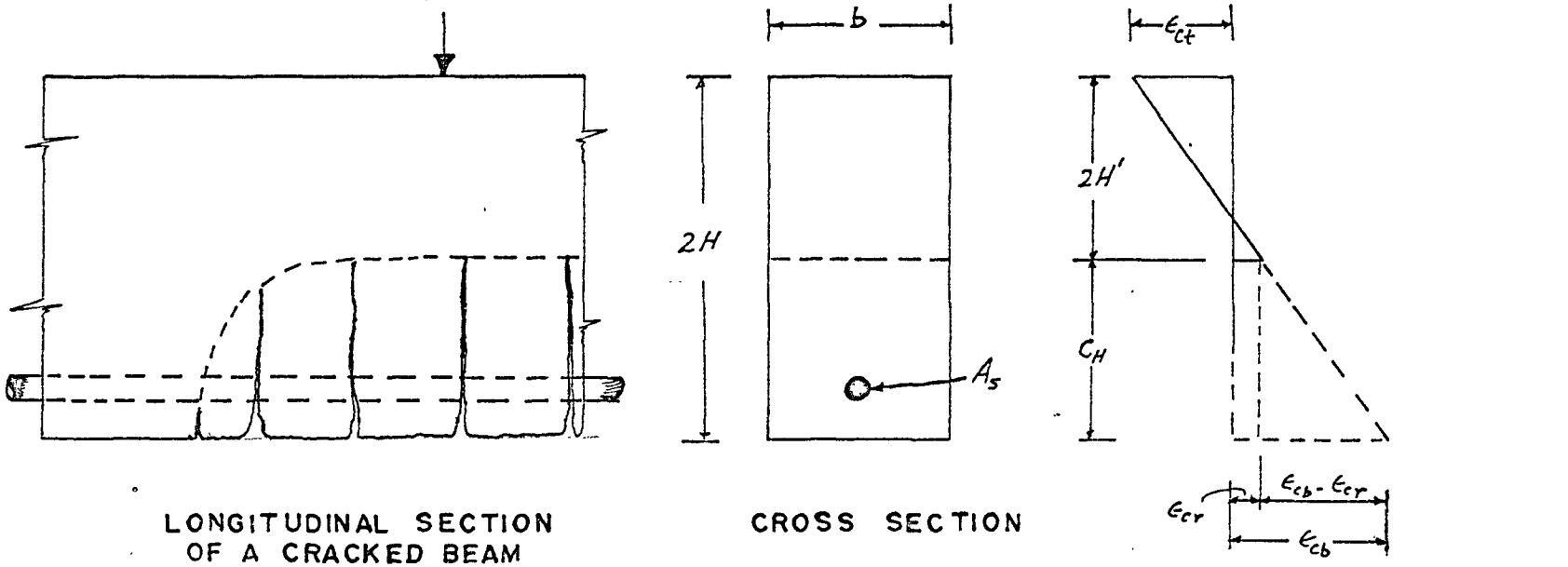

DEVELOPMENT OF A FLEXURAL CRACK

FIG. 3.1

$$2H' = 2H - C_H$$

and

$$C_H = \Delta_{ch} .$$

The new remaining depth, 2H', can be reused in equation 3.1 in place of 2H and another increment in crack height can be obtained. This is an iterative process repeated until a stable section is obtained and then:

$$C_H = \sum_{I=1}^{N} \Delta_{ch} \quad \text{where} \begin{cases} \Delta_{ch} = 0 \\ \text{and} \qquad \text{at } I=N \\ \varepsilon_{cb} = \varepsilon_{cr} \end{cases}$$

Here C_H = total crack height.

3.2 Non-Linearity of Concrete

3.2.1 It is well recognized that the stress-strain distribution for concrete is always non-linear and if a more rigorous solution and computation are desired for a reinforced concrete beam, this has to be taken into account.

A variety of stress-strain curves represented by equations having parabolic, hyperbolic and elliptical cubic parabolic have been used for analytical studies. Other simple forms such as triangular, rectangular or trapezoidal have also been used[21].

In this analysis the area under the stress-strain curve of concrete up to crushing strain has been taken from the Madrid[22] parabolic equation, given below.

$$\sigma = \sigma_o \left[2 \left(\frac{\varepsilon}{\varepsilon_o}\right) - \left(\frac{\varepsilon}{\varepsilon_o}\right)^2\right] \qquad 3.2$$

where ε_o is the strain at the maximum specified stress σ_o. The same equation has been used by Brown[23] in his book and Wong[16] in his analysis.

Fig. 3.2 shows the stress-strain curve obtained from the above equation.

3.2.2 In order to use the composite beam theory of Newmark the materials, concrete and steel should be linearly elastic. Hence, in order to use this theory the stress-strain behavior of concrete should be linear. Although Yam and Chapman[24] have developed a solution for a composite beam having an inelastic continuous shear connection as well as non-linear characteristic of steel and concrete, this, however, cannot be used for non-prismatic sections such as the reinforced concrete beam has after cracking and also the method is quite tedious and time consuming. Therefore, the question arises of approximating the area under the stress-strain curve of Fig. 3.2 into some linear distribution .

3.2.3 There are many ways to approximate the area under the curve. One approach (method I) is to take the value of the modulus of elasticity of concrete, E_c, equal to

EQUATION OF THE CURVE

$$\frac{\sigma}{\sigma_0} = 2\left(\frac{\epsilon}{\epsilon_0}\right) - \left(\frac{\epsilon}{\epsilon_0}\right)^2$$

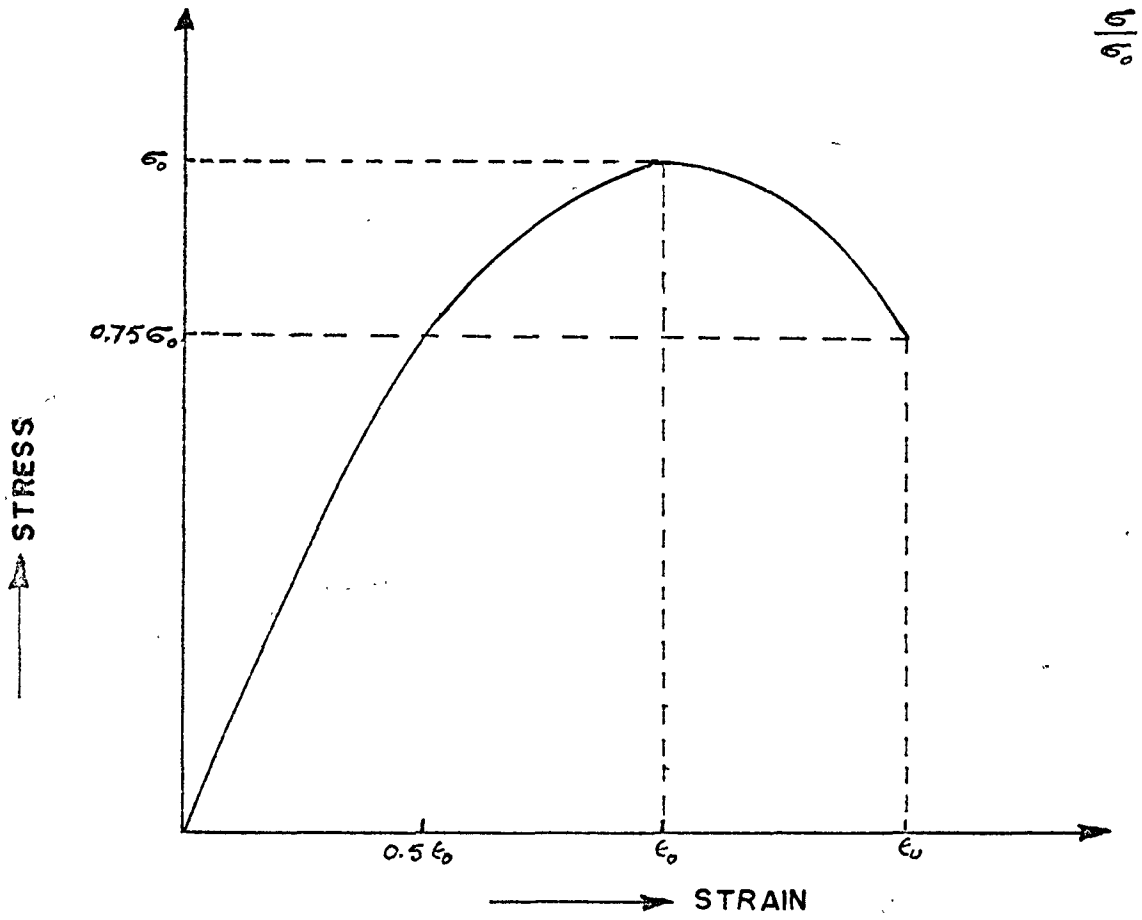

STRESS STRAIN CURVE OF CONCRETE

FIG. 3.2

the initial slope of the parabolic curve (Fig. 3.2), by differentiating equation 3.2:

$$E_c = 2 \frac{\sigma_o}{\varepsilon_o} \quad . \qquad 3.3$$

Then determine the stress and strain which give the same area under a linear stress-strain curve as that under the parabolic curve of equation 3.2. This approximation is shown in Fig. 3.3 by a triangle (method I). Here the strain of 1550 micro in/in, for σ_o = 3800 psi, ε_o = 2000 micro in/in and ε_u = 3000 micro in/in, in the linear case is approximated by a strain of 3000 micro in/in in the non-linear case, when $E_c = 3.8 \times 10^6$ psi.

This means, in this method, that when the strain at the top fibre of concrete, ε_{ct}, reaches 1550 micro in/in then the curvature of the concrete, ϕ_c, must be increased to almost double, in order to have the strain at failure 3000 micro in/in; to satisfy the conditions of equilibrium; to keep the crack height constant and to maintain the bottom fibre strain of the uncracked concrete, ε_{cb}, at the cracking strain, ε_{cr}. Here the conditions of equilibrium can be satisfied but the conditions of compatibility required by the composite theory, i.e. that the curvature of the concrete, ϕ_c, be equal to the curvature of the steel, ϕ_s, can no longer be satisfied.

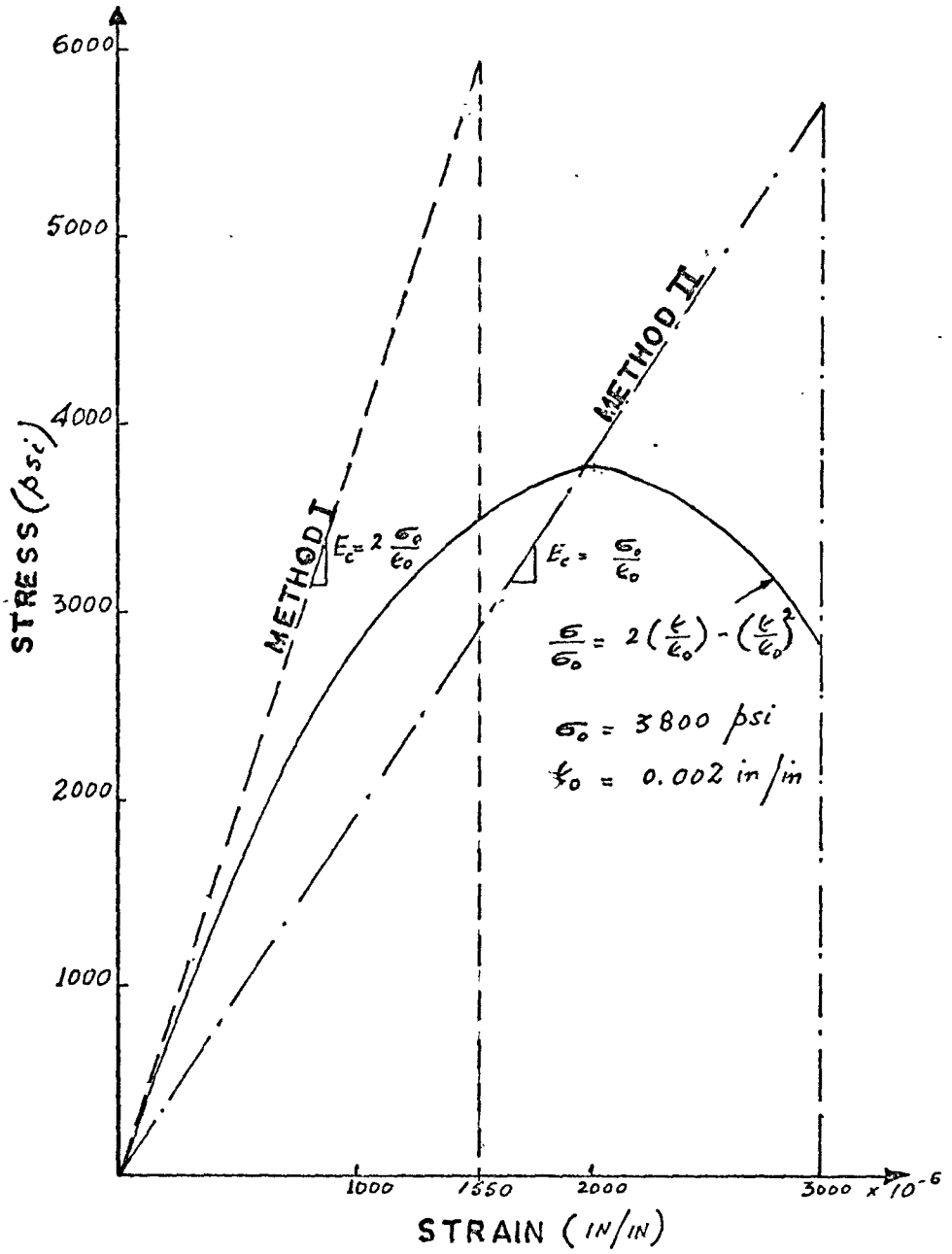

APPROXIMATION OF STRESS-STRAIN CURVE INTO LINEAR DISTRIBUTION

FIG. 3.3

3.2.4 Another approach (method II) is to keep the ultimate strain, ε_u, constant and reduce the value of modulus of elasticity of concrete, E_c, so that the area under the linear curve is equal to the area under the parabolic curve. It is found, by doing this, that for this parabolic stress-strain relationship, the value of $E_c = \frac{\sigma_o}{\varepsilon_o}$, is exactly half that proposed by Brown[23]. This equivalent linear stress-strain curve is shown in Fig. 3.3. (method II). In this method the conditions of compatibility as well as equilibrium conditions can be satisfied. Therefore, it is thought that method II is better and hence this is used in this analysis.

3.3 Stability of the Flexural Crack

Tensile cracks are frequently formed in reinforced concrete beams well below the service loads. Usually they are harmless and stabilise due to presence of reinforcing steel and the member possesses additional load capacity.

Krahl[10] et al. in their paper "Stability of Tensile Cracks in Concrete Beams", mentioned that the crack stability is of obvious importance in relation to the load carrying capacity of a concrete member. Oladapo[25] studied the stability of cracks in prestressed concrete beams, and MacGregor and Walters[11] analysis was based on crack stability.

A typical reinforced concrete beam cross-section considered herein is shown in Fig. 3.4. It has a breadth b = 6 in, total depth D = 12 in. and effective depth d=10.7 in.

The reinforced concrete beam has two symmetrical point loads situated a distance 'a' from each support, the distance between the point loads is 36 in. and the length of the beam, L = (2a+36) in. This beam is called a 'Typical Beam' throughout this analysis. This 'Typical Beam' is one of a type tested by Kani[19] in his experiments at the University of Toronto.

It can be shown by the composite beam theory[14,16,18] and confirmed by experimental observations[9] that the maximum height of a flexural crack occurs under the load points. Therefore, the stability and development of a flexural crack is considered at a cross-section under the point loads. As the crack starts to propogate into the beam, the depth of the uncracked cross-section of the beam at that particular section reduces and hence the moment carried by uncracked concrete, M_c, the interaction coefficient, $\frac{1}{C}$, and the horizontal force, F, are bound to be affected.

All these variables have been computed by the two methods discussed in the preceeding paragraphs and are plotted in Figures 3.4 and 3.5.

Figure 3.4 shows the variation of M_c, F, $\frac{1}{C}$ and ε_{cb} under the load point, as a tensile crack starts at the bottom fibre of concrete, penetrates vertically into the beam and stabilizes after reaching a certain depth, for $E_c = 1.9\times10^6$ psi (method II) and bond-slip modulus, K = 17000 lb/in. It

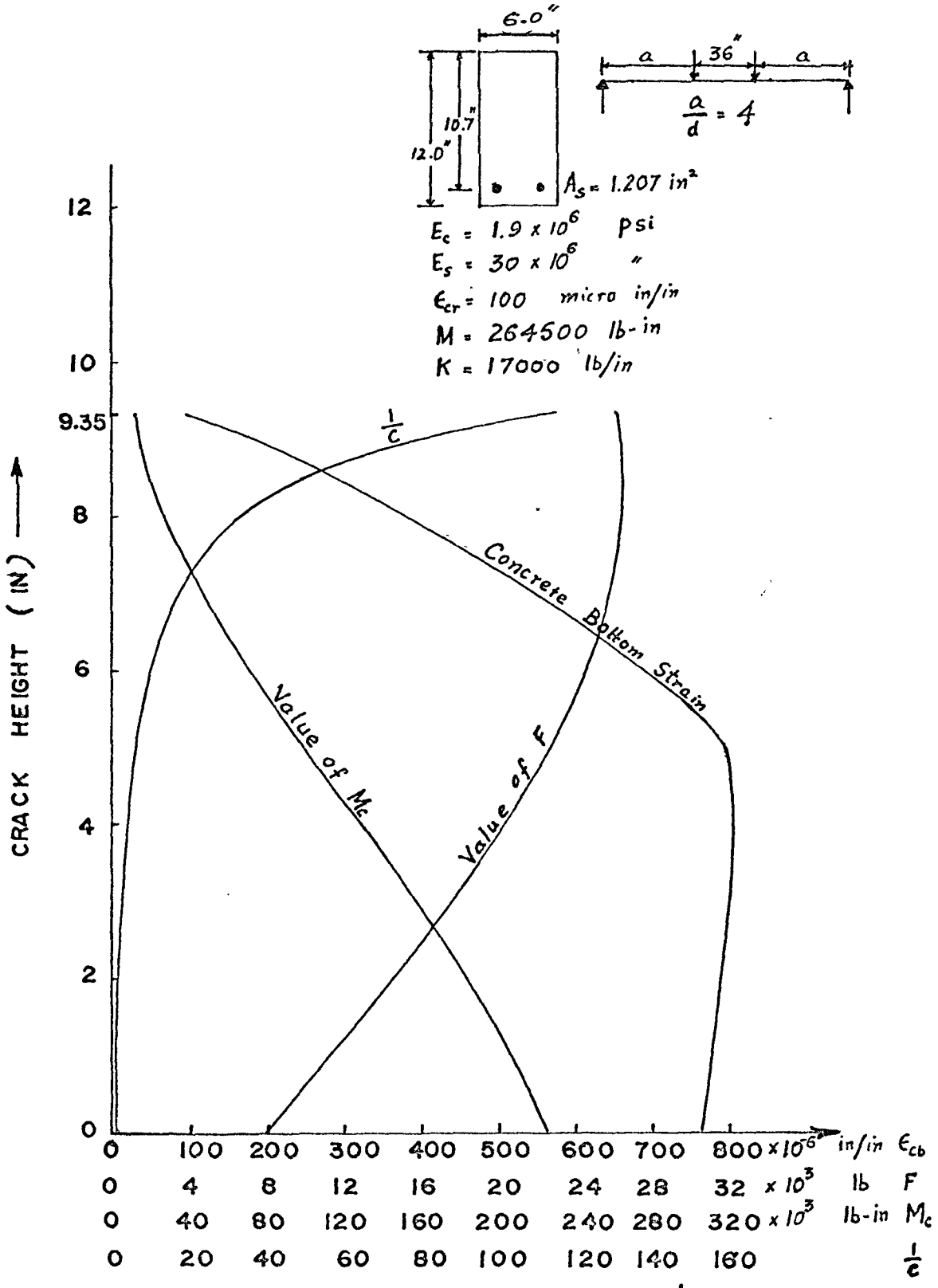

VARIATION OF ϵ_{cb}, M_c, F AND $\frac{1}{C}$

AS CRACK DEVELOPS

FIG. 3.4

can be noted that the crack height is 9.35 in.

Figure 3.5 shows the variation of M_c, F, $\frac{1}{C}$ and ε_{cb} for $E_c = 3.8\times10^6$ psi (method I) and it has been found that in order to get the same crack height, 9.35 in., as obtained for lower value of E_c, the magnitude of bond-slip modulus, K, has to be increased up to 36000 lb/in., otherwise the crack height will be 10.42 in. for K = 17000 lb/in (not shown in the figure). Figure 3.5 also shows the variation of M_c, F, $\frac{1}{C}$, and ε_{cb} for $E_c = 1.9\times10^6$ psi K = 36000 lb/in. (method II). It is to be noted that the crack height is lower for $E_c = 1.9\times10^6$ psi than for $E_c = 3.8\times10^6$ psi and it is 8.38 in.

A conclusion can be made that by keeping the bond-slip modulus, K, constant and changing the modulus of elasticity of concrete, the crack height at a particular section also changes. It has been found that the lower the magnitude of E_c the lower the crack height and vice versa, as shown in Fig. 3.5 for K = 36000 psi and $E_c = 3.8\times10^6$ psi and 1.9×10^6 psi. The difference in crack heights obtained for this particular case is 1.07 in. at a section under the point loads.

Also the magnitude of bond-slip modulus has significant influence on the flexural crack heights. This can be observed by comparing Fig. 3.4 and 3.5. For a constant value of $E_c = 1.9\times10^6$ psi the crack height is greater for K = 17000 lb/in as compared to K = 36000 lb/in. Hence, the

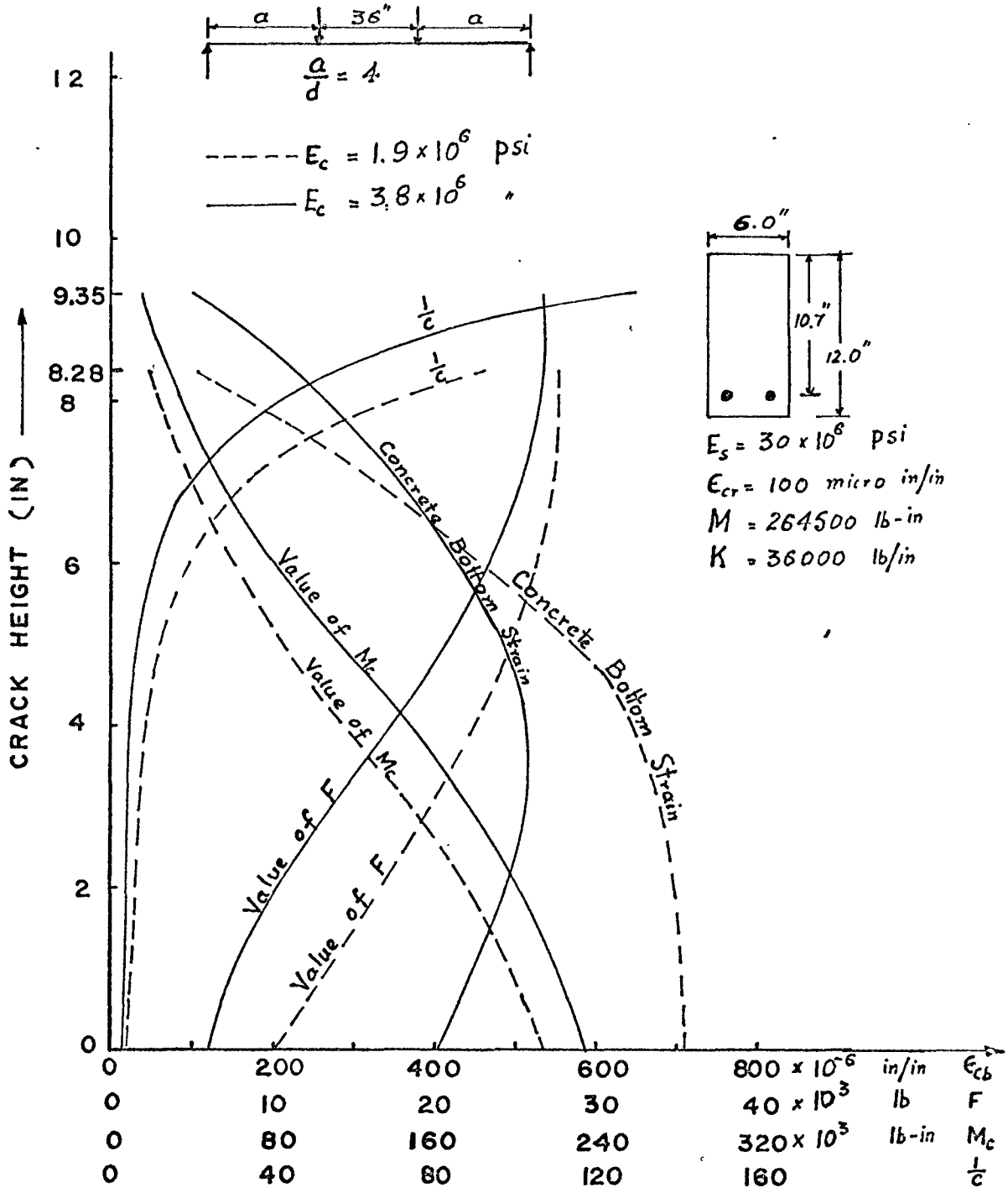

VARIATION OF ϵ_{cb}, M_c, F AND $\frac{1}{C}$
AS CRACK DEVELOPS
FIGURE ALSO SHOWS EFFECT OF E_c

FIG. 3.5

greater the values of K or in other words the greater the interaction between steel and concrete, the smaller will be the crack height.

CHAPTER IV

MOMENT CARRYING CAPACITY

4.1 Kani[19] suggested that for a reinforced concrete beam without web reinforcement the ultimate moment capacity, M_u, depends upon the $\frac{a}{d}$ ratio and the minimum is about 50 percent at $\frac{a}{d} = 2.5$ for the 'Typical Beam' of chapter III.

Morrow and Viest [9][26] and Leonhardt and Walther[9][27] also observed the same behavior. Figures 4.1 and 4.2 show the relative beam strength and ultimate moment carrying capacities, M_u, versus shear-span to depth ratio , $\frac{a}{d}$, as obtained experimentally by Kani, Morrow and Viest and Leonhardt and Walther, respectively.

It has been observed experimentally[9] and has been shown analytically[14,16,18] that the maximum flexural crack height occurs under the load points. The computed flexural crack profile of a reinforced concrete beam is shown in Fig. 2.7. Fig. 4.3 shows typical flexural cracking in a beam loaded with a two-point load system.

As the shear-span to depth ratio, $\frac{a}{d}$, of a reinforced concrete beam varies, the maximum computed flexural crack height under the load point also varies[16], even though the applied moment is constant, being higher as the shear-span is reduced.

DUE TO KANI

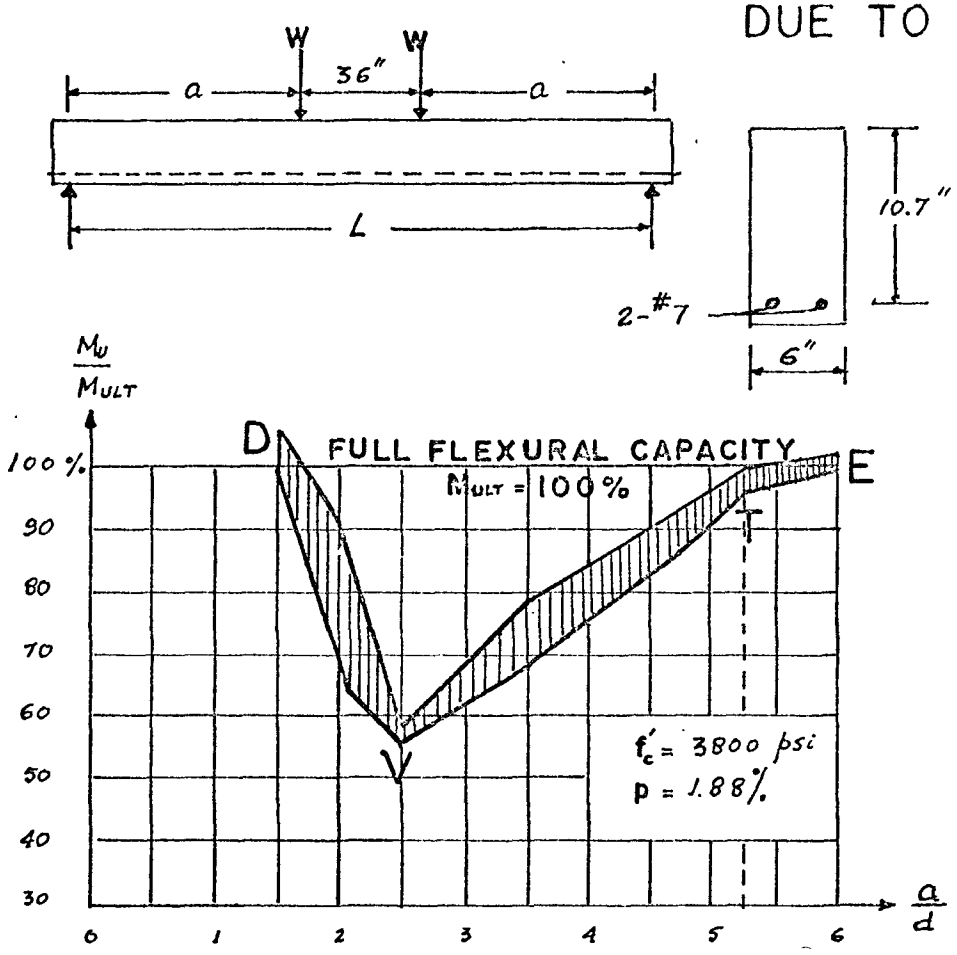

RELATIVE BEAM STRENGTH

$\frac{M_u}{M_{ULT}}$ VERSUS $\frac{a}{d}$

FIG. 4.1

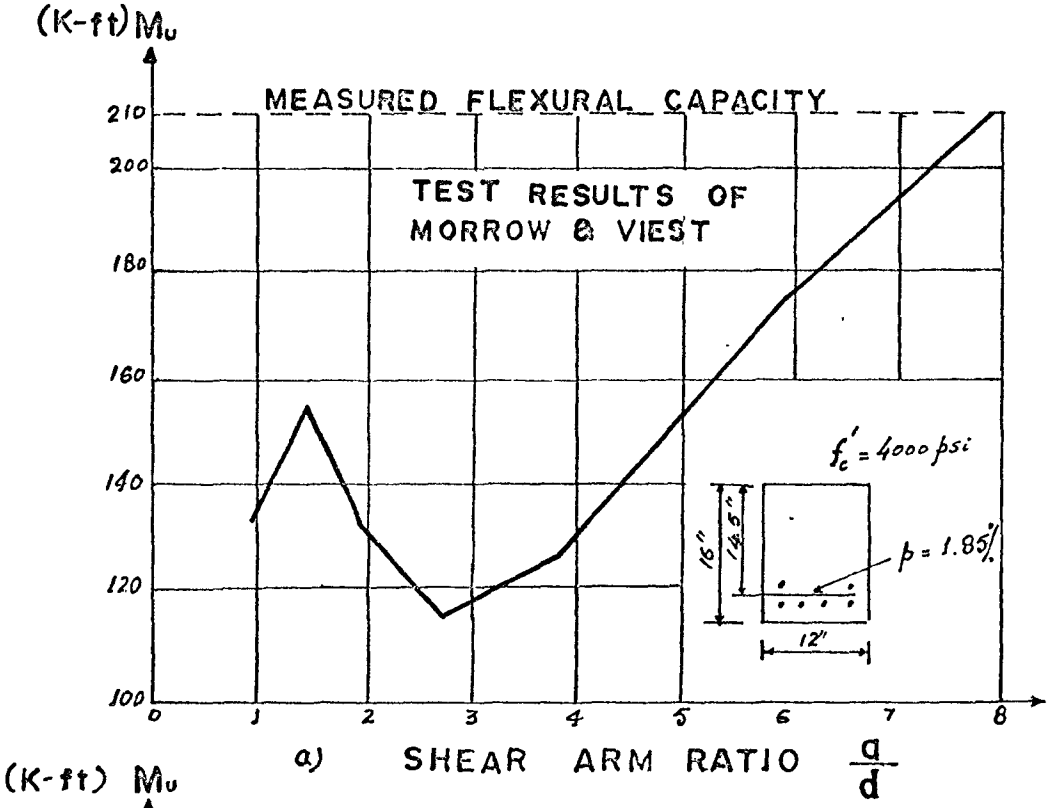
(K-ft) M_u
MEASURED FLEXURAL CAPACITY
TEST RESULTS OF MORROW & VIEST
f'_c = 4000 psi
16"
14.5"
p = 1.85%
12"
210
200
180
160
140
120
100
0
1
2
3
4
5
6
7
8
a) SHEAR ARM RATIO $\frac{a}{d}$

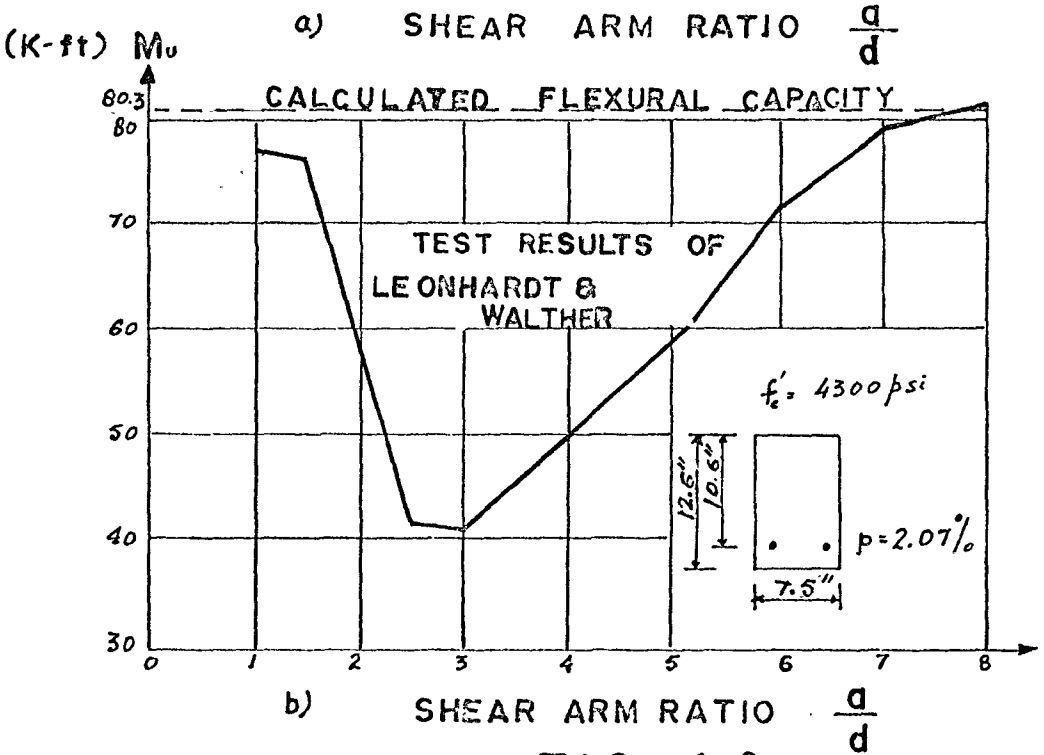
(K-ft) M_u
80.3
CALCULATED FLEXURAL CAPACITY
TEST RESULTS OF LEONHARDT & WALTHER
f'_c = 4300 psi
12.6"
10.6"
p = 2.07%
7.5"
80
70
60
50
40
30
0
1
2
3
4
5
6
7
8
b) SHEAR ARM RATIO $\frac{a}{d}$

FIG. 4.2

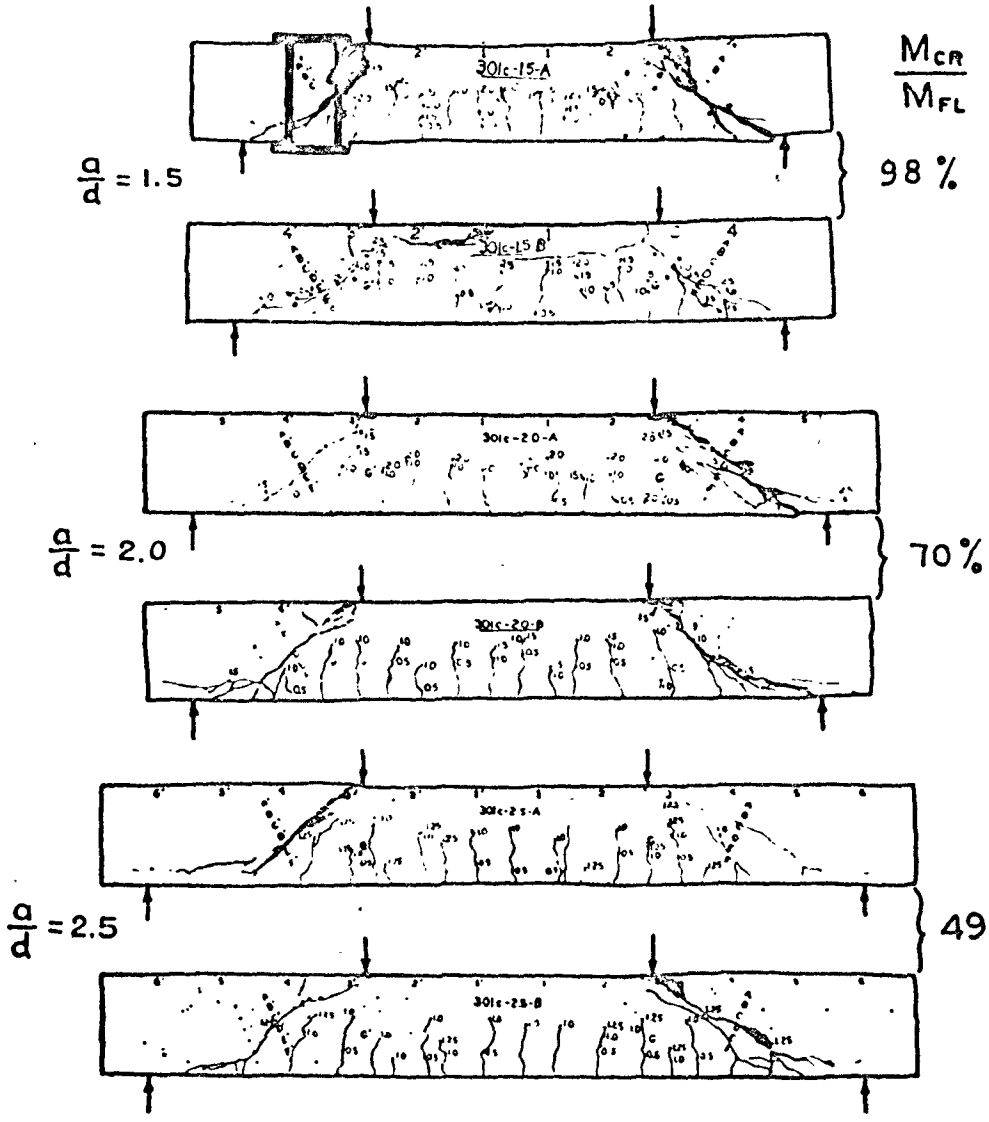

-Beams of Toronto Test Series C DUE TO KANI

FIG. 4.3

4.2 Fig. 4.4 shows the influence lines for the concrete top strain, ε_{ct}, and the average or mid-height steel strain, ε_{sm}, at a section under the load point versus the shear-span to depth ratio, $\frac{a}{d}$, for a constant bending moment 264500 lb-in (half of the moment as obtained by ACI Code formula). It may be noted that the concrete strains have much larger values for smaller $\frac{a}{d}$ ratios, while on the other hand the steel strain has larger magnitude at greater $\frac{a}{d}$ ratios.

It is interesting to note that by limiting the magnitude of strains, ε_{ct} and ε_{sm} to some constant values, the flexural capacity of the beam can be governed either by concrete strain or steel strain or both. For the purpose of demonstration assume that the maximum compressive strain of concrete, $\varepsilon_{ct_{max}}$ = 1500 micro in/in (half the crushing strain of concrete) and maximum strain that the steel can take, $\varepsilon_{sm_{max}}$ = 750 micro in/in (half the yield strain of steel), for the 'Typical Beam' having p = 1.88%, then it can be observed that for $\frac{a}{d}$ less than 5.3 the concrete strain, ε_{ct} is more than $\varepsilon_{ct_{max}}$ and for $\frac{a}{d}$ higher than this the steel strain, ε_{sm}, is more than $\varepsilon_{sm_{max}}$. Hence, between $\frac{a}{d}$ = 0.5 to $\frac{a}{d}$ = 5.3, the concrete governs the strength of the beam and for $\frac{a}{d}$ more than 5.3, the steel governs the strength. It will be shown that, in addition, the governing factor also depends upon the percentage of steel, p, shape of cross-

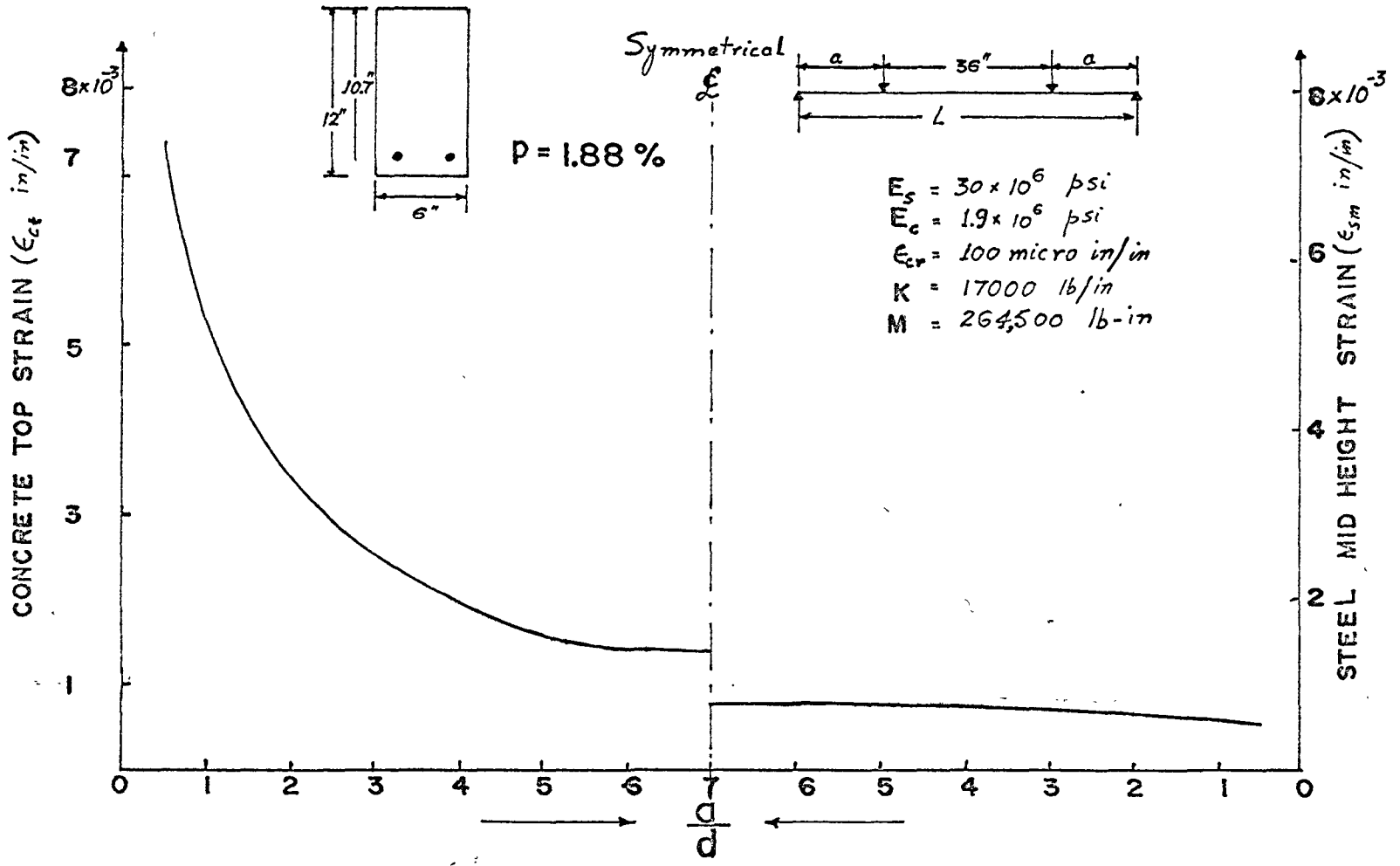

EFFECT OF SHER ARM RATIO ON CONCRETE TOP AND STEEL MID HEIGHT STRAIN

FIG. 4.4

section, strength of concrete, strength of steel etc.

4.3 Thus the moment capacity of a section under the load point can be determined analytically for certain values of $\varepsilon_{ct_{max}}$ and $\varepsilon_{sm_{max}}$, and this will be the maximum moment carried at that particular section.

In computing the influence lines for maximum moment, M_u, under the load point, the dimensions of the 'Typical Beam' of chapter III are considered. The same beam dimensions have been used by Kani [19] in his experiments. Hence, by doing this the validity of the theory can be established. It is assumed that the maximum compressive strain of concrete is 3000 micro in/in and steel yield strain is 1500 micro in/in.

4.4 In Kani's experimental beam series the distance between the point loads was kept constant and to achieve the different a/d values the length of the beam was changed. The geometry of the beam, span, cross-section , etc. has a significant influence on the interaction coefficient.

$$\frac{1}{C} = \frac{K}{s} \frac{\overline{EI}}{\overline{EA}\ \Sigma EI} \frac{L^2}{\pi^2} \qquad 4.1$$

where K = bond-slip modulus

L = length of the beam.

This means that if K along with all other parameters, except L, is kept constant, then $\frac{1}{C}$ is directly proportional to the square of length, L. It should be noted, however, that $\frac{1}{C}$ does not remain constant in a cracked beam, as can be observed in Figs. 3.4 and 3.5, because the geometry of the cross-section changes where cracking occurs. Therefore,in this analysis instead of taking an initial value of $\frac{1}{C}$, the bond-slip modulus, K, has been assumed to be constant. By doing this the interaction coefficient, $\frac{1}{C}$, changes with different a/d ratios, even for an uncracked beam. Hence, 1/C is small for short span beams and it has a higher value for greater spans.

Therefore,an important conclusion can be made that the span length, L, is one of the significant parameters in the behavior of reinforced concrete beams.

4.5.1 The moment carrying capacity has been computed under the load point for the 'Typical Beam' with various values of a/d. These computed values of M_u versus a/d are shown in Fig. 4.5 for bond-slip modulus, K = 17000 lb/in. The dotted line in the same figure is the ultimate flexural capacity, M_{ult}, value for beams with the cross-section of the 'Typical Beam', computed by the ACI Code formula:

$$M_{ult} = A_s f_y (d - a'/2) \qquad 4.2$$

where

$$a' = \frac{A_s f_y}{0.85 \cdot f'_c \cdot b}$$

$$f_y = E_s \cdot \varepsilon_{sm_{max}}$$

$$f'_c = E_c \cdot \varepsilon_{ct_{max}} \quad .$$

4.5.2 Fig. 4.5 shows that the influence line for moment carrying capacity, M_u, has two distinct portions, one slopes downward and the other one is almost horizontal. Concrete governs the strength of the beam in the sloping part, and in the horizontal region steel reaches the yield strain first and hence governs the strength of the beam. The concrete and steel both reach their ultimate strains at the transition point, T, where both the curves intersect each other.

4.5.3 The variation in the computed capacities of the beam ranges from 22 percent for a/d = 0.5 to 100 percent of the M_{ult} at a/d = 5.3, in the region where the concrete strain governs the strength of the beam. The strength is almost uniform and varies only between 100 percent to 98.5 percent of the M_{ult} in the region where the steel strain governs.

4.5.4 If the results of Fig. 4.5 are compared to that of Fig. 4.1 (Kani's experimental results) it may be seen that there is a very close agreement qualitatively as well as quantitatively for $a/d \geq 2.5$. Thus analysis of the reinforced

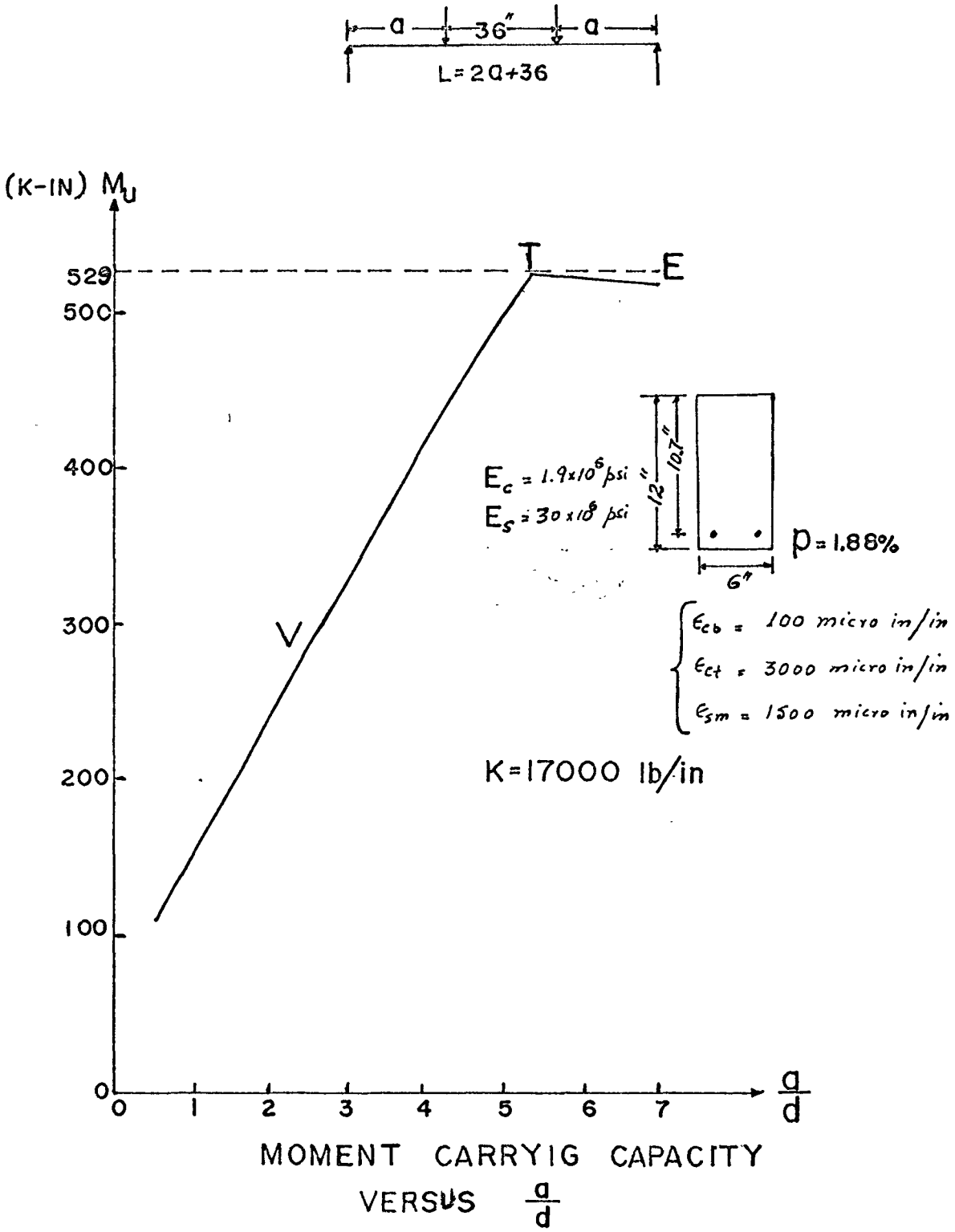
a
36"
a
L=2a+36
(K-IN) M_u
529
500
400
300
200
100
0
T
E
V
$E_c = 1.9 \times 10^6$ psi
$E_s = 30 \times 10^6$ psi
12"
10.2"
6"
p = 1.88%
ϵ_{cb} = 100 micro in/in
ϵ_{ct} = 3000 micro in/in
ϵ_{sm} = 1500 micro in/in
K=17000 lb/in
0 1 2 3 4 5 6 7
a/d
MOMENT CARRYIG CAPACITY
VERSUS a/d

FIG. 4.5

concrete beam in accordance with the composite beam theory enables the moment carrying capacities, M_u, to be computed for concrete beam without shear reinforcement, for various values of shear-span to depth ratios. The validity of the theory has been checked against Kani's experimental results.

It was found that, in order to bring the computed results closer to the Kani's experimental values, a particular magnitude of bond-slip modulus, K, was required, and in general the flexural capacity, M_u, is largely dependent upon K. This is discussed in more detail in the following paragraphs.

4.6.1 As discussed earlier the interaction coefficient, $\frac{1}{C}$ has a remarkably significant influence on the reinforced concrete beam; reflecting the influence of bond-slip modulus, K. This is shown in Fig. 4.6 for the 'Typical Beam' with p = 1.88 percent. Five different values of K were selected, namely, K = 10,000, 15,000, 17,000, 20,000 and 30,000 lb/in. It is interesting to note that the reduction in K has two effects on the influence line for flexural capacity; first, decrease in the magnitude of K causes the transition point, T, to be displaced towards the right and for smaller value of K such as 10,000 lb/in the transition almost vanishes, indicating that the carrying capacity cannot reach the maximum possible flexural capacity. The

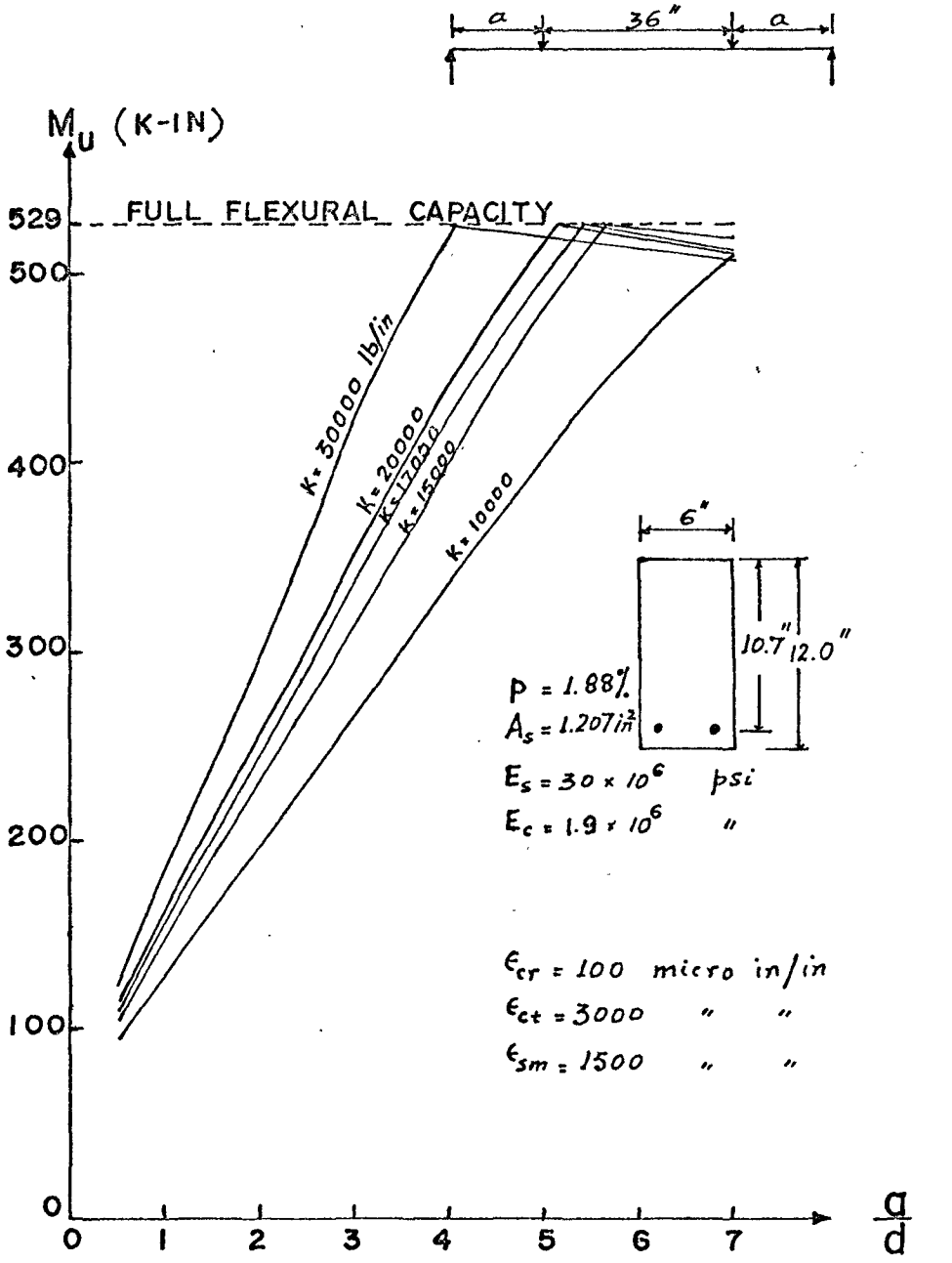

EFFECT OF BOND-SLIP MODULUS ON MOMENT CARRYING CAPACITY

FIG. 4.6

second effect is that the higher values of K increase the flexural capacity in the region governed by the concrete strain and decrease the capacity in the region governed by the steel strain. This means a decrease in the magnitude of K increases the strength of the beam where steel is the governing factor and decreases the strength where concrete is the governing factor and vice-versa.

4.6.2 Now the question arises that what is the exact magnitude of bond-slip modulus, K, for a particular reinforced concrete beam and what should be the criterion for selecting a particular value of K for any beam? In fact K depends upon a number of parameters, such as strength of concrete and steel; percentage of steel; shape and dimensions of cross-section; number, placing and diameter of longitudinal bars, etc. Unfortunately, the importance of bond-slip modulus has not been considered by research workers. Hence, further research in this field is required.

Therefore, the criterion for selecting the bond-slip modulus, K, is that the value which gives closest agreement with Kani's experimental results, is considered to be the magnitude of K. Close examination of Fig. 4.6 clearly reveals that the magnitude of K = 17000 lb/in for p = 1.88 percent gives almost the same results as obtained by Kani.

For the various values of percentage of steel, p, in the beam tested by Kani, in order to find the effect of p, on the relative beam strength, this analysis reveals that there must be different magnitudes of K for each series having different steel percentages. It may be noted that K increases for higher values of p and decreases for smaller percentages of steel. This is shown in Fig. 4.7.

4.7 Comparison with Kani's Results

4.7.1 Kani has done an extensive experimental[8,9,19] investigation in the field of shear and diagonal tension. He performed large numbers of tests[19] on the same 'Typical Beam' to find the influence of concrete strength, f'_c, percentage of steel, p, and shear-span to depth ratio, a/d, on the strength of reinforced concrete beams. Figs. 4.1 and 4.8 show the $\frac{M_{test}}{M_{ult}}$ versus a/d ratio for p = 2.80, 1.88, 0.8 and 0.5 percent and f'_c = 5000, 3800 and 2500 psi. Kani's experimental and the computed results of this analysis are compared in Fig. 4.9 for f'_c = 3800 psi and p = 1.88. It is found that there is a significantly close agreement between the experimental and computed results for a/d ratios more than 2.5. Kani observed an increase in the ultimate flexural capacity for a/d < 2.5. Agreement with the experimental results has not been achieved over that range using the composite beam theory because of different phenomenon governing

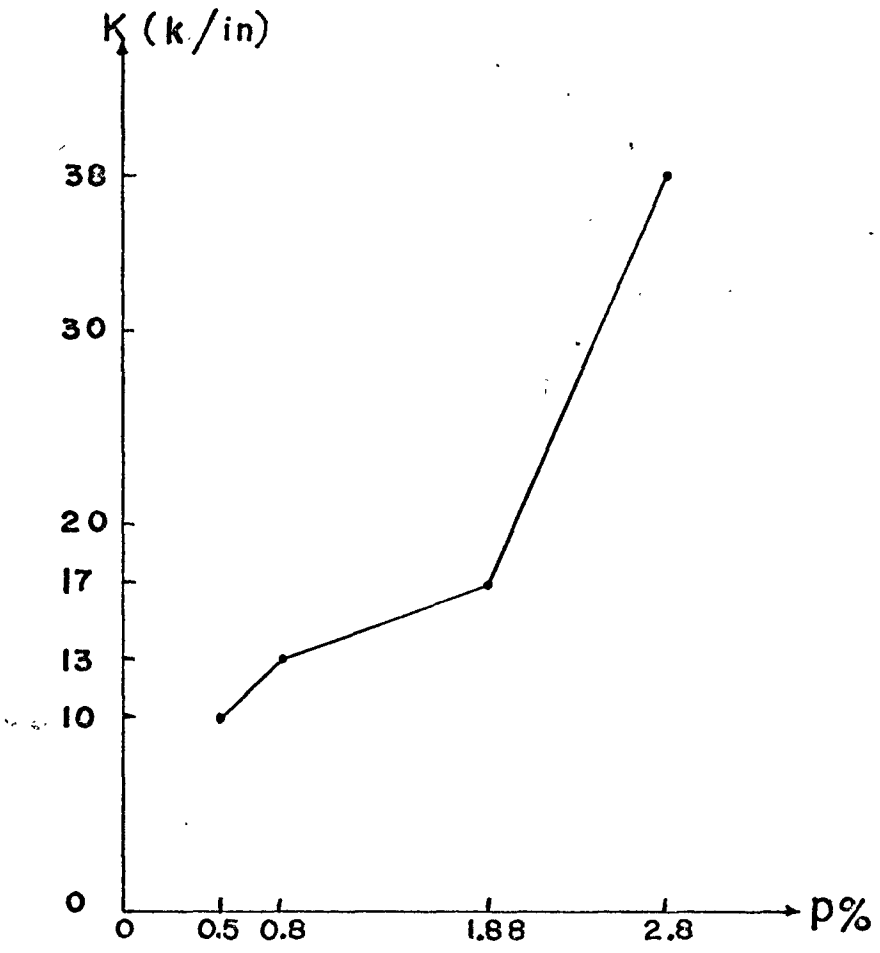

PERCENTAGE OF STEEL
VERSUS BOND-SLIP MODULUS

FIG. 4.7

DUE TO KANI

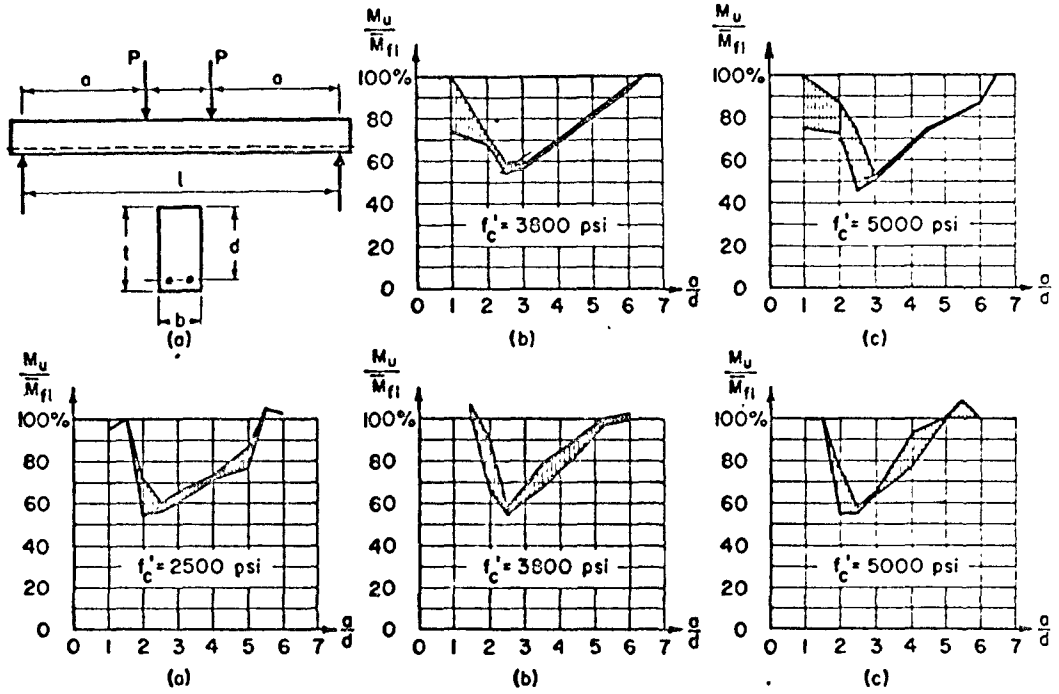

Fig. 5 (top) — Influence of the basic parameters, f_c' and a/d, on the relative beam strength for $p = 2.80$ percent

Fig. 6 (bottom) — Influence of the basic parameters, f_c' and a/d, on the relative beam strength for $p = 1.88$ percent

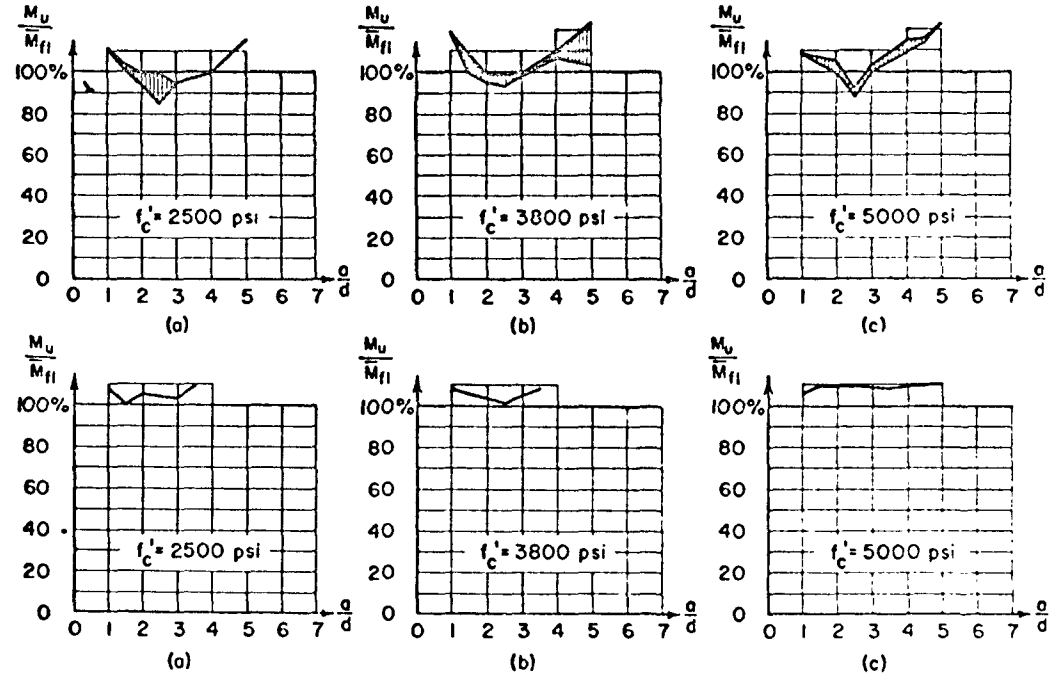

Fig. 7 (top) — Influence of the basic parameters, f_c' and a/d, on the relative beam strength for p 0.80 percent

Fig. 8 (bottom) — Influence of the beam strength, f_c' and a/d, on the relative beam strength for p 0.50 percent

FIG. 4.8

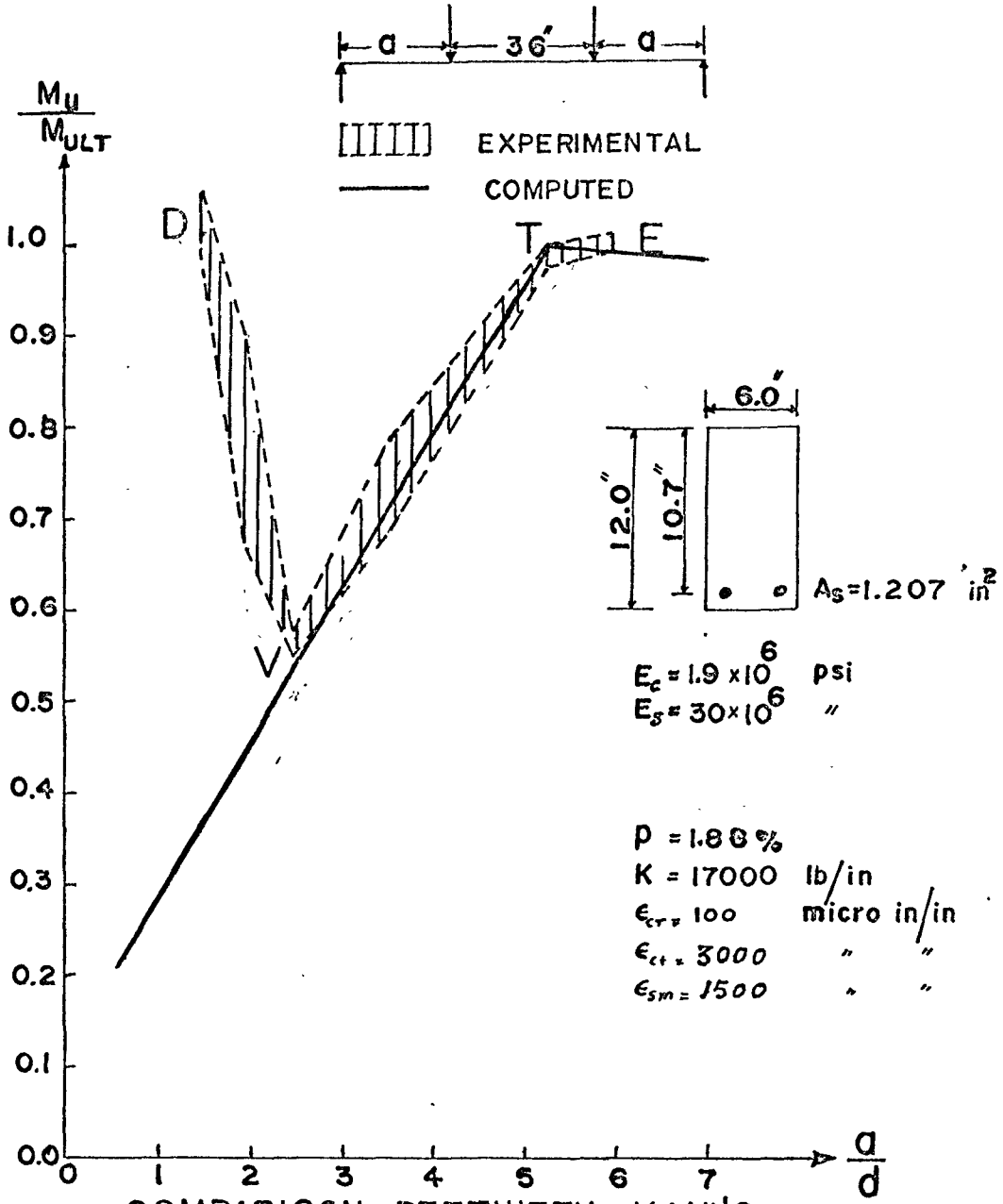

COMPARISON BEETWEEN KANI'S EXPERIMENTAL AND AUTHOR'S THEORETICAL RESULTS FOR p = 1.88%

FIG. 4.9

the strength of the beam. This aspect is discussed in detail elsewhere in this chapter.

4.7.2 Kani[9] states that as the load on the beam increases the reinforced concrete beam transforms into a 'comb-like' structure. The compressive zone of the beam is the backbone of the 'concrete-comb' and in the tensile zone there are more or less vertical cracks, which form the 'concrete-teeth'. The applied load is resisted by the transfer of stresses between concrete and steel through the bond between the materials. After the resistance of the concrete teeth has disappeared, the longitudinal profile of the concrete beam resembles a 'tied-arch'. This transformation of the reinforced concrete beam may occur suddenly or develop gradually.

Kani[9] also stated that for beams having a/d ratios less than 2.5, the capacity of the concrete teeth is lower than that of the concrete arch, therefore, under increasing loads, the transformation from beam action to tied arch occurs gradually and the failure occurs when the capacity of the arch is exceeded.

For beams having a/d ratios between 2.5 and the transition point, T, the capacity of the concrete-teeth is more than the capacity of the arch, however failure does not occur until the concrete teeth capacity is exceeded and at

this stage transformation begins. In this case a sudden collapse follows, because the concrete arch capacity is lower than the applied moment. Beyond the transition point, T, only normal flexural failure is possible.

Hence, in Fig. 4.1, according to Kani[9], the portion DV represents the capacity of the remaining arch. In the region VTE the relative beam strength is governed by the capacity of the concrete teeth. Point V is the intersection of the remaining arch capacity line to the concrete teeth capacity line and this point shows the minimum relative beam strength. After the transition point, T, only normal flexural failure is possible.

4.7.2 It has been observed that the computed moment carrying capacity, M_u, under the load point versus a/d ratio is influenced by certain parameters in the same way as found experimentally by Kani. But as discussed above the computed results do not show any rise in carrying capacity for smaller values of a/d.

Figs. 4.10a and 4.10b show the influence of percentage of steel, p, on the relative beam strength versus a/d ratio computed by the composite theory. Kani[19] found similar relative beam strengths for various values of percentage of steel, p. In order to compare the results the same

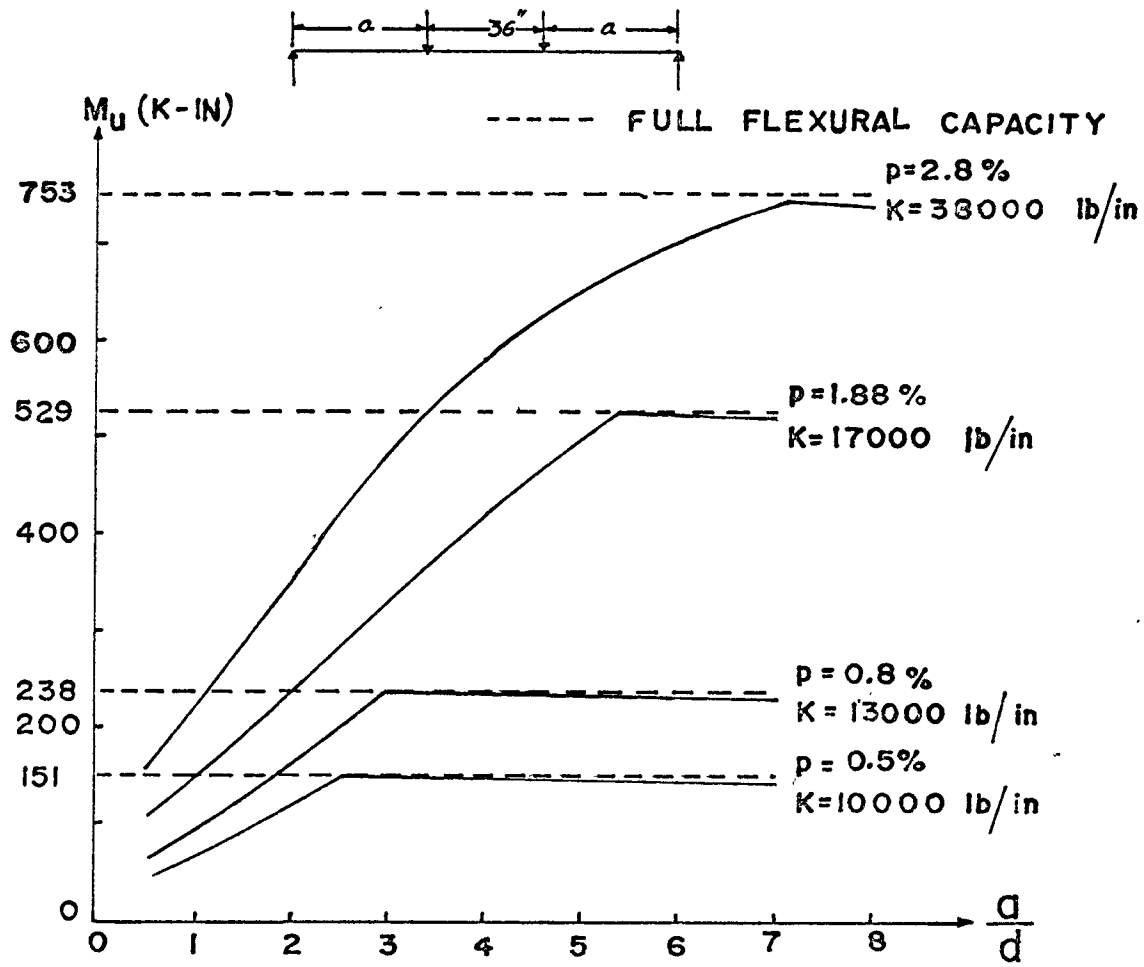

EFFECT OF PERCENTAGE OF STEEL ON MOMENT CARRYING CAPACITY

FIG. 4.10a

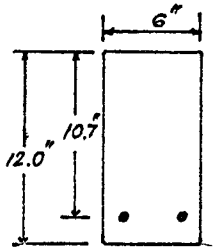

$E_c = 1.9 \times 10^6$ psi
$E_s = 30 \times 10^6$ "
$\epsilon_{cr} = 100$ micro in/in
$\epsilon_{ct} = 3000$ " "
$\epsilon_{sm} = 1500$ " "

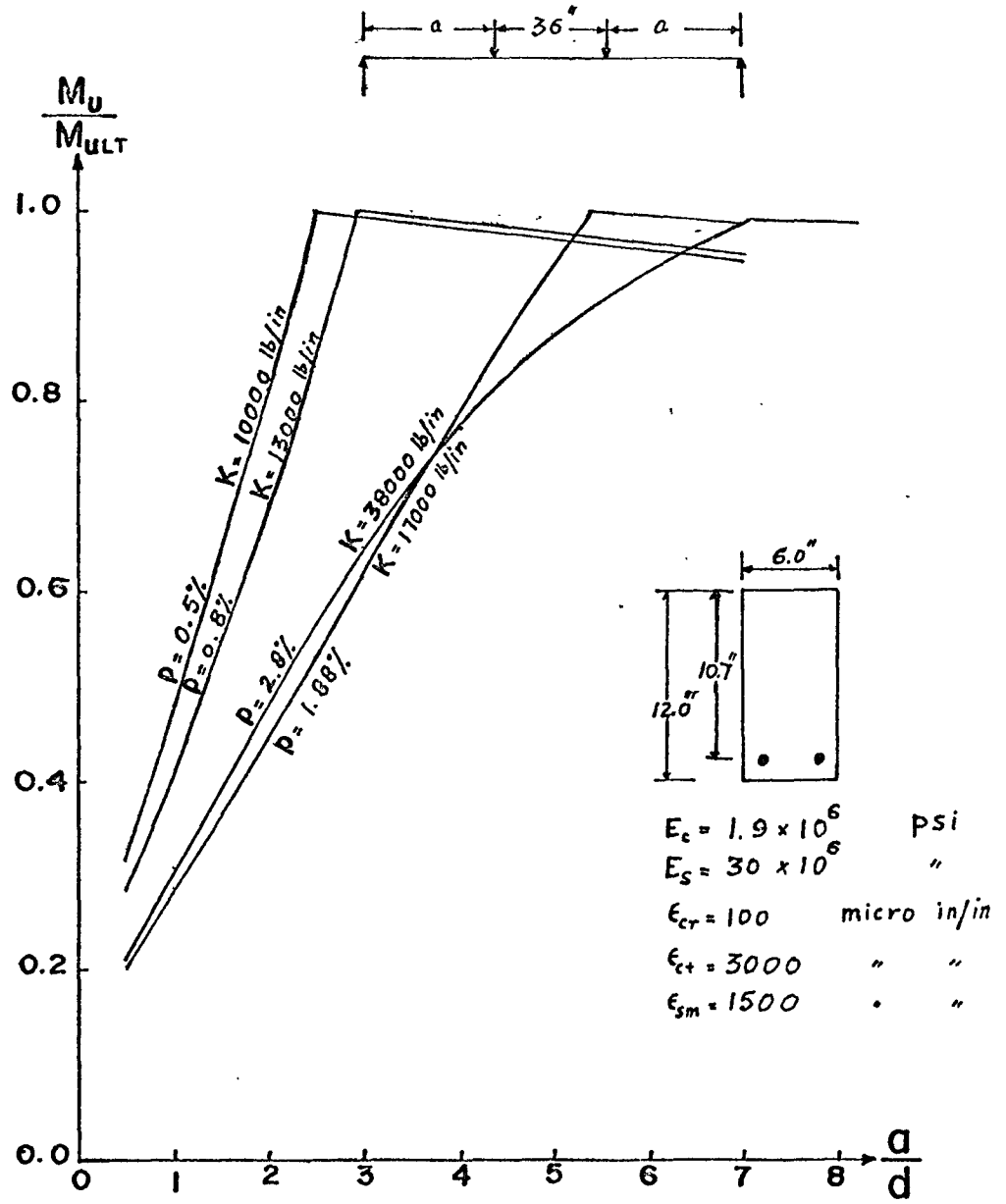

RELATIVE BEAM STRENGTH
EFFECT OF
PERCENTAGE OF STEEL

FIG. 4.10b

percentages of steel, p = 0.5, 0.8, 1.88 and 2.80 are used.

It is interesting to note that p has two effects on the moment carrying capacity; the ultimate flexural capacity is greater for higher values of p and also the transition point, T, moves towards right, Fig. 4.10a. Increase in the flexural capacity with increase in p has also been demonstrated analytically by MacGregor and Walters[11]. Kani[19] states that the amount of longitudinal reinforcement has a significant influence on the location of transition point. If the amount of reinforcement varies from 2.80, 1.88 to 0.80 percent then the transition points, obtained from the test results, are at a/d = 6.5, 5.5 and 3.5 respectively. For smaller percentage of steel such as 0.50, the valley of diagonal tension disappeared completely. This is evident from Fig. 4.8.

In order to compare the results for different percentages of steel, consider for example when p = 0.50 percent, the $\frac{M_u}{M_{ult}}$ computed by this analysis is 100 percent (Fig. 4.10b) at a/d = 2.5 and the experimental findings of Kani also give 100 percent. At p = 0.80 percent, the computed value of $\frac{M_u}{M_{ult}}$ is 84 percent at a/d = 2.5 (Fig. 4.10b), the same percentage of $\frac{M_u}{M_{ult}}$ is obtained by Kani for this amount of reinforcement.

For p = 1.88 percent and 2.80 percent the computed results and Kani's experimental results are shown in Figs.

4.9 and 4.11.

Fig. 4.9 shows the agreement of the theory with the test results[19] for p = 1.88 percent. The transition point, T, is found to be at a/d = 5.4 whereas Kani's tests indicate the transition point at a/d = 5.6. Kani[19] stated that the results showed a scatter. The minimum relative beam strength at a/d = 2.5 (point V in the diagram) is 57 percent as obtained by Kani and the computed results give 54 percent.

Similarly, if the results for p = 2.80% are compared, the transition point, T, occurs at a/d = 7.1 while Kani's tests gave the transition at a/d = 6.6. Fig. 4.11 shows the comparison. The minimum relative beam strength at a/d = 2.5, according to Kani is 58% whereas the computed one is 57%. However, there is a slight difference in the magnitudes of carrying capacity between V and T varying from 1 to 8%. This is because the test results showed almost the same capacity at a/d = 3 as for a/d = 2.5, but, according to theory the carrying capacity will increase for increasing ratios of a/d up to transition point T.

4.8 Discussion

4.8.1 In this chapter the experimental results of Kani, Morrow and Viest, and Leonhardt and Walther are presented. They show qualitative agreement amongst them for the variation

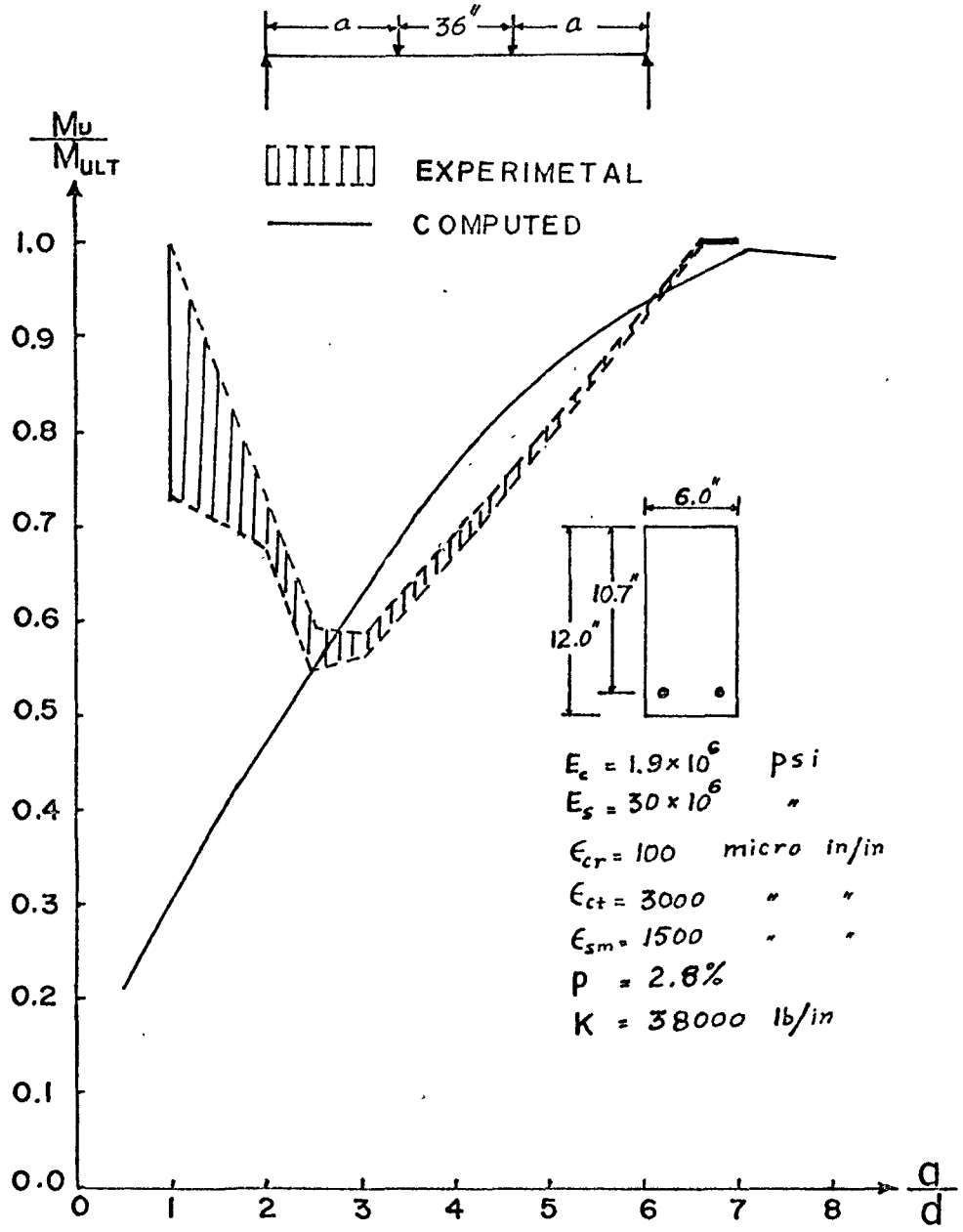

COMPARISON BETWEEN KANI'S EXPERIMENTAL AND AUTHOR'S THEORETICAL RESULTS FOR p= 2.80%

FIG. 4.11

of ultimate flexural capacity with variation in the shear-span to depth ratio, a/d. Three distinct regions can be identified, namely DV, VT and TE as in Fig. 4.1.

The theoretical computations based on the concept of loss of interaction in a composite beam have shown good agreement with Kani's experimental results over the region VT and TE. The only qualitative assumption made in the theoretical computations was that the bond-slip modulus should have that magnitude that would give the closest agreement between the computed and experimental value of ultimate flexural capacity at the experimental transition points V and T for beams having a particular steel percentage, p.

Fitting the theoretical results to the experimental transition points, V and T, resulted in the bond-slip modulus, K,having different values for different steel percentages, p. Although the resulting magnitudes of K are not equal and have not been identified with any experimental results, since the bond-slip modulus does not appear to have been investigated experimentally; qualitatively the computed values of K appear acceptable since they show an increase of K with increase in percentage of steel (i.e. either an increase in bar diameter or an increase in number of bars).

It is interesting to note that in the computation no account has been made directly for the vertical applied shear

or diagonal cracking and the analysis is entirely based on flexural capacity at the cross-sections under the load points. In spite of this the computed results are very much in agreement with experimental results of Kani.

4.8.2 Figs. 4.5, 4.9, 4.10a, 4.10b and 4.11 show the computed ultimate moment, M_u, carried by the section under the load point for various ratios of a/d. It has been observed that it is influenced by the same parameters as found experimentally by Kani over the range VTE. However, this method does not result in any increase in ultimate flexural capacity of the beams for a/d less than 2.5 as has been observed experimentally.

It is evident that some other factor comes into play in this region. Kani[9] has suggested that the 'tied-arch' phenomenon governs the strength of the beam for a/d ratios less than the transition point, V. Hence, in order to have a complete theoretical explanation of the reinforced concrete beams behavior, the arch analogy should be investigated.

4.8.3 In fact Kani[9] has presented a semi-empirical method for calculating the capacity of the remaining arch and the capacity of the concrete teeth, but, that method cannot be generalized because it depends upon certain factors such as spacing and height of the flexural crack which have to be determined from experiments.

Kani's method of analysis is summarized in the following paragraph.

1. The full flexural capacity, M_{FL}, of the beam can be expressed by:

$$M_{FL} = \frac{7}{8} \cdot d \cdot A_s \, f_y \, . \qquad 4.3$$

2. The capacity of the concrete teeth can be expressed by:

$$M_{CR} = \frac{7}{8} \frac{f'_t}{6} \frac{\Delta x}{s} \, b \, a \, d \, . \qquad 4.4$$

3. If M_o is the moment depends only on the properties of the section, then:

$$M_o = \frac{7}{8} \frac{f'_t}{6} \, bd^2 \qquad 4.5$$

The equation 4.4 can be written as:

$$M_{CR} = M_o \cdot \frac{\Delta x}{s} \cdot \frac{a}{d} \qquad 4.6$$

4. At the point where the carrying capacity line reaches the line of full flexural capacity, the:

$$M_{FL} = M_{CR} = M_o \frac{\Delta x}{s} \frac{a}{d}$$

then the transition point α_{TR} can be given by

$$\alpha_{TR} = \frac{M_{FL}}{M_o} \cdot \frac{s}{\Delta x}$$

putting the values of M_{FL} and M_o from equations 4.3 and 4.4 into above equation:

$$\alpha_{TR} = \frac{6pf_y}{f'_t} \frac{s}{\Delta x} \quad . \qquad 4.7$$

Hence the magnitude of α_{TR} can be determined.

5. In the region of low a/d ratios the capacity of the beam can be calculated as the strength of the remaining arch which can be expressed as:

$$M_{CR} = \frac{M_{FL}}{k} \frac{d}{a} \qquad 4.8$$

where k is a constant and is equal to 0.9.

6. In the medium region of a/d values the concrete teeth capacity determines the strength of the structure:

$$M_{CR} = \frac{M_{FL}}{\alpha_{TR}} \frac{a}{d} \quad . \qquad 4.9$$

7. The common boundary point of the two regions is given by:

$$\alpha_{min} = \sqrt{\frac{\alpha_{TR}}{k}} \qquad 4.10$$

and the minimum capacity at α_{min} can be calculated by:

$$\min M_{CR} = \frac{\alpha_{min}}{\alpha_{TR}} M_{FL}$$

where α_{TR} = the magnitude of transition point

f'_t = tensile strength of concrete

p = percentage of longitudinal tension reinforcement

s = average height of the crack

Δx = average spacing of crack

k = constant factor = 0.9 - suggested by Kani[9]

M_{FL} = full flexural capacity

M_{CR} = moment at failure of concrete-teeth or the capacity of remaining arch

a/d = shear-arm depth ratio

CHAPTER V

SHEAR STRESS DISTRIBUTION

5.1 The formation of flexural cracks, particularly in the shear span, leaves a comparatively small cross-section of concrete to support the external shear force with the result that many authors[1,11,15] reason that additional resistance must be provided by 'dowel action' in the reinforcing bars and 'aggregate interlock' or 'shear due to friction'.

Acharya[15] argued that the presence of dowel force cannot be ingored in any quantitative analysis of shear failure.

Some research workers[11] in the analysis of diagonal failure assume some contribution of dowel and aggregate interlock forces. Fenwick and Pauley[1] in their paper "Mechanism of Shear Resistance of Concrete Beams" attributed a significant percentage of shear resistance to aggregate interlock. Their experiments suggest that aggregate interlock action provides 50 percent of the resistance to shear force in a cracked beam, with 20 percent due to dowel action and the remainder carried in by uncracked portion of a cross-section.

It was therefore of interest to study the distribution of shear stresses and the contribution of shear force resis-

tance by different components, at various sections along the length of a cracked beam.

Since there are three major components resisting the shear force, namely, uncracked concrete, aggregate interlock action and dowel action, two different approaches are considered. One for calculating the shear stress distribution in the uncracked concrete and the other to determine the contribution of dowel and aggregate interlock actions and the distribution of shear stresses in the cracked portion of the beam. These are discussed in the following.

5.2 Shear Stress Distribution in Uncracked Concrete

5.2.1 The method presented here is primarily based on equilibrium of the horizontal forces. The equilibrium conditions are applied to an uncracked portion between any two sections of a cracked beam. Fig. 5.1a shows such an uncracked portion, C-C, between sections 1-1 and 2-2. Referring to Fig. 5.1a, the strain at any level can be computed by:

$$\left.\begin{aligned} \varepsilon_{y_1} &= \varepsilon_{ct_1} \left(\frac{n_1 - y_1}{n_1}\right) \\ \varepsilon_{y_2} &= \varepsilon_{ct_2} \left(\frac{n_2 - y_2}{n_2}\right) \end{aligned}\right\} \qquad 5.1$$

where n_1 and n_2 are the distances of the neutral axes for section 1-1 and 2-2 respectively from the top concrete fibre.

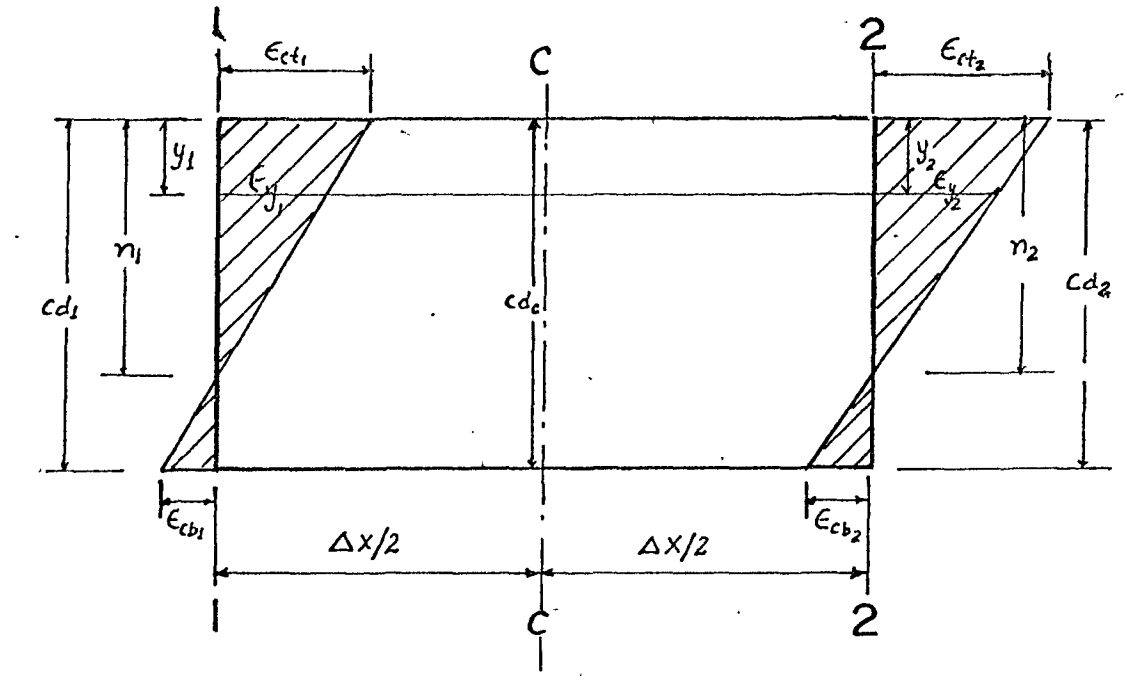

a) FLEXURAL STRAINS

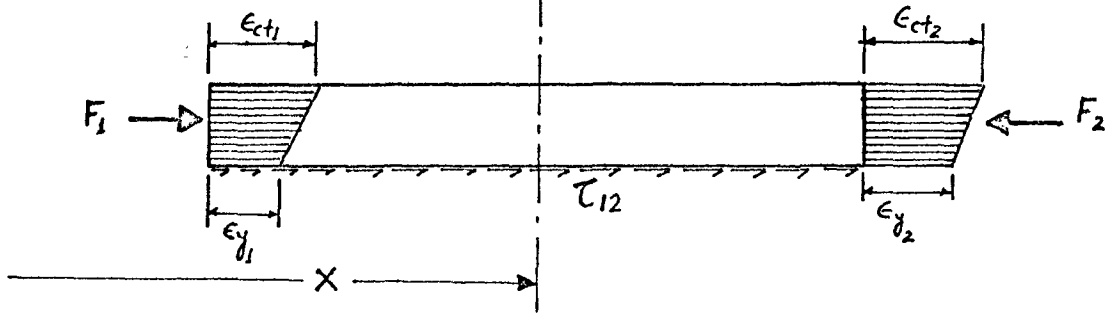

b) FREE BODY FOR τ_{12}

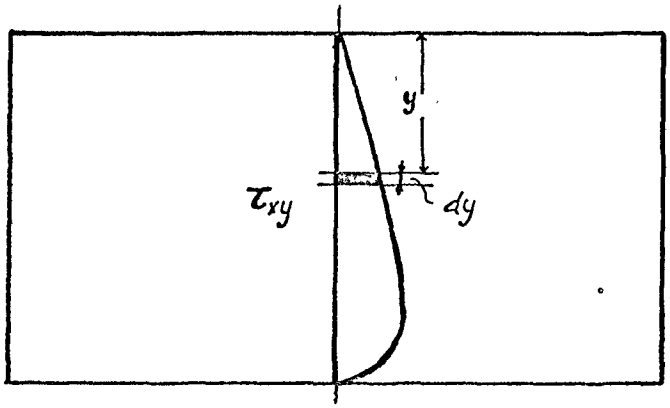

c) TOTAL SHEAR

DETERMINATION OF VERTICAL SHEAR STRESS DISTRIBUTION IN UNCRACKED CONCRETE

FIG. 5.1

Δx in Fig. 5.1 is the distance between section 1-1 and 2-2; that is the middle section C-C where the shear stress distribution is to be determined is $\Delta x/2$ in. from each section 1-1 or 2-2. It is assumed that the flexural crack heights at all the three sections 1-1, C-C and 2-2 are the same and the height is equal in magnitude to that obtained for section C-C, that is,

$$Cd_1 = Cd_c = Cd_2$$

where Cd is the uncracked concrete depth. Since the magnitude of $\Delta x/2$ is very small, therefore, the difference between the actual computed uncracked depth is insignificant.

5.2.3 Shear Stresses

The uncracked portion C-C can be divided into a number of rectangular laminas . The average shear stress determined, from the equilibrium of the free body above the base level, at the base of each lamina is shown in Figs. 5.1b and 5.1c.

Therefore $$\tau_{12} = \frac{F_2 - F_1}{b \cdot \Delta x} \qquad 5.2$$

where $$F_1 = \left(\frac{\varepsilon_{ct_1} + \varepsilon_{y_1}}{2}\right) y_1 \, bE_c$$

and $$F_2 = \left(\frac{\varepsilon_{ct_2} + \varepsilon_{y_2}}{2}\right) y_2 \, bE_c$$

here b = width of the beam

τ_{12} = average shear stress over the base of free body.

If τ_{xy} is the vertical shear stress at a depth, y, and at a distance, x, from left support, then

$$\tau_{xy} = \tau_{12}.$$

5.2.4 Shear Force

The total shear force, S, carried by the section C-C at a distance x from left support, as per Fig. 5.1c can be given by:

$$S = b \int_{o}^{c_{d_c}} \tau_{xy} \, dy \quad . \qquad 5.3$$

5.2.5 Zero shear stress at the root of the crack

From the method stated above the shear stress is not zero at the root of the crack and the computation shows that there is a certain amount of shear stress existing at the base of the crack. But, for the requirements of the boundary condition it is reasoned that the shear stress should be zero at the root of the crack, since it is zero at the top or bottom fibres of concrete. Also the method for the determination of shear stresses in the cracked region of the section, as dis-

cussed in the following paragraphs, requires the shear stress to be zero at the base of the crack.

5.3 Shear Stress Distribution in Cracked Concrete

5.3.1 Most research workers[1,2,9,11,28] agree that the formation of flexural tension cracks in a beam, divide the tension zone into a number of blocks; each of them may be considered as a cantilever spanning from the compression zone to just beyond the tension reinforcement. These blocks are called 'concrete-cantilevers' and the compression zone is the backbone of these cantilevers. The structure formed may be likened to a 'comb-like' structure. This is shown in Fig. 5.2a.

5.3.2 If only two adjacent concrete cantilevers are considered at a time and all the other minor forces acting on them are neglected then the only major force acting is the bond force, ΔF_B, which is the incremental increase of the tensile force in the flexural reinforcement, as shown in Fig. 5.2.b. These two cantilevers can be idealized as a 'composite cantilever beam' having a continuous shear connection throughout the length at the interface due to aggregate interlock or friction action, and a stiff connector due to horizontal steel at the level of reinforcement (dowel action). This composite cantilever beam has a

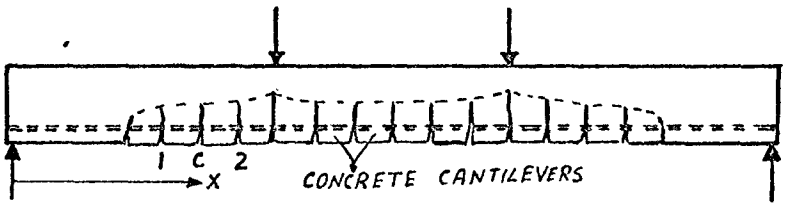

a) COMB-LIKE STRUCTURE

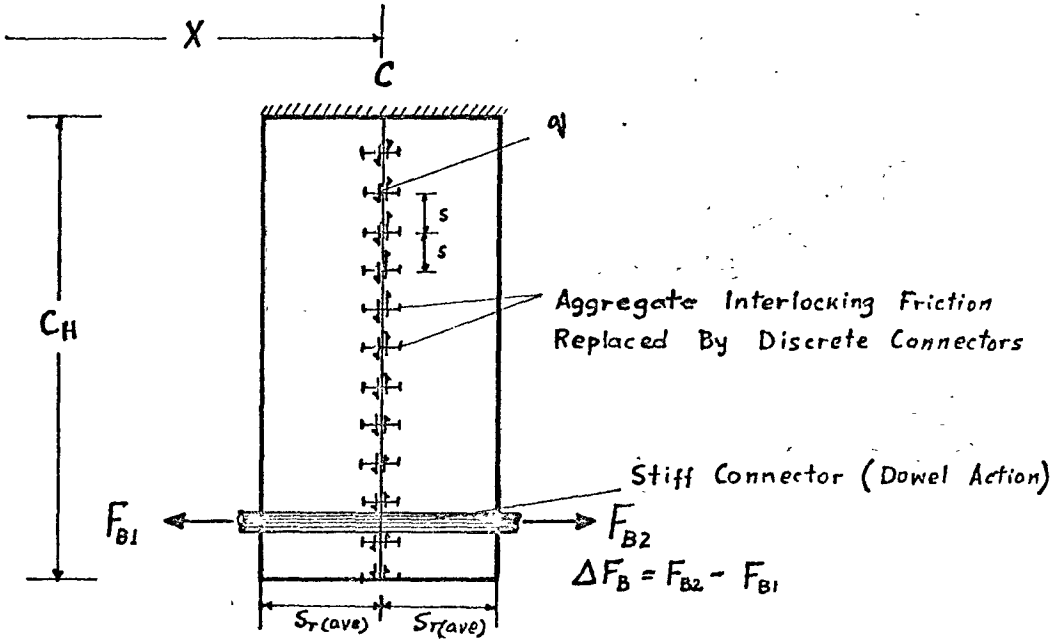

b) TWO ADJACENT CANTILEVERS
IDEALISE AS COMPOSITE BEAM

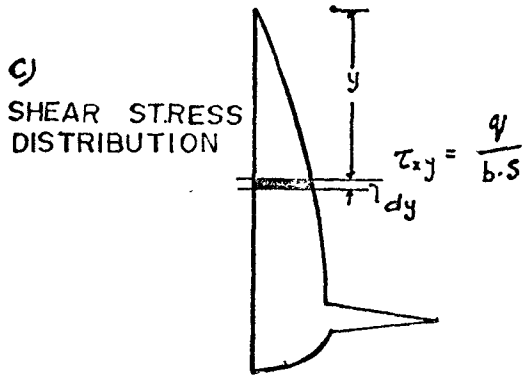

DETEMINATION OF VERTICAL SHEAR STRESS DISTRIBUTION IN CRACKED ZONE - CONTRIBUTION OF AGGREGATE INTERLOCK & DOWEL ACTIONS

FIG. 5.2

horizontal shear, q, at the interface, which can be determined by Stussi[20] composite theory. The continuous connection can be replaced by discrete connectors of any desired spacing, s. If the horizontal shear, q, is divided by the product of breadth of beam and spacing of connectors then the vertical shear stress can be obtained:

$$\tau_{xy} = \frac{q}{b \cdot s} \qquad 5.4$$

5.3.3 This approach, discussed above, has been used to determine the shear stress distribution in the tensile zone.

For any composite beam the magnitude of the shear modulus of the connector must be known. In this case there are two different connectors, friction or aggregate interlocking action (replaced by discrete connectors of spacing,s) and a stiff shear connector due to reinforcement (dowel action). Now the question arises as to the magnitude of the shear module of the two types of connectors. In order to determine the contribution of dowel action in a reinforced concrete beam Fenwick and Pauley[1] conducted tests on long and short dowels. They stated that"the long dowels were intended to throw some light on the conditions which prevail in the vicinity of the first diagonal crack near the support of a beam ----," "The short dowel tests were designed to

give some information on the contribution of dowel action to the resistance of the concrete cantilevers". Their test arrangements and the results obtained in the form of a graph (dowel force versus displacement of dowels) are shown in Fig. 5.3a to 5.3c.

Since the short dowel tests were intended to determine the conditions in concrete cantilevers, the initial slope of the dowel force versus displacement of dowel curve (which can be regarded as a load-slip curve) has been used for the determination of the modulus of the stiff connector (flexural reinforcement). The average value obtained from Fig. 5.3b (tension side) is:

$K_D = 1.75 \times 10^5$ lb/in for a $\frac{7}{8}$" diameter bar.

In this way an approximate value of shear modulus of dowel, K_D, has been determined. The magnitude of the friction modulus, K_{AG}, still remains unknown. At this stage no work appears to have been done to determine the friction modulus. Therefore, the magnitude of the friction modulus, K_{AG}, is left undefined in the computation.

From the approach of section 5.2 of this chapter the shear force contribution of uncracked concrete is known. The remaining shear force must be carried by aggregete interlock plus dowel action. Therefore, the magnitude of the friction modulus, K_{AG}, which gives the appropriate percentage contri-

DUE TO FENWICK AND PAULEY

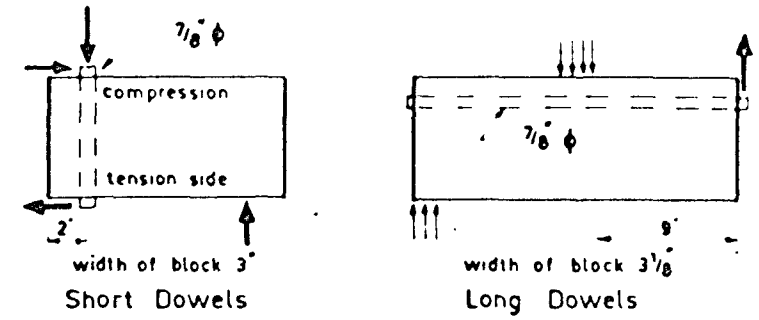

(a)

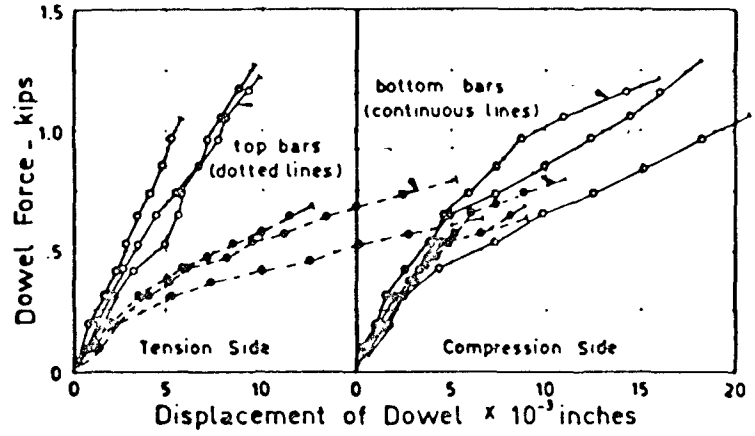

(b)

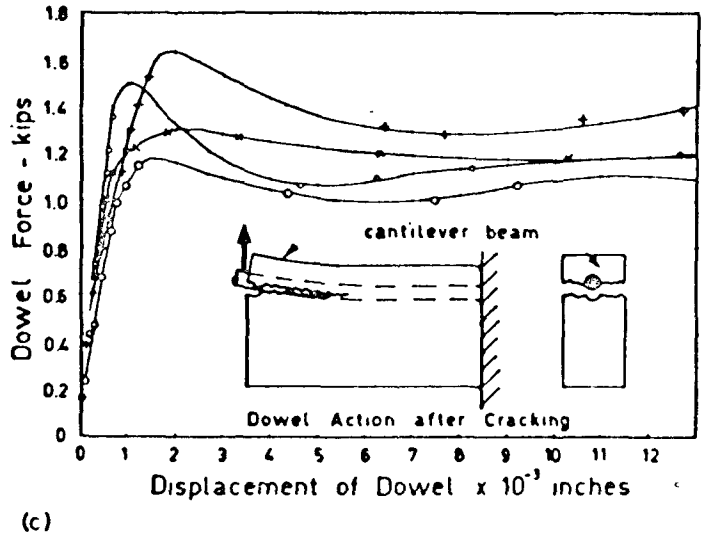

(c)

DOWEL TESTS; (*a*) TEST ARRANGEMENTS; (*b*) TYPICAL RESULTS SHORT DOWEL TESTS; (*c*) RESULTS OF LONG DOWEL TESTS

FIG. 5.3

bution to the total shear force is taken as the value of aggregate interlocking modulus.

5.3.4 In order to find the shear stress distribution in the tensile zone by Stussi's composite beam theory the dimensions of the 'composite cantilever beam' such as length, breadth and depth, must be known. The length is the crack height from the bottom of the concrete beam to the root of the crack, for the crack which forms the interface between the two cantilevers. The depth of each element of the composite beam cantilever is taken as the spacing of the cracks. Broms [13] suggested that the average crack spacing is approximately twice the distance of the concrete cover, d_s, to the tension reinforcement.

$$S_{cr(ave)} = 2d_s \qquad 5.5$$

where $S_{cr(ave)}$ is the average crack spacing.

In the computation this spacing has been used. The influence of crack spacing on the shear stress distribution along a crack has also been determined and is summarized elsewhere in this chapter.

5.4 Shear Stress Distribution Along A Flexural Crack

The particular beam considered for this purpose is the same 'typical beam' of chapter III, having p = 1.88 percent. The bending moment on the beam is 264500 lb-in, half

the ultimate bending moment carried by such a section, as obtained by ACI Code formula.

Since in the beam considered here two number 7 bars are used, the modulus of dowel action is:

$$K_D = 2 \times 1.75 \times 10^5 \text{ lb/in}$$
$$= 3.5 \times 10^5 \text{ lb/in.}$$

Two shear-arm to depth ratios, a/d, are considered, namely $\frac{a}{d} = 3$ and $\frac{a}{d} = 5$, in order to have a better picture of shear stress distribution for the same bending moment.

Fig. 5.4a and 5.4b shows the computed shear stress distribution at different sections along the length of the beam for $\frac{a}{d} = 3$ and $\frac{a}{d} = 5$, respectively. The figures also show the required magnitude of friction or aggregate interlocking modulus, K_{AG}, for every particular section, since it varies for different sections, when it is required that the internal resisting shear force must equal the external applied shear force. The percentage of total shear force carried by different components in a cracked beam is also shown in Figs. 5.4a and 5.4b.

It is to be noted that the percentage shear force carried by the uncracked concrete varies from section to section; for example for $\frac{a}{d} = 3$ and x=4 in., where the section is uncracked throughout the depth of the beam 99.7 percent of the total shear force is carried by concrete and the distri-

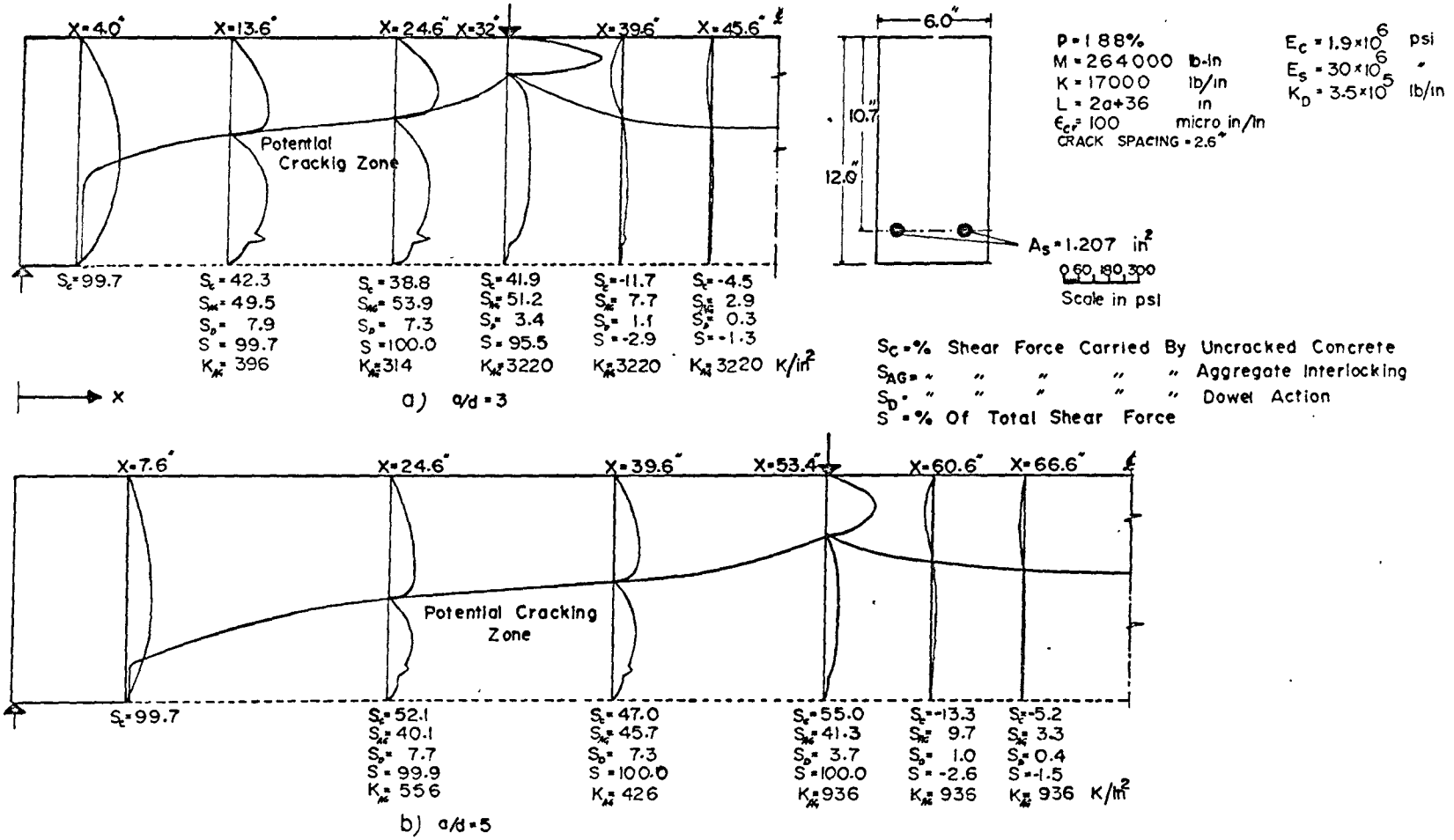

DISTRIBUTION OF SHEAR STRESSES IN A CRACKED BEAM

FIG. 5.4

bution of shear stress is a parabolic curve. In the cracked zone in the shear span the percentage contribution of shear force varies from 42.3 percent to 38.0 percent for $\frac{a}{d} = 3$ and 55 percent to 47 percent for $\frac{a}{d} = 5$. The dowel force is almost constant and is about 7.5 percent except just to the left of the point load where it is about 3.5 percent, for both the a/d ratios. The aggregate interlocking resistance ranges from 54 percent to 49.5 percent and 45.5 percent to 40 percent of the total shear force for $\frac{a}{d} = 3$ and 5, respectively.

In the constant moment region the shear stress in the uncracked concrete reverses its sign (negative). Since the 'tooth' deflection would remain in the same direction, because, the stress in the tensile reinforcement continues to increase up to midspan. Therefore, a balance of internal shear force is possible and zero total shear force can be obtained. However, in order to achieve zero resultant shear a very large magnitude of K_{AG} is required. For example, for $\frac{a}{d} = 3$ the K_{AG} in the constant moment region is about 10 times greater than the K_{AG} in the combined moment and shear region. Even then a negative shear of magnitude 2.94 percent at x=39.6 in. and 1.28 percent at x = 45.6 in. remained. One conclusion to be drawn from this is that the computed shear force contribution due to friction is extremely insensitive to the change in the magnitude of the friction

shear modulus, K_{AG}, in the constant moment region.

The magnitude of K_{AG} just to the left of the load point, as shown in Fig. 5.4a, is 3,220,000 lb/in^2 for a/d=3 and 936,000 lb/in^2 for a/d=5. These are also the maximum values of K_{AG} in the combined shear and bending moment region. It can also be noted that for $\frac{a}{d} = 3$ and at x = 32 in.(just left of the load point) the total shear force carried by all the components is 96.5 percent; a difference of 3.5 percent. Here the same difficulty arises and in order to get another 3.5 percent due to friction the value of K_{AG} would have to be more than 7 times the used value of K_{AG} = 3,220,000 lb/in^2, which is already 10 times higher than the other K_{AG} values for the same a/d ratio in the increasing moment region.

5.5 Influence of Crack Spacing and Δx

5.5.1 The choice of crack spacing has a great influence on the magnitude of K_{AG}. It has been found that the greater the value of average crack spacing (tooth width), the greater the magnitude of K_{AG} required to balance the external shear force and vice versa. For example, if a crack spacing of 1.3 in. is used in the computation instead of 2.6 in. then the magnitude of K_{AG} is reduced to 200,000 lb/in^2 from 396,000 lb/in^2 for $\frac{a}{d} = 3$ and at x = 13.6 in. and it reduced to 210,000 lb/in^2 from 426,000 lb/in^2 for $\frac{a}{d} = 5$

and at x = 39.6 in. Similarly for other sections. Also the reduction in the crack spacing slightly increases the percentage of shear force carried by dowel action and it is observed that the average shear force carried by dowel action in the shear span is 8.5 percent for crack spacing of 1.3 in.; an increase of 1 percent from that with 2.6 in. crack spacing. This means that the aggregate interlocking force decreased by 1 percent.

5.5.2 It has been found that the magnitude of Δx used in the computation of the shear stress distribution in the uncracked concrete does not have any effect on the shear force carried by the uncracked concrete. The value of Δx was varied from 1.0 in. to 0.01 in., but the percentage of shear force and the magnitude of shear stresses remains the same for each particular section.

5.6 Discussion

The methods considered here for the determination of shear stress distribution in a cracked beam, throughout its depth, and subsequently used to find the contribution of the different components to resist the external shear force are based on simplified assumptions, such as equilibrium of horizontal forces and on a composite cantilever beam model. However, the shear stress distribution and the

percentage contribution of different components seems to be reasonable.

Acharya[15] argued that only 40 percent of the total shear force is carried by uncracked concrete and the rest by dowel action. On the other hand Fenwick and Pauley[1] claim that the shear force carried by uncracked concrete, aggregate interlock and dowel actions is 30 percent, 50 percent and 20 percent respectively. MacGregor and Walters[11] in their analytical analysis considered 11 percent contribution of shear force from dowel action, 23 percent from the aggregate interlock and the remaining from uncracked concrete.

From the approach described above the percentage shear force carried by the uncracked concrete ranges from 39 percent to 55 percent; aggregate interlock action contribution in resisting the shear force varied from 40 percent to 54 percent and the dowel action resists almost 7.5 percent of the total shear force. This is for a particular beam cross-section (typical beam) and for two a/d ratios: 3 and 5.

In the light of the above discussion it is concluded that the calculated shear stress distribution in uncracked concrete and the percentage contribution in resisting the shear force is reasonable. Although the method for finding the shear stress distribution and the contribution of dowel and aggregate interlocking actions is based on simplified

assumptions the distribution of shear stress on a cross-section in the tensile zone seems to be reasonable. Dowel action does not seem to contribute much to the resistance to shear force for this particular beam. It is to be mentioned that a different beam having the dimensions of those tested by Plowman[29] was also examined analytically. The maximum bending moment on the beam is 36200 lb-in (design moment), the magnitude of K and E_c is 17000 lb/in and 1.9×10^6 psi, respectively. It was found that the dowel action in this particular beam is significantly larger; having a magnitude of almost 20 percent, while the shear force carried by uncracked concrete is 46.6 percent and the remaining was carried by aggregate interlocking action. The distance of the particular section was 20 in. from left hand support.

Therefore, the percentage of shear force carried by dowel action and aggregate interlocking vary considerably and depend upon the dimensions of the beam.

It should be emphasized that the computed values of the friction shear modulus (or aggregate interlock modulus) are the result of determining a magnitude of K_{AG} which would provide the remainder of the shear resistance not carried by the computed components due to dowel action and the uncracked part of the concrete.

It is difficult to pass a judgement on the magnitudes

and variation of K_{AG} values obtained from the computation, since there does not appear to have been any experimental results with which to compare them. Therefore, a more realistic approach is required to determine the magnitudes of the friction modulus.

Also in a real beam the width of the crack is not constant. The maximum width occurs at the level of the longitudinal reinforcement and the minimum width at the root of the crack. Therefore, the magnitude of aggregate interlocking modulus is not in fact likely to be constant, because the maximum friction will occur near the root of the crack and the minimum at the level of reinforcement. Hence, it is also emphasized that the variation in the magnitude of aggregate interlocking modulus should also be investigated and should be considered in the computation.

Once these coefficients are established, it would then be possible to determine the distribution of shear stresses in the tensile zone of a cracked beam and the contribution of the different actions in resisting it, especially if a multi-layered composite beam solution is tried. Then it is hoped the analysis could be extended to trace the path of diagonal cracks and to study the cause of such a failure.

CHAPTER VI

INCLINED CRACKING

6.1 Diagonal cracking is often regarded as a combined stress problem. Therefore, in this chapter the maximum principal tensile strains (combination of flexural and shear strains) are studied on an element above the flexural crack. It is based on the assumption that cracking will start to occur whenever the principal tension strain exceeds the critical cracking strain, ε_{cr} (100 micro in/in).

6.2.1 From the previous chapter the distribution and magnitude of shear stresses in a cracked reinforced concrete beam are known. The flexural strain distribution at any particular section can also be computed as shown in Fig. 5.1.

6.2.2 Shear Strain

Consider a section at a distance x from the left hand support, then at any level 'y' from the top concrete fibre, the shear stress, τ_{xy} is known. The shear strain would be:

$$\gamma_{xy} = \frac{\tau_{xy}}{G_c} \qquad 6.1$$

where G_c = shear modulus of concrete = $\frac{E_c}{2(1+\nu)}$.

Here ν is the Poisson's ratio. The value of ν for concrete is taken as 0.16.

6.2.3 Principal Strain

If ε_{xy} is the flexural strain at a distance x from left hand support and at a depth y from top fibre of concrete then the magnitude and direction of maximum principal strain at the same position can be computed by the conventional combined strain formula, as:

$$\varepsilon_{max} = \frac{\varepsilon_{xy}}{2} + \sqrt{(\frac{\varepsilon_{xy}}{2})^2 + (\frac{\gamma_{xy}}{2})^2} \quad . \qquad 6.2$$

Here any effect of transverse strains has been neglected. Also

$$\theta = \frac{1}{2} \tan^{-1} (\frac{\gamma_{xy}}{\varepsilon_{xy}}) \qquad 6.3$$

6.3 Since the computed shear stress is zero at the root of the crack any inclined crack likely to occur must be some distance above the root of the flexural crack. The uncracked concrete cross-section at any particular location is divided into a number of intervals and at each level the combination of shear and flexural strains (maximum principal strain) is computed. Since in this computation the magnitude of the applied bending moment is arbitrary, the largest of the maximum principal strains will be regarded as the cause of

inclined cracking if it is greater than or equal to the critical cracking strain ε_{cr}. The more correct computational procedure is to apply incremental loading and trace the location and direction of the top of the crack.

6.4 Numerical Example

6.4.1 Consider the "typical Beam' having p = 1.88%, K = 17000 lb/in and a/d = 3. Fig. 6.1 shows the computed flexural and inclined crack pattern in the combined bending and shear region. The procedure of computing the inclined cracks is as follows.

6.4.2 Procedure

The flexural crack heights are obtained in the usual manner as outlined in chapter III. In computing the inclined cracks, the shear stress distribution in the remaining uncracked concrete portion at a particular cross-section is determined. The uncracked concrete portion is divided into 50 equal intervals; at each interval the maximum principal strain is computed as outlined above. The largest of all the maximum principal tensile strains is regarded as the cause of inclined cracking if it is greater than or equal to ε_{cr}. The first increment in the crack height is then computed in the same way as explained in Chapter III. Then the new total cracked height will be the sum of the

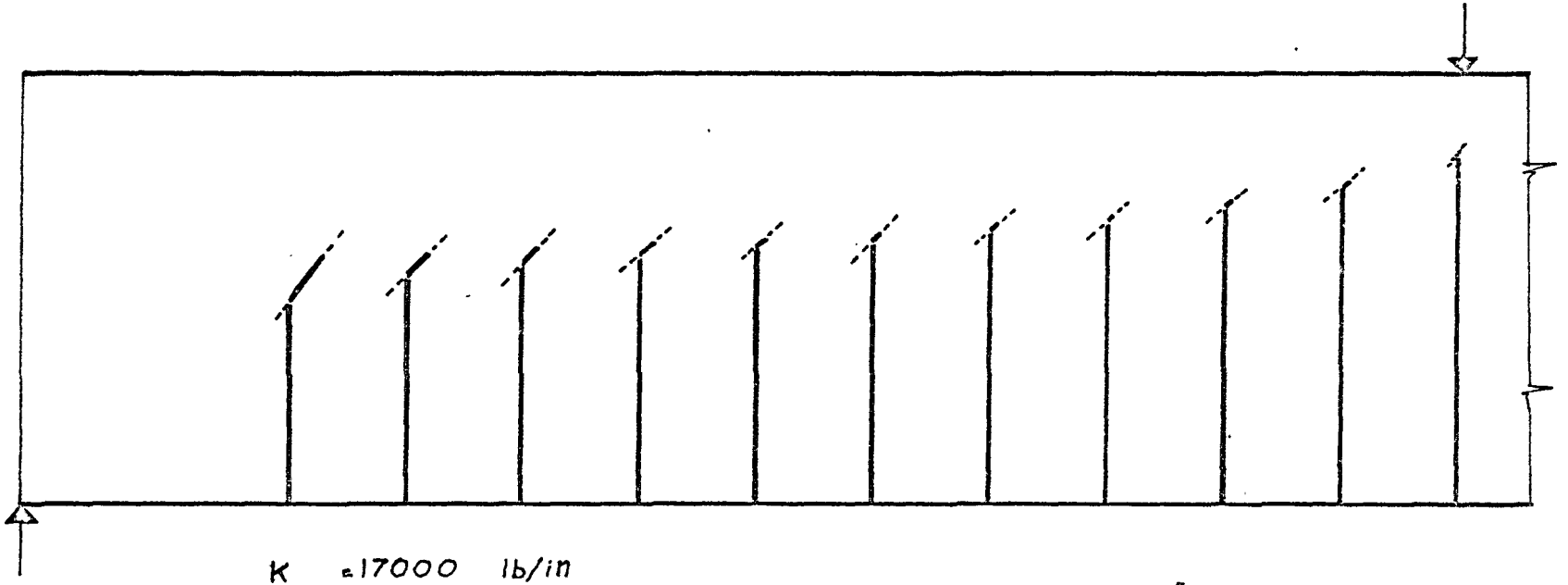

K	= 17000	lb/in
E_c	= 1.9×10^6	psi
E_s	= 30×10^6	"
M	= 264500	lb-in
a/d	= 3	
ϵ_{cr}	= 100	micro in in
Crack Spacing	= 2.6	in

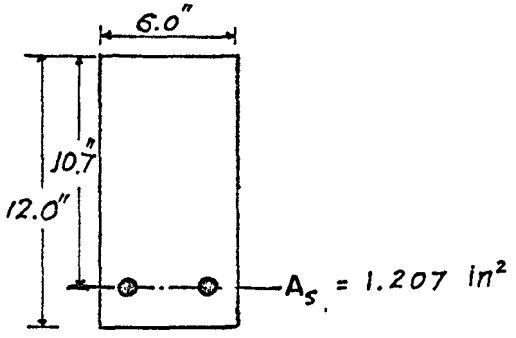

DIAGRAM SHOWING INCLINED CRACKS (above the flexural cracks) IN THE SHEAR SPAN

FIG. 6.1

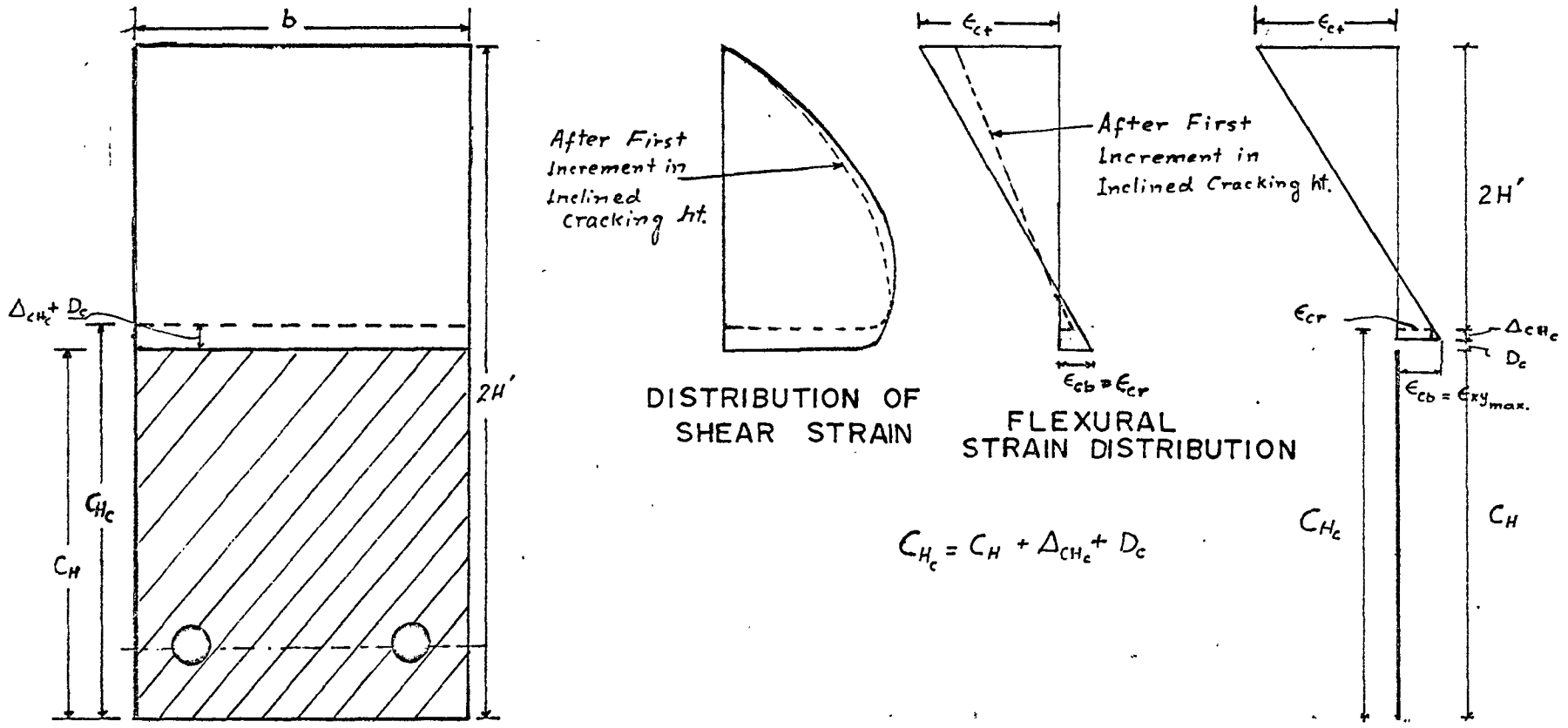

$$C_{H_c} = C_H + \Delta_{CH_c} + D_c$$

DEVELOPMENT OF AN INCLINED CRACK

FIG. 6.2

flexural crack height, the first increment in the crack height due to maximum principal tensile strain and the height between the root of the flexural crack and the depth over which the maximum principal tensile strain is equal to or more than ε_{cr}, see Fig. 6.2.

$$C_{H_c} = C_H + \Delta_{ch_c} + D_c$$

and

$$2H' = 2H - C_{H_c} \quad . \qquad 6.4$$

The new remaining depth, 2H', is reused in equation 3.1 in place of 2H and another increment in the crack height is obtained. All the above procedure, is repeated until a stable section is obtained, as explained in chapter III, section 3.1, except that the magnitude of ε_{cb} in this case is equal to the largest of the maximum principal tensile strains.

It was found that vertical shear capacity of a particular section in the uncracked concrete diminishes as the inclined crack height increases. For example at x = 11.2 in. the shear force carried by the uncracked concrete above the root of the flexural crack is 45 percent. After the stabilization of the inclined crack the percentage shear force carried by the uncracked concrete is reduced to 41.5 percent.

6.5 Discussion

The maximum principal strains computed in the remaining uncracked portion of the beam are in fact greater than the critical cracking strain, ε_{cr} (100 micro in/in), hence an inclined crack is obtained. An inclination of up to 40 degrees with the vertical has been obtained. This suggests that inclined cracks may be developed when the principal strains are computed.

By computing and plotting the development of cracks during incremental loading it may be possible to trace the development of inclined cracks.

CHAPTER VII

SUMMARY, CONCLUSION AND SUGGESTIONS FOR FUTURE STUDIES

7.1 Summary

In this thesis a reinforced concrete beam has been treated as a composite beam with incomplete interaction.

The solution for a composite beam with stepped profile was obtained. It takes into account the compatibility conditions at the change of cross-section, i.e., at the first flexural crack. It was found that the maximum crack height under the load point calculated by this method (Newmark 2B) remains the same as obtained by Newmark 1, which does not take into consideration the compatibility conditions, see Fig. 2.7. However, the crack profile obtained by Newmark 2B, in the increasing moment region, is better than the crack profile obtained by Newmark 1, as the cracks are not so high in the initial flexural cracking zone. It has been found that the Newmark 1 solution can well be applied to the study of reinforced concrete beam, since the difference between the two approaches when computing the moment capacity under the load point is negligible.

The non-linear behavior of concrete has been considered and the area under the parabolic stress-strain curve

of concrete has been approximated to a triangle, by reducing the modulus of elasticity of concrete. It has been found that the crack height, in general depends upon the bond-slip modulus, K, and modulus of elasticity of concrete, E_c. The decrease in K results in higher crack heights. On the other hand the decrease in E_c also decreases the crack height, see Figs. 3.4 and 3.5.

The stability of flexural cracks has also been discussed and it was found that the tensile crack stabilizes, after penetrating vertically into the beam to a certain height until the lower fibre concrete strain, ε_{cb}, is equal to critical cracking strain, ε_{cr}, as well as there being equilibrium between internal and external forces. The analysis of Krahl[10] et al. and MacGregor and Walters[11] also depends upon stability of the tension crack, but the analysis presented in this thesis differs in the sense that they did not account for the relative movement (slip) between the concrete and steel.

It was found that the interaction diminishes as the shear-arm to depth-ratio, a/d, is reduced, consequently the concrete top strain, ε_{ct}, increases and steel mid height strain, ε_{sm}, decreases. Hence, the influence lines for the maximum moment carrying capacity were obtained. These are almost the same as obtained experimentally by Kani, Leonhardt and Walther, and Morrow and Viest (see Fig. 4.1, 4.2 and

compare with Fig. 4.5 for a/d $\geq$ 2.5). These carrying capacity curves are only based on the consideration of flexural stresses and no account has been taken of shear stresses. Figs. 4.9 and 4.11 show the comparison between Kani's [19] experimental results and the computed results of this thesis. It is interesting to note that these curves are similar in magnitude and shape for a/d $\geq$ 2.5. It is to be noted that each curve consists of two parts, namely one sloping down (portion VT in Fig. 4.5) and the other which is almost horizontal (portion TE in Fig. 4.5). In the sloping portion concrete governs the strength of the beam while in the horizontal part the steel reaches its yield strain first. Point 'T' in Fig. 4.5 represents the transition point which divides the two governing factors and also at this point the concrete and steel both fail simultaneously.

The transition point, T, as reasoned by Kani [9] differentiates between the two modes of failure. Beams having a/d ratios less than T fail in diagonal cracking and after the transition point only normal flexural failure is possible.

It was established that the value of bond-slip modulus, K, affects the moment carrying capacity and the location of the transition point. The carrying capacity increases slightly on the right side of transition point and decreases on the left side of transition point, as the value of K reduces for

a given percentage of steel. Also the transition point moves more towards the support for higher values of K, Fig. 4.6.

It has been found that the percentage of steel, p, has a significant influence on carrying capacity and also on the position of transition point. The transition point moves towards a larger a/d ratio for greater percentages of steel, Figs. 4.10a and 4.10b.

Kani[19], in describing the influence of p on relative beam strength stated, "for those beams with a high percentage of reinforcement (p = 2.80 percent), the 'valley of diagonal failure' has a low point in the vicinity of $M_u/\bar{M}_{fl}$ = 50 percent, whereas for those beams with a low percentage of reinforcement (p = 0.5 percent with $M_u/\bar{M}_{fl}$ = 100 percent), the 'valley of diagonal failure' disappears". Kani also stated that the amount of reinforcement influences the location of the transition point, T. Varying the main reinforcement from p = 2.80 percent to 1.88 percent and 0.80 percent, the test results produced locations of the transition point, T, at a/d = 6.5, 5.5 and 3.5,respectively.

The computed results show that for p = 0.50, 0.80, 1.88 and 2.80 percent, the transition point T occurs at a/d = 2.5, 3.0, 5.4 and 7.1,respectively. The computed relative beam strength,M_u/M_{ult} at a/d = 2.5 is 100 percent, 84 percent, 54 percent and 58 percent for p = 0.50,0.80,1.88

and 2.80 percent, respectively. In spite of the fact that certain simplifying assumptions were made for this analytical approach, the computed values are in very close agreement with the experimental results. The only qualitative assumption made in the analysis is that the bond-slip modulus should have the magnitude that would give the closest agreement between the computed and Kani's experimental results at the experimental transition points V and T.

The analysis was further extended to determine the shear stress distribution and the contribution of different actions in a cracked beam. Shear studies were carried out by two different methods, one to determine the shear distribution in uncracked concrete and the other to find out the distribution in the tensile zone. The analysis indicated that the contribution of uncracked concrete varies from 39 percent to 55 percent depending upon the remaining uncracked depth and shear span to depth ratio. Dowel action contributes about 7.5 percent of the total shear force and the rest, presumably, is carried by aggregate interlock action. The opinion of research workers varies widely regarding the share of total shear force by different actions. MacGregor and Walters[11] suggested that 66 percent of the total shear force is carried by the uncracked concrete, 23 percent is carried by aggregate interlock action and the rest, 11 percent, by dowel action.

Fenwick and Pauley[1] claim that the contribution of uncracked concrete is 30 percent and the remaining 70 percent is carried by aggregate interlock and dowel actions; out of this 70 percent $\frac{1}{3}$rd to $\frac{1}{4}$th is the contribution of dowel action. Acharya[15] assumed that as much as 60 percent of the total shear force is carried by the dowel action.

It is also suggested that shear stress at the root of the flexural crack is zero. This differs with the opinion of Krahl et al.[10] and MacGregor and Walters[11] who argued that for an inclined crack (extension of the flexural crack) there must be some shear stress at the root of the crack. But, in many instances the diagonal crack is above the flexural crack, therefore, the assumption of zero shear stress at the root of the flexural crack is reasonable.

It has been shown that inclined cracking is possible above the root of the flexural crack and an inclination of as much as 40 degrees is possible. This inclination was obtained by combining the bending and shear stress. No account has been taken of normal stresses. A more rigorous analysis is required to determine the path of the diagonal cracks, and an incremental loading technique should be utilized. It is hoped that this may provide more insight into the problem of diagonal cracking.

7.2 Conclusion

The following conclusions are drawn from this study:

1. The composite beam solution of Newmark[17] (called Newmark 1) can be applied, giving reasonable accuracies, to determine the crack profile and moment carrying capacity, particularly with respect to the crack height at the load points.
2. The magnitude of modulus of elasticity of concrete has a significant influence on crack height. For higher values of E_c, the crack height will be higher.
3. The bond-slip modulus affects the final height of the flexural crack. The lower the magnitude of K, the greater will be the height of the flexural crack.
4. After flexural cracking, the value of the interaction coefficient, $\frac{1}{C}$, increases, as the depth of the remaining uncracked concrete diminishes.
5. Due to reduction in the remaining uncracked depth during the process of flexural cracking, the horizontal force, F, increases, as the moment carried by the remaining uncracked concrete, M_c, decreases.
6. The bond-slip modulus, K, percentage of reinforcement, p, and the shear-arm to depth ratio, a/d, have a significant influence on moment carrying capacity of the beam. The lower the a/d ratio, the lower will be the carrying

capacity. Increase in the magnitude of K increases the carrying capacity to the left of the transition point, T, and also it shifts 'T' more towards the support. The percentage of steel has two effects; it increases the moment carrying capacity if p increases and also moves the transition point away from the support.

7. Shear studies show that 39 percent to 55 percent of the total shear force is carried by the uncracked concrete, 7.5 percent by dowel action and the rest by aggregate interlocking action. (The study of shear force carrying capacity at a cracked section in beams with different dimensions, however, indicates that the proportions can vary significantly. A study of a typical beam tested by Plowman showed that the dowel actions can contribute up to 20 percent with the uncracked section supporting 46 percent and aggregate interlock taking the remaining 34 percent.)
8. Inclined cracking can occur above the root of the flexural crack, since the principal strain can be more than the critical cracking strain. An inclination of as much as 40 degrees to the vertical was obtained.

7.3 Suggestions for Future Work

1. The flexural cracking, based on composite beam theory with incomplete interaction, should be extended to include curvilinear stress-strain characteristics of concrete. This should lead to more realistic cracking profiles and probably better understanding of the problems of diagonal cracking.
2. The values of bond-slip modulus, modulus of aggregete interlock action and dowel action modulus should be investigated and the effect of various parameters, such as percentage of steel (diameter and number of bars), breadth and depth of cross-section and the strength of concrete and steel on the magnitudes of these moduli should be determined.
3. A theoretical arch model should be investigated for the determination of moment carrying capacity of a beam for smaller values of shear-span to depth ratios (i.e. $a/d < 2.5$), in order to establish a complete theoretical explanation of the behavior of reinforced concrete beams.
4. The distribution of shear stresses in the cracked region (tensile zone) of the beam should be investigated more rigorously. In particular the cantilever action of the concrete 'teeth' in the cracked zone should be treated as a multilayer composite beam problem.

5. This method of analysis should be extended to study the effect of incremental loading. Such an approach may lead to a better production of the path of diagonal cracks and better understanding of such a failure.

BIBLIOGRAPHY

1. Fenwick, R.C. and Pauley, T., "Mechanism of Shear Resistance of Concrete Beams", Journal of the Structural Division, Proceedings of the ASCE, Vol. 96, No. ST10, October 1968, pp 2325-2350.

2. Bresler, B. and MacGregor, J.G., "Review of Concrete Beams Failing in Shear", Journal of the Structural Division, Proceedings of the ASCE. Vol. 93 ,No. ST2, February 1967, pp 343-372.

3. Report of ACI-ASCE 326, "Shear and Diagonal Tension", Journal of the ACI, Proceedings V.59, January to March 1962.

4. Robinson, H., "Discussion of a Paper by Plowman, J.M., Measurement of Stress in Concrete Beam Reinforcement", The Institution of Civil Engineers, Proceedings Vol. 28, July 1966, pp 412-419.

5. Hognested, E., "What do we Know About Diagonal Tensions and Web Reinforcement in Concrete?", Circular Series No. 64, University of Illinois, Engineering Experiment Station, March, 1952, 47 pp.

6. Talbot, A.N., "Tests on Reinforced Concrete Beams", Bulletin No. 14, University of Illinois, Engineering Experiment Station, 1907.

7. Clark, A.P., "Diagonal Tension in Reinforced Concrete Beams", Journal of the ACI, Proceedings V. 48, October, 1951, pp 145-156.

8. Kani, G.N.J. "The Mechanism of So-Called Shear Failure", Trans. of Engng. Inst. of Canada, April 1963.

9. Kani, G.N.J., "The Riddle of Shear Failure and the Solution", Journal of the ACI, Proceedings Vol. 61, No. 4, April 1964, pp 441-467.

10. Krahl, N.W., Khachaturian, N. and Siess, C.P., "Stability of Tensile Cracks in Concrete Beams", Journal of the Structural Division, Proceedings of ASCE, Vol. 93, No. ST1, February 1967, pp 235-254.

11. MacGregor, J.G. and Walters, J.R.V., "Analysis of Inclined Cracking in Slender Reinforced Concrete Beams", Journal of the ACI, Proceedings Vol. 64, No. 10, October 1967, pp 644-653.

12. Ferguson, P.M., "Some Implications of Recent Diagonal Tension Tests", Journal of the ACI, Proceedings Vol. 53, No. 2, August 1956, pp 157-172.

13. "Cracking in Reinforced Concrete Members", Authorised Reprint from Copyright Journal of the ACI, Dec. 1964, Jan. 1965, Sept. 1965, Oct. 1965 and Nov. 1965, with Discussions, Bulletin No. 17.

14. Uppal, A.S., "Composite Action in the Reinforced Concrete Beam", M. of Eng. Thesis, McMaster University, Hamilton, Ontario, January 1969.

15. Acharya, D.N. and Kemp, K.O., "Significance of Dowel

Forces on the Shear Failure of Rectangular Reinforced Concrete Beams Without Web Reinforcement", Journal of the ACI, Proceedings Vol. 62, No. 10, October 1965, pp 1265-1279.

16. Wong, A.C.C., "The Influence of Loss of Bond on the Mechanism of Failure of Reinforced Concrete Beams", M. of Eng. Thesis, McMaster University, Hamilton, Ontario, October 1964.

17. Siess, C.P., Viest, J.M. and Newmark, N.M., "Studies of Slab and Beam Highway Bridges: Part III, University of Illinois, Engineering Experiment Station, Bulletin Series No. 396.

18. Ho, H.H.H., "The Influence of Loss of Bond on the Failure Mechanism of Reinforced Concrete Beams", M. of Eng. Thesis, McMaster University, Hamilton, Ontario, May 1966.

19. Kani, G.N.J., "Basic Facts Ccncerning Shear Failure", Journal of the ACI, Proceedings Vol. 63, No. 6, June 1966, pp 675-692.

20. Stussi, F., "Zusammengesetzte Vollwandtrager", Publications, International Association for Bridge and Structural Engineering, Vol. VIII, pp 249-269, 1947.

21. Desayi, P. and Krishnan, S., "Equation for the Stress-Strain Curve of Concrete", Journal of the ACI, Proceedings Vol. 61, No. 3, March 1964, pp 345-350.

22. Luis, P.S., Ignacio, Martin and Rafael Tamergo, "Discussion of a Paper by Franco and Levi, Work of European Concrete Committee", Journal of the ACI, Proceedings V. 58, No. 3, September 1961.

23. Brown, E.H., "Structural Analysis Vol. 1", John Wiley and Sons, Inc., New York, Publication 1967.

24. Yam, L.C.P. and Chapman, J.C., "The Inelastic Behavior of Simply Supported Composite Beams of Steel and Concrete, Paper No. 7111, Proc. I.C.E., Dec. 1968.

25. Oladapo, I.O., "Stability of Tensile Cracks in Prestressed Concrete Beams", Journal of the Structural Division Proceedings of the ASCE, Vol. 95, No. ST1, January 1969, pp 17-31.

26. Morrow, J. and Viest, I.M., "Shear Strength of Reinforced Concrete Frame Members Without Web Reinforcement", Journal of the ACI, Proceedings Vol. 53, No. 9, March, 1957, pp 833-870.

27. Leonhardt, F. and Walther, , "Contribution to the Treatment of Shear Problems in Reinforced Concrete" ("Beiträge zur Behardlung der Schubprobleme in Stahlbetonbau"), Beton-und Strahlbetonbau (Berlin), V. 56, No. 12, Dec. 1961, and V.57: No. 2, Feb. 1962; No. 3, Mar. 1962; No. 6, June 1962; No. 7, July 1962; and No. 8, Aug. 1962 (in German).

28. Moe, J., "Discussion of a Report of ACI-ASCE Committee 326, Shear and Diagonal Tension", Journal of the ACI, Proceedings Vol. 59, No. 9, September 1962, pp 1323-1349.

29. Plowman, J.M., "Measurement of Stress in Concrete Beam Reinforcement", The Institution of Civil Engineers, Proceedings Vol. 25, Paper No. 6659, June 1963, pp 127-146.

30. Evan, R.H. and Robinson, G.W., "Bond Stresses in Pre-stressed Concrete from X-Ray Photographs", The Institution of Civil Engineers, Proceedings Part 1, 1955, Vol. 4, Paper No. 6025, pp 212-235.

APPENDIX A

FLEXURAL CRACKING THEORY

A.A.1 The conventional theories for the analysis of reinforced concrete beams assume that there is perfect bond between the steel and the concrete and that no slip occurs. However, it is well recognized by the experiments of many research workers[1,2,30] that the two materials in a reinforced concrete beam do not act perfectly together and there is always some relative movement between them. In a cracked beam this phenomenon is much more pronounced where slip is partially due to the breakdown in interaction (between the concrete and steel) and partially due to deformation of the concrete teeth.

Although a reinforced concrete beam does not possess a distinct interfacial plane between the concrete and steel. The composite beam theory[17] can be applied if a pseudo-interface is assumed.

The following assumptions are made for the derivation of the formulae:

1) Concrete and steel are perfectly elastic materials.
2) Concrete and steel deflect equal amounts at all points along the length of the beam, i.e., they have equal curvatures at any cross-section.

3) The horizontal force, F, transmitted to each component by the bond is considered to act at the centroids of each section.

4) There is a linear strain distribution across the depth of the section.

5) The bond-slip modulus is assumed to remain constant before and after cracking and is uniform and continuous along the length of the beam.

6) The amount of slip between the concrete and steel is directly proportional to the horizontal shear.

7) The total external moment, M_t, at any location along the length of the beam is equal to the sum of the individual moments, in the concrete, M_c, and in the steel, M_s, and the additional couple due to horizontal force, F, hence:

$$M_t = M_c + M_s + F \cdot Z.$$

The line joining the extremities of the flexural crack is called the crack profile. This profile will be treated as a pseudo-interface. Referring to Fig. A.A.I, the stress-strain at the pseudo-interface can be written as:

$$\frac{d\gamma}{dx} = \varepsilon_1 - \varepsilon_{cb} \qquad \text{A.A.1}$$

where

$$\varepsilon_1 = - (\varepsilon_r - \varepsilon_{st})$$

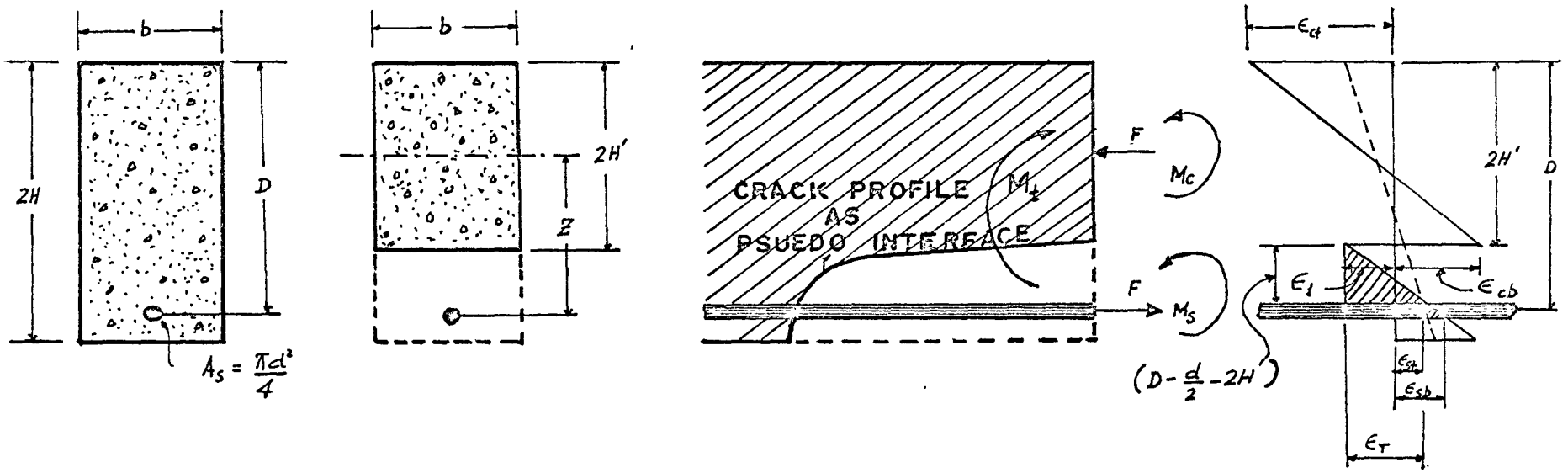

a) UNCRACKED SECTION

b) CRACKED SECTION

c) FORCES
$(M_t = M_c + M_s + F \cdot Z)$

d) STRAINS

REINFORCED CONCRETE BEAM IN THE LIGHT OF COMPOSITE THEORY

FIG. A.A.I

$$\therefore \quad \frac{d\gamma}{dx} = \varepsilon_{st} - \varepsilon_r - \varepsilon_{cb} \qquad \text{A.A.2}$$

From the similarity of the shaded triangles,

$$\varepsilon_r = (\varepsilon_{sb} - \varepsilon_{st}) \left(\frac{D - \frac{d}{2} - 2H'}{d}\right) \qquad \text{A.A.3}$$

where ε_r is the strain due to distortion of the 'concrete teeth' in a cracked beam. Since the strain distribution has been assumed to be linear across the section, analogous to composite beam theory the following expressions can be written:

$$\left.\begin{aligned} \varepsilon_{sb} &= \frac{F}{E_s A_s} + \frac{M_s C_s}{E_s I_s} \\ \varepsilon_{st} &= \frac{F}{E_s A_s} - \frac{M_s C_s}{E_s I_s} \\ \varepsilon_{cb} &= -\frac{F}{E_c A_c} + \frac{M_c C_c}{E_c I_c} \\ \varepsilon_{ct} &= -\frac{F}{E_c A_c} - \frac{M_c C_c}{E_c I_c} \end{aligned}\right\} \qquad \text{A.A.4}$$

Therefore:

$$\varepsilon_r = \left(\frac{F}{E_s A_s} + \frac{M_s C_s}{E_s I_s} - \frac{F}{E_s A_s} + \frac{M_s C_s}{E_s I_s}\right) \left(\frac{D - \frac{d}{2} - 2H'}{d}\right)$$

or

$$\varepsilon_r = \frac{2 M_s C_s}{E_s I_s} \left(\frac{D - \frac{d}{2} - 2H'}{d}\right) \qquad \text{A.A.5}$$

Substituting this value of ε_r in equation A.A.2, the rate of change of slip will be:

$$\frac{d\gamma}{dx} = \varepsilon_{st} - \varepsilon_{cb} - \frac{2M_s C_s}{E_s I_s d}\left(D - \frac{d}{2} - 2H'\right). \qquad \text{A.A.6}$$

According to composite beam theory:

$$q = \frac{dF}{dx} \qquad \text{A.A.7}$$

$$\gamma = q \cdot \frac{s}{K} \qquad \text{A.A.8}$$

where q = load transmitted per unit length of the beam (here, between concrete and steel reinforcement)

F = Interaction force

s = Spacing of connector

= 1 in. (For reinforced concrete beam)

K = Bond-slip modulus.

Differentiating eqs. A.A.7, and A.A.8 with respect to x, yields:

$$\frac{dq}{dx} = \frac{d^2F}{dx^2} \qquad \text{A.A.9}$$

and $$\frac{d\gamma}{dx} = \frac{dq}{dx} \cdot \frac{1}{K}, \quad \text{where } s = 1 \qquad \text{A.A.10}$$

Substitution of eq. A.A.9 in eq. A.A.10, yields:

$$\frac{d\gamma}{dx} = \frac{d^2F}{dx^2} \cdot \frac{1}{K}$$

Therefore, eq. A.A.6 will then be:

$$\frac{1}{K}\frac{d^2F}{dx^2} = \varepsilon_{st} - \varepsilon_{cb} - \frac{2M_sC_s}{E_sI_sd}\left(D - \frac{d}{2} - 2H'\right). \qquad \text{A.A.11}$$

Now substituting values of ε_{st} and ε_{cb} in eq. A.A.11 from eq. A.A.4

$$\frac{1}{K}\frac{d^2F}{dx^2} = \left(\frac{F}{E_sA_s} - \frac{M_sC_s}{E_sI_s}\right) - \left(-\frac{F}{E_cA_c} + \frac{M_cC_c}{E_cI_c}\right) - \frac{2M_sC_s}{E_sI_sd}\left(D - \frac{d}{2} - 2H'\right).$$

Re-arranging,

$$\frac{1}{K}\frac{d^2F}{dx^2} = F\left(\frac{1}{E_sA_s} + \frac{1}{E_cA_c}\right) - \left[\frac{M_sC_s}{E_sI_s} + \frac{M_cC_c}{E_cI_c} + \frac{2M_sC_s}{E_sI_sd}\left(D - \frac{d}{2} - 2H'\right)\right] \qquad \text{A.A.12}$$

Since it is assumed that the concrete and steel reinforcement deflect equally at all points i.e., they have equal curvatures, therefore:

$$\frac{M_s}{E_sI_s} = \frac{M_c}{E_cI_c} \qquad \text{A.A.13}$$

Also from the equilibrium of composite section

$$M_t = M_c + M_s + F\cdot Z\ . \qquad \text{A.A.14}$$

Therefore:

$$\frac{M_c}{E_cI_c} = \frac{M_s}{E_sI_s} = \frac{M_t - F\cdot Z}{\Sigma EI} \qquad \text{A.A.15}$$

where

$$\Sigma EI = E_sI_s + E_cI_c.$$

$$\frac{1}{K}\frac{d^2F}{dx^2} = F\left(\frac{1}{E_sA_s} + \frac{1}{E_cA_c}\right) - \frac{M_t - F\cdot Z}{\Sigma EI}\left[C_s + C_c + \frac{2C_s}{d}\left(D - \frac{d}{2} - 2H'\right)\right]$$

or
$$\frac{1}{K}\frac{d^2F}{dx^2} = F\left\{\frac{1}{E_sA_s} + \frac{1}{E_cA_c}\frac{Z^2}{\Sigma EI}\right\} - \frac{M_tZ}{\Sigma EI} \qquad \text{A.A.16}$$

where
$$Z = C_s + C_c + \frac{2C_s}{d}\left(D - \frac{d}{2} - 2H'\right)$$

by definition
$$C_c = H'$$

and
$$C_s = \frac{d}{2}\ .$$

If
$$\frac{1}{\overline{EA}} = \frac{1}{E_sA_s} + \frac{1}{E_cA_c}$$

and
$$\overline{EI} = \Sigma EI + \overline{EA}\cdot Z^2\ .$$

Then eq. A.A.16 can be written as:

$$\frac{1}{K}\frac{d^2F}{dx^2} = F\cdot\frac{\overline{EI}}{\overline{EA}\Sigma EI} - \frac{M_tZ}{\Sigma EI}\ .$$

By re-arranging the above equation:

$$\frac{d^2F}{dx^2} - F\cdot K\cdot\frac{\overline{EI}}{\overline{EA}\Sigma EI} = -K\cdot\frac{Z}{\Sigma EI}\ M_t(x) \qquad \text{A.A.17}$$

For a cracked section,

$$Z = C_s + C_c + \frac{2C_s}{d}\left(D - \frac{d}{2} - 2H'\right)$$

or
$$Z = \frac{d}{2} + H' + \frac{2d}{2d}\left(D - \frac{d}{2} - 2H'\right).$$

Therefore,
$$Z = D - H'.$$

For an uncracked section, where there are no concrete teeth, $D - \frac{d}{2} - 2H' = 0$ and so $\varepsilon_r = 0$. Therefore, equation A.A.2. reduces to:

$$\frac{d\gamma}{dx} = \varepsilon_{st} - \varepsilon_{cb}.$$

The equation for the uncracked section will be obtained in a manner similar to that for the cracked section (Eq. A.A.17) then, $Z = D-H$

This shows that slip occurs only between the reinforcement and the concrete surrounding it, in an uncracked beam, whereas in a cracked beam there would be an additional slip due to deformation of the concrete teeth.

It is therefore concluded the differential equation A.A.17 is applicable to both a cracked as well as uncracked section of a reinforced concrete beam.

Equation A.A.17 is a second order differential equation in F. The solution of this equation can be obtained for various loadings and end and compatibility conditions by expressing the external moment M_t in terms of distance x of the section from left hand support.

APPENDIX B

PROGRAM TO FIND THE CRACK PROFILE OF R.C. BEAM

(NEWMARK 1 METHOD)

FUNCTION

THIS PROGRAM COMPUTES THE FLEXURAL CRACK PROFILE OF A REINFORCED CONCRETE BEAM - TREATING IT AS A COMPOSITE BEAM WITH INCOMPLETE INTERACTION.

INPUT DATA

AS A PARTICULAR CASE THE DIMENSIONS OF ' TYPICAL BEAM ' HAVE BEEN USED.

NOTATIONS

AC,AC1	AREA OF CONCRETE
AS	AREA OF THE REINFORCEMENT
B	WIDTH OF THE BEAM
BM	MAXIMUM EXTERNAL MOMENT
BMC	MOMENT CARRIED BY CONCRETE
BMS	MOMENT CARRIED BY STEEL
BMX	APPLIED MOMENT AT A SECTION X FROM LEFT SUPPORT
COI	INTERACTION COEFFICIENT - INITIAL VALUE
CCCC	INTERACTION COEFFICIENT - TERMINAL VALUE AS OUTPUT
CH	TOTAL CRACK HEIGHT
CI,CI1	MOMENT OF INERTIAS OF CONCRETE
DELCH	INCREMENT IN THE CRACK HEIGHT
DIS	DIAMETER OF THE STEEL REINFORCEMENT
ED	EFFECTIVE DEPTH OF CONCRETE
EC,ES	MODULI OF ELASTICITY OF CONCRETE AND STEEL RESPECTIVELY
F,FP	INTERACTION FORCE FOR INCOMPLETE AND COMPLETE INTERACTIONS RESPECTIVELY
FFP	DEGREE OF INTERACTION
RD	UNCRACKED DEPTH OF CONCRETE
SI	MOMENT OF INERTIA OF STEEL
STCR	PERMISSIBLE CRACKING STRAIN
STCB,STCT	STRAINS AT BOTTOM AND TOP FIBRES OF UNCRACKED CONCRETE RESPECTIVELY
STSB,STST	STRAIN AT BOTTOM AND TOP FIBRES OF STEEL RESPECTIVELY
STSM	MID-HEIGHT STRAIN IN STEEL
TD	TOTAL DEPTH OF CONCRETE
U	LENGTH OF THE SHEAR SPAN
UOD	SHEAR DEPTH RATIO
W	EXTERNAL APPLIED LOAD
X	DISTANCE OF ANY SECTION FROM LEFT HAND SUPPORT
Z,Z1	INTERNAL LEVER ARM
ZK(I)	BOND-SLIP MODULUS

```
C      ZL                LENGTH OF THE BEAM
C      ZL2               HALF THE LENGTH OF BEAM
C
C
C      D E C K
C      *******
C
       DIMENSION F(100),FP(100),FFP(100),C(10),ZK(10)
C      DATA INPUT AND CALCULATION OF SECTION PROPERTIES
       TD=12.0
       ED=10.7
       B=6.0
       AS=1.207
       STCR=0.0001
       UOD=4.0
       BM=264500.0
       U=UOD*ED
       ZL=2.0*U+36.0
       WRITE(6,2) TD,B,AS,STCR,U,BM,ED,ZL
    2  FORMAT(3F12.5,5X,F12.6,5X,2F15.5,5X,2F12.5)
       S=1.0
       PI=22.0/7.0
       ZL2=ZL*0.5
       EC=3.8E+06
       ES=30.0E+06
       AC1=B*TD
       CI1=B*TD**3./12.0
       Z1=ED-(0.5*TD)
       ASS=0.5*AS
       DIS=SQRT(4.0*ASS/PI)
       SI=2.0*(ASS**2./(4.0*PI))
       SEI1=EC*CI1+ES*SI
       EAB1=ES*AS*EC*AC1/(ES*AS+EC*AC1)
       EIB1=SEI1+EAB1*Z1*Z1
       X=3.0
       I=1
       ZK(I)=17000.0
       C(I)=S*EAB1*SEI1*PI*PI/(ZK(I)*EIB1*ZL*ZL)
       COI=1.0/C(I)
   11  W=BM/U
       WRITE(6,14) X
   14  FORMAT(1H0,26HSECTION CONSIDERED IS AT =,F6.2)
       CH=0.0
C      CALCULATION OF INTRACTION FORCE AND CRACK HEIGHT INCREMENTS
    5  RD=TD-CH
       AC=B*RD
       CI=B*RD**3./12.0
       SEI=EC*CI+ES*SI
       EAB=ES*AS*EC*AC/(ES*AS+EC*AC)
       Z=ED-0.5*RD
       EIB=SEI+EAB*Z*Z
       CR=S*EAB*SEI*PI*PI/(ZK(I)*EIB*ZL*ZL)
       PPI=SQRT(CR)
       AA=PI*X/(ZL*PPI)
```

```
      EE=PI*(0.5-U/ZL)/PPI
      FF=PI*(0.5-X/ZL)/PPI
      BB=PI*U/(ZL*PPI)
      DD=0.5*PI/PPI
      GG=SINH(AA)
      HH=SINH(BB)
      PP=COSH(EE)
      PPP=COSH(FF)
      PIP=COSH(DD)
      IF(X.GT.U) GO TO 30
      BMX=W*X
      FFP=1.0-((GG*PP)/(PIP*AA))
      FP=EAB*Z*BMX/EIB
      F=FP*FFP
      GO TO 7
   30 BMX=BM
      FFP=1.0-((HH*PPP)/(PIP*BB))
      FP=EAB*Z*BMX/EIB
      F=FP*FFP
    7 CC=0.5*RD
      CS=0.5*DIS
      BMC=(BMX-F*Z)*EC*CI/SEI
      BMS=BMX-BMC-F*Z
      STCB=-F/(EC*AC)+BMC*CC/(EC*CI)
      STCT=-F/(EC*AC)-BMC*CC/(EC*CI)
      STSB=F/(ES*AS)+BMS*CS/(ES*SI)
      STST=F/(ES*AS)-BMS*CS/(ES*SI)
      STSM=0.5*(STST+STSB)
      CCCC=1.0/CR
      IF(STCB.LE.STCR) GO TO 8
      IF(ABS(STCB-STCR).LT.1.0E-06) GO TO 8
      IF(CH.GE.TD) GO TO 8
      DELCH=RD*(STCB-STCR)/(STCB-STCT)
      CH=CH+DELCH
      GO TO 5
    8 WRITE(6,10) RD,CH,DELCH,F(I),BMC,CCCC,ZK(I),STCB,STCT,STSM
   10 FORMAT(1H0,7F11.3,3E15.4)
      IF(X.EQ.U) GO TO 27
      RRR=1.0
   15 X=X+RRR
      IF(X.LE.ZL2) GO TO 11
      X=U
      GO TO 11
   27 STOP
      END
```

APPENDIX C

PROGRAM TO FIND THE CRACK PROFILE OF R.C. BEAM

(NEWMARK 2B METHOD)

FUNCTION

THIS PROGRAM COMPUTES THE FLEXURAL CRACK PROFILE OF A REINFORCED CONCRETE BEAM - TREATING IT AS A COMPOSITE BEAM WITH INCOMPLETE INTERACTION.

INPUT DATA

AS A PARTICULAR CASE THE DIMENSIONS OF ' TYPICAL BEAM ' HAVE BEEN USED. THE DISTANCE OF THE FIRST FLEXURAL CRACK FROM THE SUPPORT, AS COMPUTED IN THE PROGRAM OF APPENDIX B (NEWMARK 1 METHOD), HAS BEEN USED AS THE MAGNITUDE OF 'ALP'(THE LENGTH OF THE FULL CROSS-SECTION FROM THE SUPPORT).

NOTATIONS

ALL NOTATIONS ARE SAME AS USED IN THE APPENDIX B PROGRAM.

D E C K

```
*******

      DIMENSION C(10),ZK(10)
      TD=12.0
      B=6.0
      AS=1.207
      STCR=0.0001
      ED=10.7
      UOD=3.0
      BM=264500.0
      ALP=4.1
      U=ED*UOD
      ZL=2.0*U+36.0
      WRITE(6,2) TD,B,AS,STCR,U,BM,ED,ZL
    2 FORMAT(3F12.5,5X,F12.6,5X,2F15.5,5X,2F12.5)
      S=1.0
      PI=22.0/7.0
      ZL2=ZL/2.0
      W=BM/U
      ZK(1)=17000.0
      EC=3.8E+06
      ES=30.0E+06
      AC=B*TD
      CI=B*TD**3/12.0
      Z=ED-TD/2.0
      ASSS=0.5*AS
```

```
      DIS=SQRT(4.0*ASSS/PI)
      SI=2.0*ASSS*2./(4.0*PI)
      SEI=EC*CI+ES*SI
      EAB=ES*AS*EC*AC/(ES*AS+EC*AC)
      EIB=SEI+EAB*Z*Z
      X=1.0
11    WRITE(6,12) X,BM
12    FORMAT(1H0,31HTHE SECTION CONSIDERED IS AT X=,F10.2,10X,F12.2)
      IF(X.GT.U) GO TO 3
      BMX=W*X
      GO TO 4
3     BMX=BM
4     CH=0.0
5     RD=TD-CH
      AC1=B*RD
      CI1=B*RD**3/12.0
      SEI1=EC*CI1+ES*SI
      EAB1=ES*AS*EC*AC1/(ES*AS+EC*AC1)
      Z1=ED-RD/2.0
      EIB1=SEI1+EAB1*Z1**2.
      QQ=ZK(1)*EIB/(S*EAB*SEI)
      QQ1=ZK(1)*EIB1/(S*EAB1*SEI1)
      RR=ZK(1)*Z*W/(S*SEI)
      RR1=ZK(1)*Z1*W/(S*SEI1)
      SQQ=SQRT(QQ)
      SQQ1=SQRT(QQ1)
      AA=COSH(ALP*SQQ)
      BB=COSH(ALP*SQQ1)
      CC=SINH(ALP*SQQ)
      DD=SINH(ALP*SQQ1)
      EE=ZL2-U
      FF=COSH(EE*SQQ1)
      GG=SINH(SQQ1*ZL2)
      PP=COSH(SQQ1*ZL2)
      SS=SINH(U*SQQ1)
      TT=COSH(U*SQQ1)
      VV=SQQ1*BB*AA-SQQ*DD*CC
      UU=RR1*FF/(GG*QQ1**1.5)
      YY=SQQ*CC*BB-SQQ1*DD*AA
      XX=RR1/QQ1-RR/QQ
      ZZ=SQQ*CC*XX/SQQ1
      CC1=0.0
      CC4=-(ZZ+UU*VV)/(YY+(VV*PP/GG))
      CC3=-(CC4*PP/GG)-UU
      CC2=QQ1*(CC3*BB+CC4*DD)/(QQ*CC)
      CC5=CC3-(RR1*SS/(QQ1**1.5))
      CC6=CC4+(RR1*TT/(QQ1**1.5))
40    IF(X.GT.ALP) GO TO 101
      F=CC1*COSH(X*SQQ)+CC2*SINH(X*SQQ)+RR*X/QQ
      FP=RR*X/QQ
      FFP=F/FP
      CCC=TD/2.0
      CS=DIS/2.0
```

```
      BMC=(BMX-F*Z)*EC*CI/SEI
      BMS=BMX-BMC-F*Z
      STCB=-F/(EC*AC)+BMC*CCC/(EC*CI)
      STCT=-F/(EC*AC)-BMC*CCC/(EC*CI)
      STSB=F/(ES*AS)+BMS*CS/(ES*SI)
      STST=F/(ES*AS)-BMS*CS/(ES*SI)
      STSM=0.5*(STST+STSB)
      GO TO 7
  101 IF(X.GT.0) GO TO 102
      F=CC3*COSH(X*SQQ1)+CC4*SINH(X*SQQ1)+RR1*X/QQ1
      FP=RR1*X/QQ1
      FFP=F/FP
      CCC=RD/2.0
      CS=DIS/2.0
      BMC=(BMX-F*Z1)*EC*CI1/SEI1
      BMS=BMX-BMC-F*Z1
      STCB=-F/(EC*AC1)+BMC*CCC/(EC*CI1)
      STCT=-F/(EC*AC1)-BMC*CCC/(EC*CI1)
      STSB=F/(ES*AS)+BMS*CS/(ES*SI)
      STST=F/(ES*AS)-BMS*CS/(ES*SI)
      STSM=0.5*(STSB+STST)
      GO TO 7
  102 IF(X.GT.ZL2) GO TO 60
      F=CC5*COSH(X*SQQ1)+CC6*SINH(X*SQQ1)+RR1*U/QQ1
      FP=RR1*U/QQ1
      FFP=F/FP
      CCC=RD/2.0
      CS=DIS/2.0
      BMC=(BMX-F*Z1)*EC*CI1/SEI1
      BMS=BMX-BMC-F*Z1
      STCB=-F/(EC*AC1)+BMC*CCC/(EC*CI1)
      STCT=-F/(EC*AC1)-BMC*CCC/(EC*CI1)
      STSB=F/(ES*AS)+BMS*CS/(ES*SI)
      STST=F/(ES*AS)-BMS*CS/(ES*SI)
      STSM=0.5*(STSB+STST)
    7 CONTINUE
      CCCC=1.0/CR
      IF(STCB.LE.STCR) GO TO 8
      IF(ABS(STCB-STCR).LT.1.0E-06) GO TO 8
      IF(CH.GE.TD) GO TO 8
      DELCH=RD*(STCB-STCR)/(STCB-STCT)
      CH=CH+DELCH
      GO TO 5
    8 WRITE(6,10) RD,CH,DELCH,F,BMC,CCCC,ZK(1),STCB,STCT,STSM
   10 FORMAT(1H0,7F11.3,3E15.4)
   16 IF(X.EQ.0) GO TO 27
      RRR=1.0
   15 X=X+RRR
   60 IF(X.LE.ZL2) GO TO 11
      X=0
      GO TO 11
      STOP
      END
```

APPENDIX D

PROGRAM TO FIND THE MOMENT CARRYING CAPACITY OF R.C. BEAM

FUNCTION

THIS PROGRAM COMPUTES THE MAXIMUM MOMENT CARRYING CAPACITY OF A REINFORCED CONCRETE BEAM FOR DIFFIRENT SHEAR-ARM TO DEPTH RATIOS, UNDER LOAD POINT BY NEWMARK 1 THEORY. THE BEAM HAS BEEN TREATED AS A COMPOSITE BEAM WITH INCOMPLETE INTERACTION.

INPUT DATA

AS A PARTICULAR CASE THE DIMENSIONS OF ' TYPICAL BEAM ' HAVE BEEN USED.

NOTATIONS

AO	DEPTH OF NEUTRAL AXIS AS OBTAINED BY A.C.I. CODE FORMULA
EUC	ALLOWABLE ULTIMATE STRAIN IN CONCRETE
P	PERCENTAGE OF TENSILE REINFORCEMENT
SUC	ULTIMATE CRUSHING STREES OF CONCRETE
RATIO	RELATIVE BEAM STRENGTH
YST	YIELD STRESS OF STEEL
YSTS	YIELD STRAIN OF STEEL
UBMM	ULTIMATE MOMENT CAPACITY OF THE BEAM-OBTAINED BY A.C.I. CODE FORMULA

OTHER NOTATIONS ARE SAME AS USED IN APPENDIX B PROGRAM

LIMITATIONS

STCR=100 MICRO IN/IN
STCT=3000 MICRO IN/IN
STSM=1500 MICRO IN/IN

D E C K

```
*******

DIMENSION C(25),ZK(25)
DATA INPUT AND CALCULATION OF SECTION PROPERTIES
TD=12.0
B=6.0
P=1.88
STCR=0.0001
ED=10.7
AS=B*ED*P/100.0
NN=10
NN IS THE NUMBER OF A/D RATIOS TO BE CONSIDERED
```

```
C       INITIALLY ASSUME ANY SUITABLE VALUE OF ULTIMATE BENDING MOMENT
C             FOR EACH PARTICULAR A/D RATIO
        DO 27 M=1,NN
        READ(5,28) UOD,BM
   28   FORMAT(2F12.0)
        U=UOD*ED
        ZL=2.0*U+36.0
        WRITE(6,53) TD,B,AS,ED,ZL,P,STCR
   53   FORMAT(1H0,21HPROPERTIES OF SECTION,6F12.3,E15.4)
        WRITE(6,54) UOD
   54   FORMAT(1H0,11HU/D RATIO =,F5.2)
        S=1.0
        KNT=0
        PI=22.0/7.0
        ZL2=ZL*0.5
        EUC=0.003
        EC=1.9E+06
        SUC=EUC*EC
        ES=30.0E+06
        YST=45000.0
        YSTS=YST/ES
        AC1=B*TD
        CI1=B*TD**3./12.0
        Z1=ED-(0.5*TD)
        ASS=0.5*AS
        DIS=SQRT(4.0*ASS/PI)
        SI=2.0*(ASS**2./(4.0*PI))
        EAB1=ES*AS*EC*AC1/(ES*AS+EC*AC1)
        SEI1=EC*CI1+ES*SI
        EIB1=SEI1+EAB1*Z1*Z1
        X=U
C       FOR THE CALCULATION OF ULTIMATE CARRYING CAPACITY SECTION UNDER
C            LOAD POINT IS CONSIDERED
        I=1
        ZK(I)=17000.0
        C(I)=S*EAB1*SEI1*PI*PI/(ZK(I)*EIB1*ZL*ZL)
        COI=1.0/C(I)
    6   W=BM/U
        CH=0.0
C       FOR EVERY SET OF BENDING MOMENT AND A/D RATIO FLEXURAL CRACK
C            STABILISES FIRST
    5   RD=TD-CH
        AC=B*RD
        CI=B*RD**3./12.0
        SEI=EC*CI+ES*SI
        EAB=ES*AS*EC*AC/(ES*AS+EC*AC)
        Z=ED-0.5*RD
        EIB=SEI+EAB*Z*Z
        CR=S*EAB*SEI*PI*PI/(ZK(I)*EIB*ZL*ZL)
        CCCC=1.0/CR
        PPI=SQRT(CR)
        AA=PI*X/(ZL*PPI)
        BB=PI*U/(ZL*PPI)
        DD=0.5*PI/PPI
        EE=PI*(0.5-U/ZL)/PPI
```

```
      FF=PI*(0.5-X/ZL)/PPI
      GG=SINH(AA)
      HH=SINH(BB)
      PP=COSH(EE)
      PPP=COSH(FF)
      PIP=COSH(DD)
      IF(X.GT.0) GO TO 30
      BMX=W*X
      FFP=1.0-((GG*PP)/(PIP*AA))
      FP=EAB*Z*BMX/EIB
      F=FP*FFP
      GO TO 7
   30 BMX=BM
      FFP=1.0-((HH*PPP)/(PIP*BB))
      FP=EAB*Z*BMX/EIB
      F=FP*FFP
    7 CC=0.5*RD
      CS=0.5*DIS
      BMC=(BMX-F*Z)*EC*CI/SEI
      BMS=BMX-BMC-F*Z
      STCB=-F/(EC*AC)+BMC*CC/(EC*CI)
      STCT=-F/(EC*AC)-BMC*CC/(EC*CI)
      STSB=F/(ES*AS)+BMS*CS/(ES*SI)
      STST=F/(ES*AS)-BMS*CS/(ES*SI)
      STSM=0.5*(STST+STSB)
      T=STSM*ES*AS
      IF(STCB.LE.STCR) GO TO 20
      IF(ABS(STCB-STCR).LT.1.0E-06) GO TO 20
      DELCH=RD*(STCB-STCR)/(STCB-STCT)
      CH=CH+DELCH
      GO TO 5
   20 WRITE(6,3) RD,CH,FFP,CCCC,COI,STCB,STCT,STSM
    3 FORMAT(1H0,5F14.3,3E18.4)
C     AFTER STABILISATION OF CRACK CHEK FOR THE CONCRETE TOP STRAIN AND
C          STEEL MID-HEIGHT STRAIN.IF EITHER ONE IS GRETER THAN THE
C          RESPECTIVE ALLOWABLE LIMIT REDUCE THE BENDING MOMENT.IF ANY
C          STRAIN EQUAL TO THE ALLOWABLE LIMIT TAKE ANOTHER A/D RATIO,
C          OTHERWISE INCREASE THE BENDING MOMENT AND REPEAT THE PROCESS
      IF(STSM.GT.(YSTS+10.0E-06)) GO TO 103
      IF(ABS(STCT).GT.(EUC+25.0E-06)) GO TO 103
      IF(STSM.GE.YSTS) GO TO 48
      IF(ABS(STSM-YSTS).LE.10.0E-06) GO TO 48
      IF(ABS(STCT).GE.3.0E-03) GO TO 49
      IF(ABS(STCT+3.0E-03).LE.25.0E-06) GO TO 49
      GO TO 31
  103 BM=BM-5000.0
      KNT=KNT+1
      GO TO 6
   31 IF(KNT.GT.1) GO TO 50
      BM=BM+5000.0
      GO TO 6
C     CALCULATION OF ULTIMATE BENDING MOMENT BY ACI CODE FORMULA
   49 AO=AS*YST/(0.85*SUC*B)
      UBMM=AS*YST*(ED-0.5*AO)
      RATIO=BMX/UBMM
```

```
      WRITE(6,11) UBMM,BMX,RATIO,STCT,STSM
   11 FORMAT(1H0,14H CONC CRUSHES ,3F15.3,2E20.4)
      GO TO 27
C     CALCULATION OF ULTIMATE BENDING MOMENT BY ACI CODE FORMULA
   48 AO=AS*YST/(0.85*SUC*B)
      UBMM=AS*YST*(ED-0.5*AO)
      RATIO=BMX/UBMM
      WRITE(6,47) UBMM,BMX,RATIO,STCT,STSM
   47 FORMAT(1H0,14H STEEL YIELDS ,3F15.3,2E20.4)
      GO TO 27
C     CALCULATION OF ULTIMATE BENDING MOMENT BY ACI CODE FORMULA
   50 AO=AS*YST/(0.85*SUC*B)
      UBMM=AS*YST*(ED-0.5*AO)
      RATIO=BMX/UBMM
      WRITE(6,51) UBMM,BMX,RATIO,STCT,STSM
   51 FORMAT(1H0,55HUSE LESSER INCREMENT OF BM-SECTION IS NEARER TO FAIL
     1URE,3F12.3,2E15.4)
   27 CONTINUE
      STOP
      END
```

APPENDIX E

PROGRAM TO FIND THE SHEAR STRESS DITRIBUTION THROUGHOUT THE DEPTH OF A CRACKED OR UNCRACKED R.C. BEAM

PART 1) IN THE REMAINING UNCRACKED CONCRETE

FUNCTION

THIS PROGRAM COMPUTES THE SHEAR STRESS DITRIBUTION IN THE UNCRACKED CONCRETE AND ITS CONTRIBUTION IN RESISTING THE EXTERNAL SHEAR FORCE. THE BEAM HAS BEEN TREATED AS A COMPOSITE BEAM WITH INCOMPLETE INTERACTIONAND NEWMARK 1 THEORY HAS BEEN USED.

INPUT DATA

AS A PARTICULAR CASE THE DIMENSIONS OF ' TYPICAL BEAM ' HAVE BEEN USED.

NOTATIONS

CRSP	SPASING OF THE FLEXURAL CRACKS OR TOOTH WIDTH
DDNA1 AND DDNA2	DISTANCE OF ANY PARTICULAR LEVEL FROM THE TOP CONCRETE FIBRE FOR SECTIONS 1-1 AND 2-2 RESPECTIVELY
DX	DISTANCE BETWEEN THE SECTIONS 1-1 AND 2-2
FOR 1 AND FOR2	HORIZONTAL FORCE AT ANY LEVEL FROM TOP CONCRETE FIBRE AT SECTONS 1-1 AND 2-2, RESPECTIVELY
GC	SHEAR MODULUS OF CONCRETE
POR	POISON'S RATIO FOR CONCRETE
RSHF	RATIO OF THE SHEAR FORCE CARRIED BY THE UNCRACKED CONCRETE
SHF	SHEAR FORCE AT ANY LEVEL FROM TOP CONCRETE FIBRE
STY1 AND STY2	CONCRETE STRAIN AT ANY LEVEL AT SECTIONS 1-1 AND 2-2 , RESPECTIVELY
TSHF	TOTAL SHEAR FORCE ABOVE ANY DESIRED LEVEL

OTHER NOTATIONS ARE SAME AS USED IN APPENDIX B, C AND D PROGRAM

D E C K

```
*******
DIMENSION X(50),XX(5),RD(5),CH(5),FFP(5),FP(5),F(5),BMX(5),BMC(5)
DIMENSION BMS(5),STCB(5),STCT(5),STSB(5),STST(5),STSM(5),DELCH(5)
DIMENSION DNA(5),DDNA1(50),DDNA2(50),STY1(50),STY2(50),FOR1(50)
```

```
      DIMENSION FOR2(50),SHS(50),SHST(50),SHSTM(50),T(50),SHF(50)
      DIMENSION TSHF(50),RDD(50),CHH(50)
C     DATA INPUT AND CALCULATION OF SECTION PROPERTIES
      TD=12.0
      B=6.0
      AS=1.207
      STCR=0.0001
      ED=10.7
      POR=0.16
      S=1.0
      PI=22.0/7.0
      ZK=17000.0
      WRITE(6,2) TD,ED,B,AS,STCR
    2 FORMAT(1H0,4F20.3,F20.4)
      CRSP=2.6
      DX=0.1
      UOD=3.0
      BM=264500.0
      U=UOD*ED
      ZL=2.0*U+36.0
      ZL2=0.5*ZL
      WRITE(6,62) UOD,BM
   62 FORMAT(1H0,11HA/D RATIO =,F7.2,5X,16HBENDING MOMENT =,F10.0)
      NN=11
C     NN IS THE NUMBER OF SECTIONS AT WHICH SHEAR CALCULATION DESIRED
      READ(5,13) (X(I),I=1,NN)
   13 FORMAT(16F5.0)
      EC=1.9E+06
      ES=30.0E+06
      GC=0.5*EC/(1.0+POR)
      AC1=B*TD
      CI1=B*TD**3./12.0
      Z1=ED-(0.5*TD)
      DIS=SQRT(4.0*AS/PI)
      SI=AS**2./(4.0*PI)
      SEI1=EC*CI1+ES*SI
      EAB1=ES*AS*EC*AC1/(ES*AS+EC*AC1)
      EIB1=SEI1+EAB1*Z1**2.
      C=S*EAB1*SEI1*PI*PI/(ZK*EIB1*ZL*ZL)
      DO 47 I=1,NN
      RDD(I)=TD
      CHH(I)=0.0
   47 CONTINUE
      W=BM/U
C     SECTIONS 1-1 AND 2-2 ARE AT AT A DISTANCE DX/2 TO THE LEFT AND
C     RIGHT OF THE PARTICULAR SECTION C-C
      DO 15 J=1,NN
      XX(1)=X(J)-0.5*DX
      XX(2)=X(J)
      XX(3)=X(J)+0.5*DX
      WRITE(6,56) X(J)
   56 FORMAT(1H0,14HSECTION AT X =,F7.2)
      DO 16 I=1,3
      RD(I)=RDD(J)
```

```
      CH(I)=CHH(J)
   16 CONTINUE
C     THE FLEXURAL CRACK HEIGHT AT THE PARTICULAR SECTION C-C IS CALCUL-
C          ATED FIRST AND THE HEIGHT OF CRACK FOR RESPECTIVE SECTIONS
C          1-1 AND 2-2 MADE EQUAL TO THAT FOR SECTION C-C AND THEN THE
C          STRAIN DISTRIBUTION FOR SECTIONS 1-1 AND 2-2 ARE DETERMINED
   21 K=2
    5 AC=B*RD(K)
      CI=B*RD(K)**3./12.0
      SEI=EC*CI+ES*SI
      EAB=ES*AS*EC*AC/(ES*AS+EC*AC)
      Z=ED-(0.5*RD(K))
      EIB=SEI+EAB*Z*Z
      CR=S*EAB*SEI*PI*PI/(ZK*EIB*ZL*ZL)
      PPI=SQRT(CR)
      AA=PI*XX(K)/(ZL*PPI)
      BB=PI*U/(ZL*PPI)
      DD=0.5*PI/PPI
      EE=PI*(0.5-U/ZL)/PPI
      FF=PI*(0.5-XX(K)/ZL)/PPI
      GG=SINH(AA)
      HH=SINH(BB)
      PP=COSH(EE)
      PPP=COSH(FF)
      PIP=COSH(DD)
      IF(XX(K).GT.0) GO TO 6
      BMX(K)=W*XX(K)
      FFP(K)=1.0-((GG*PP)/(PIP*AA))
      FP(K)=EAB*Z*BMX(K)/EIB
      F(K)=FP(K)*FFP(K)
      GO TO 7
    6 BMX(K)=BM
      FFP(K)=1.0-((HH*PPP)/(PIP*BB))
      FP(K)=EAB*Z*BMX(K)/EIB
      F(K)=FP(K)*FFP(K)
    7 CC=RD(K)*0.5
      CS=0.5*DIS
      BMC(K)=(BMX(K)-F(K)*Z)*EC*CI/SEI
      BMS(K)=BMX(K)-BMC(K)-F(K)*Z
      STCB(K)=-F(K)/(EC*AC)+BMC(K)*CC/(EC*CI)
      STCT(K)=-F(K)/(EC*AC)-BMC(K)*CC/(EC*CI)
      STSB(K)=F(K)/(ES*AS)+BMS(K)*CS/(ES*SI)
      STST(K)=F(K)/(ES*AS)-BMS(K)*CS/(ES*SI)
      STSM(K)=0.5*(STSB(K)+STST(K))
      T(K)=STSM(K)*ES*AS
      DNA(K)=-STCT(K)*RD(K)/(STCB(K)-STCT(K))
      IF(K.EQ.1) GO TO 42
      IF(K.EQ.2) GO TO 43
      GO TO 44
   43 IF(CH(K).GE.TD) GO TO 53
      IF(STCB(K).LE.STCR) GO TO 20
      IF(ABS(STCB(K)-STCR).LT.1.0E-06) GO TO 20
   41 DELCH(K)=RD(K)*(STCB(K)-STCR)/(STCB(K)-STCT(K))
      CH(K)=CH(K)+DELCH(K)
```

```
      RD(K)=TD-CH(K)
      RDD(J)=RD(K)
      CHH(J)=CH(K)
      GO TO 5
   20 K=K-1
      RD(K)=RD(K+1)
      CH(K)=CH(K+1)
      GO TO 5
   42 K=K+2
      RD(K)=RD(K-1)
      CH(K)=CH(K-1)
      GO TO 5
   44 WRITE(6,45) RD(2),CH(2),DNA(2),STCB(2),STCT(2),STSM(2)
   45 FORMAT(1H0,14HAFTER BENDING ,3F10.3,3E20.4)
      GO TO 54
   53 WRITE(6,59) RD(2),CH(2),DNA(2),STCB(2),STCT(2),STSM(2)
   59 FORMAT(1H0,18HWHOLE BEAM CRACKED,3F10.3,3E20.4)
      GO TO 57
C     THIS PART CALCULATE THE SHEAR STRESS AND SHEAR FORCE
   54 M=1
      KK=50
      DDM=RD(M+1)/FLOAT(KK)
      DO 18 JJ=1,KK
      IF(JJ.EQ.1) GO TO 17
      DDNA1(JJ)=DDNA1(JJ-1)+DDM
      DDNA2(JJ)=DDNA2(JJ-1)+DDM
      GO TO 19
   17 DDNA1(JJ)=DDM
      DDNA2(JJ)=DDM
   19 IF(DDNA1(JJ).GT.DNA(M)) GO TO 25
      STY1(JJ)=STCT(M)*(DNA(M)-DDNA1(JJ))/DNA(M)
      FOR1(JJ)=(STCT(M)+STY1(JJ))*0.5*DDNA1(JJ)*B*EC
      GO TO 27
   25 STY1(JJ)=STCB(M)*(DDNA1(JJ)-DNA(M))/(RD(M)-DNA(M))
      FOR1(JJ)=0.5*B*EC*STCT(M)*DNA(M)+0.5*B*EC*STY1(JJ)*(DDNA1(JJ)-DNA(
     1M))
      GO TO 27
   31 FOR1(JJ)=0.5*B*EC*STCT(M)*DNA(M)+0.5*B*EC*STCB(M)*(RD(M)-DNA(M))
   27 IF(DDNA1(JJ).LT.ED) GO TO 34
      FOR1(JJ)=FOR1(JJ)+T(M)
   34 IF(DDNA2(JJ).GT.DNA(M+2)) GO TO 26
      STY2(JJ)=STCT(M+2)*(DNA(M+2)-DDNA2(JJ))/DNA(M+2)
      FOR2(JJ)=(STCT(M+2)+STY2(JJ))*0.5*DDNA2(JJ)*B*EC
      GO TO 28
   26 STY2(JJ)=STCB(M+2)*(DDNA2(JJ)-DNA(M+2))/(RD(M+2)-DNA(M+2))
      FOR2(JJ)=0.5*B*EC*STCT(M+2)*DNA(M+2)+STY2(JJ)*0.5*B*EC*(DDNA2(JJ)-
     2DNA(M+2))
      GO TO 28
   28 IF(DDNA2(JJ).LT.ED) GO TO 35
      FOR2(JJ)=FOR2(JJ)+T(M+2)
   35 SHS(JJ)=(FOR2(JJ)-FOR1(JJ))/(B*DX)
      SHST(JJ)=SHS(JJ)/GC
      SHST(KK)=0.0
   18 CONTINUE
```

```
      SHF(1)=0.5*SHS(1)*DDM*B
      TSHF(1)=SHF(1)
      DO 51 I=2,KK
      SHF(I)=0.5*(SHS(I)+SHS(I-1))*B*DDM
      TSHF(I)=TSHF(I-1)+SHF(I)
      RSHF=TSHF(KK)/W
   51 CONTINUE
      WRITE(6,300)
  300 FORMAT(1H0,23H      SHEAR DISTRIBUTION)
      WRITE(6,22) DDM,TSHF(KK),RSHF
   22 FORMAT(1H0,3F12.3)
      WRITE(6,50) SHS(5),SHS(10),SHS(15),SHS(20),SHS(25),SHS(30),SHS(35)
     2,SHS(40),SHS(45),SHS(49)
   50 FORMAT(1H0,10E12.3)
   15 CONTINUE
   57 STOP
      END
```

PART 2) IN THE CRACKED ZONE OF CONCRETE

FUNCTION

THIS PROGRAM COMPUTES THE SHEAR STRESS DISTRIBUTION IN THE CRACKED PORTION(TENSILE ZONE) OF CONCRETE AND ALSO CALCULATE THE CONTRIBUTION OF DOWEL AND AGGREGATE INTERLOCK ACTIONS. ANY TWO ADJACENT CONCRETE TEETHS WERE IDEALISED INTO 'COMPOSITE CANTILEVER BEAM' AND STUDSI'S COMPOSITE BEAM THEORY HAS BEEN USED.

INPUT DATA

THE DIMENSIONS OF THE CONCRETE TEETHS HAVE BEEN USED.THEY ARE AS FOLLOWS WITH THE NOTATIONS.

BM	BENDING MOMENT AT ANY SECTION IN THE CANTILEVER BEAM
BMM	EXTERNAL BENDING MOMENT (LONGITUDINAL) AT THE SECTION UNDER CONSIDERATION
BR	BREDTH OF THE BEAM
DB AND DS	DEPTH OF EACH ELEMENT OF THE BEAM AND IS EQUAL TO THE AVERAGE CRACK SPASING
N	NUMBER CONNECTORS
RA	RATIO OF THE SHEAR FORCE CARRIED BY UNCRACKED CONCRETE AS OBTAINED FROM PART 1
RRS	RATIO OF THE SHEAR FORCE TO BE RESISTED BY DOWEL AND AGGREGATE INTERLOCK ACTIONS
S AND SP	CONNECTORS SPASING
U	DISTANCE BETWEEN THE FLEXURAL REINFORECEMENT TO THE CRACK HEIGHT AT THE INTERFACE
W	LOAD ON THE BEAM AND IS EQUAL TO THE INCREMENT IN THE HORIZONTAL FORCE BBETWEEN THE TWO ADJACENT CONCRETE TEETHS UNDER CONSIDERATION
WW	EXTERNAL LOAD (VERTICAL) AT THE SECTION UNDER CONSIDERATION
ZKC	AGGREGATE INTERLOCK MODULUS
ZL	LENGTH OF THE BEAM-EQUAL TO THE CRACK HEIGHT AT THE INTERFACE OF THE BEAM

OTHER NOTATIONS ARE SELF EXPLANATORY IN THE LIGHT OF THE NOTATIONS USED IN THE APPENDICES B, C, D, AND E-PART 1

D E C K
****

```
DIMENSION S(100),X(100),BM(100),A(3,100),Q(100),B(100)
DIMENSION ZK(100),SS(100),SHF(100),TSHF(100),SHS(100)
DS=2.6
DB=DS
BR=6.0
```

```
      SP=0.25
      ZL=7.337
      U=6.037
      ZKC=4840000.0
      BMM=264500.0
      RA=0.045
      ST1=786.95E-06
      ST2=781.445-06
      N=30
      N1=N-1
      N2=N-2
      S(1)=0.3
      DO 12 I=2,N2
   12 S(I)=SP
      S(N1)=0.287
      W=(ST1-ST2)*30.0E+06
      WRITE(6,13) DS,DB,BR,W,ZL,U,N,ZKC,SP
      WRITE(6,14) BMM,RA,ST1,ST2
   13 FORMAT(1H0,6F12.2,I10,2F12.2)
   10 FORMAT(1H0,12F10.3)
    3 FORMAT(1H0,4F12.4,I10)
   14 FORMAT(1H0,2F15.4,2E15.4)
      WW=BMM/32.1
      KNTT=30
      KNT=0
      RRS=RA
C     THE PARTICULAR DIMENSIONS GIVEN HERE ARE FOR THE CANTILEVERS IN
C          BETWEEN THE LOAD POINTS. IF THE SECTION LIES IN THE SHEAR
C          SPAN THEN  RRS=1.0-RA
      Z=(DS+DB)*0.5
      ES=1.9E+06
      AS=DS*BR
      AB=DB*BR
      EB=ES
      SI=BR*DS**3./12.0
      BI=BR*DB**3./12.0
      EAB=ES*AS*EB*AB/(ES*AS+EB*AB)
      SEI=EB*BI+ES*SI
      EIB=SEI+EAB*Z*Z
      AO=EIB/(EAB*SEI)
      X(1)=0.5*S(1)
      DO 4 I=2,N1
      SS(I)=(S(I-1)+S(I))*0.5
      X(I)=X(I-1)+SS(I)
    4 CONTINUE
      DO 5 I=1,5
    5 BM(I)=0.0
      DO 6 I=6,N1
    6 BM(I)=W*(X(I)-(ZL-U))
    9 DO 16 I=1,N1
   16 ZK(I)=ZKC
      ZK(6)=2.0*1.75E+05+ZKC
      ZK(1)=ZKC*S(1)/SP
      ZK(N1)=ZKC*S(N1)/SP
```

```
      KNT=KNT+1
      DO 20 I=1,N2
      A(1,I)=-1.0
      A(2,I)=1.0+ZK(I)/ZK(I+1)+AO*ZK(I)*S(I)
      A(3,I)=-ZK(I)/ZK(I+1)
      B(I)=BM(I)*Z*ZK(I)*S(I)/SEI
   20 CONTINUE
      A(1,1)=0.0
      A(3,N1)=0.0
      A(2,N1)=1.0+AO*ZK(N1)*S(N1)
      A(1,N1)=-1.0
      B(N1)=BM(N1)*Z*ZK(N1)*S(N1)/SEI
      CALL BNDSOL(A,B,3,1,N1)
      B(N)=B(N1)
      Q(1)=B(1)
      DO 11 I=2,N
   11 Q(I)=B(I)-B(I-1)
      SHS(1)=0.0
      DO 18 I=2,N1
   18 SHS(I)=Q(I)/(S(I)*BR)
      SHS(N)=0.0
      DO 19 I=1,N1
      SHF(I)=(SHS(I)+SHS(I+1))*0.5*BR*S(I)
      IF(I.GT.1) GO TO 21
      RR=0.0
      GO TO 22
   21 RR=TSHF(I-1)
   22 TSHF(I)=RR+SHF(I)
   19 CONTINUE
      RATIO=TSHF(N1)/WW
      WRITE(6,10) (B(I),I=1,N1)
      WRITE(6,10) (Q(I),I=1,N)
      WRITE(6,10) (SHS(I),I=1,N)
      WRITE(6,3) TSHF(N1),WW,ZKC,RATIO,KNT
      IF(ABS(RATIO-RRS).LE.0.001) GO TO 7
      IF(KNT.GT.KNTT) GO TO 7
      IF(RATIO.GT.RRS) GO TO 8
      ZKC=ZKC+5000.0
      GO TO 9
    8 ZKC=ZKC-5000.0
      GO TO 9
    7 STOP
      END
```